TABLE OF CONTENTS

GATHER RICH INSIGHTS FROM COATINGS ANALYSIS

Molecular Spectroscopy Application eHandbook

Agilent Technologies

TABLE OF CONTENTS

Click the links to jump immediately to that section

COATING CHALLENGES

CHALLENGES FOR COATINGS RESEARCHERS AND MANUFACTURERS

From aerospace to automotive, marine, and architectural coatings, and from paints to thin films and highly specialized optical coatings, researchers and manufacturers are constantly striving to meet the ever-increasing demands on coating function, performance, and longevity.

Demand for new and innovative products to meet the market's needs, particularly those with eco-friendly credentials

Demand for coatings with more functionality – that's maintained across the coating's lifecycle

Demand for products manufactured and applied to a consistently high quality

GATHERING RICH DATA ABOUT YOUR COATINGS WITH FTIR AND UV-VIS-NIR SPECTROSCOPY

Develop and produce market leading products with Agilent's coatings solutions. Collect a wide range of data to inform your research and development efforts, confirm product quality or help troubleshoot product application problems.

Visual appearance changes with viewing angle

Test the appearance of coatings in the visible spectrum, and characterize changes with viewing angle or the angle of the incident light.

In practice:

Measuring angular reflectance of compact visual displays

Film thickness measurement

Use UV-Vis or FTIR to accurately measure the thickness of thin films of single layer, or multi-layer, dielectric stacks.

In practice:

Determining the optical properties of thin films

Measuring epoxy primer thickness on aluminum with FTIR

Measuring aluminum anodization thickness with FTIR

Spatially profile coatings

Ensure a coating is uniform and homogeneous by mapping its properties over its surface.

In practice:

Automated spectrophotometric spatial profiling of coated optical wafers

Specular reflection from coatings and angular dependence

Automated, unattended determination of specular reflection, under s and p polarized conditions, from 6 deg near normal to grazing angle 85 deg in 1 deg increments.

In practice:

Characterizing the angular reflectance properties of silicon wafers

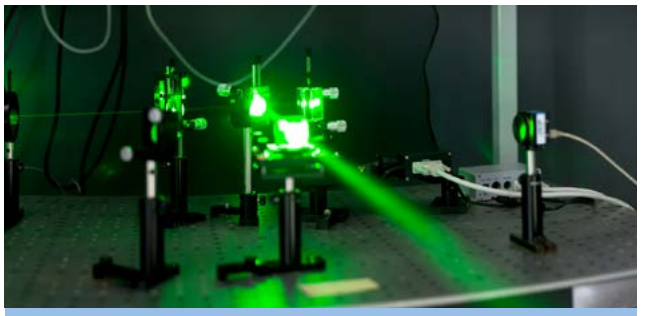

Extreme performance coatings

Improve designs through quality measurement of high performance, low loss, coatings used in high energy laser based applications.

In practice:

Quality control of beam splitters and quarter wave mirrors

Coating ageing studies

Design more robust coatings with knowledge of aging or weathering mechanisms through the use of UV and FTIR spectroscopy.

In practice:

Non-destructive testing (NDT) of an industrial 2K epoxy resin-coated panel undergoing accelerated weathering using the ASTM G155 protocol

Analysis of artificially weathered PET and a separate PET hydrolysis evaluation using handheld FTIR

Characterizing embedded optical films

Complete characterization of embedded optical films in cube beam splitters through transmission and reflection measurements without moving the sample.

In practice:

Charactertizing cube beam splitters

Coating performance studies

Use FTIR to test the impact mixture ratio has on coating performance—resistance to heat, water, chemicals, radiation, and so on—under actual use conditions. Study high performance optical coatings for laser applications at oblique angles of incidence.

In practice:

Comparison of portable FTIR interface technologies for the analysis of paints, minerals & concrete

Rapid quantification of the A:B mix-ratio of a 2K industrial OEM PU paint prior to autoclave thermal activation

Coating cure studies

Determining whether the cure process has completed or identify the optimal cure rate and temperature using FTIR spectroscopy.

In practice:

Comparison of portable FTIR interface technologies for the analysis of paints, minerals & concrete

Rapid quantification of the A:B mix-ratio of a 2K industrial OEM PU paint prior to autoclave thermal activation

Identification and evaluation of coatings using hand-held FTIR

Identifying trapped solvents

Determine if there are solvents that have been trapped within the coating due to incomplete or ineffective curing.

Determining coating mix ratios

Be confident that the mixing ratio of a 2-part coating is correct – both before and after application.

In practice:

Mix ratio identification in industrially significant two-part coating systems using handheld FTIR

Rapid quantification of the A:B mix-ratio of a 2K industrial OEM PU paint prior to autoclave thermal activation

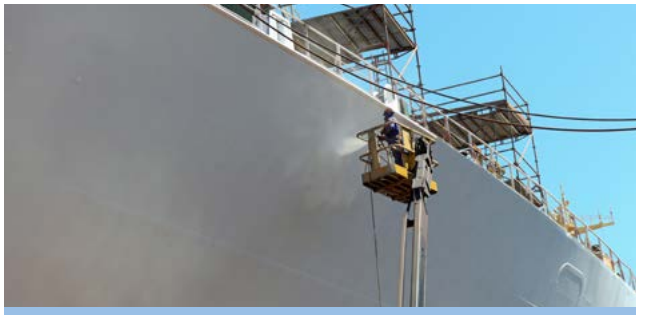

Surface contamination studies

Ensure that surfaces are clean and free of contaminants such as silicone oil or hydrocarbons, which reduce surface adhesion.

In practice:

Detection of trace contamination on metal surfaces

Measurement of composite surface contamination

Coating identification

Use the fingerprint region of the IR spectrum and a library of known spectra to positively identify a coating. This is useful when trying to match a coating or identify counterfiet products.

In practice:

Metal coatings analysis using the handheld Agilent 4100 ExoScan FTIR

Identification and evaluation of coatings using hand-held FTIR

Positive and nondestructive identification of acrylic-based coatings

Surface activation confirmation

Ensure that surfaces are properly pretreated, as required to ensure correct coating adhesion.

In practice:

Analysis of plasma treated carbon fiber reinforced polymer composites by portable FTIR

Measure release agent on a polymer reinforced with carbon fibre

HOW TO MEASURE YOUR SAMPLE – WHEN IT'S ENORMOUS... OR ATTACHED TO AN AIRCRAFT OR BUILDING?

In the past, researchers and technicians often had to sacrifice their samples for analysis – either cutting them to fit into instrumentation or destroying them during sample preparation. Agilent's unique sampling compartments and hand held measurement capabilities mean non-destructive testing is now available, in areas you may never have thought possible.

The handheld 4300 FTIR unit can be used insitu, anywhere, anytime. Instead of taking coating samples back to the lab, you can take non-destructive measurements of the coating on whatever it's been applied to – walls, aircraft, glass etc.

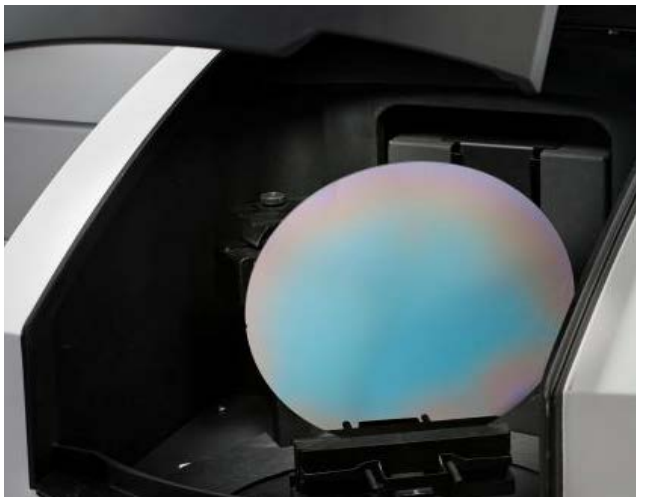

The unique sample handling capabilities of the Cary UV-Vis-NIR UMS instrument allow you to mount samples up to 200 mm in diameter in the sample compartment. The motorized sample stage moves the sample into position – allowing measurements at any position on the sample.

INSTRUMENT OVERVIEW

GET RICH INSIGHTS INTO COATING STRUCTURE AND PERFORMANCE

Agilent's FTIR and UV-VIS-NIR instruments can generate accurate data from across the spectrum, quickly and easily. Whether you are researching, manufacturing or applying coatings and thin films, data obtained using ultraviolet through to infrared wavelengths will help you delve into the identity, characteristics and functions of a coating.

The 4300 Handheld FTIR is the first of its kind combining lightweight ergonomics, ease of use, ruggedness, and flexibility into one system. The 4300 weighs in at approximately 2 kg. With its light weight and ergonomic design it's ideal for field use and deployment into non-laboratory situations.

A variety of sampling interfaces (Diffuse Reflectance, External Reflectance, Grazing Angle, Diamond ATR, Ge ATR) allows the user to easily transition from one sample type to another while on the go, with no alignment or adjustments necessary. Sample types typically include infrared absorbing and scattering surfaces, reflective metal surfaces with coatings and films as well as analysis of bulk materials including powders and granules.

The revolutionary Agilent Cary 7000 Universal Measurement Spectrophotometer (UMS) can collect hundreds of UV-Vis-NIR spectra overnight, or characterize optical components or thin films in minutes to hours rather than hours to days.

A turn-key solution for research, development and QA/QC of optics, thin films/coatings, solar and glass, the Cary 7000 UMS will advance your materials analysis. Design experiments never before possible, expand your research, and save time and money.

FTIR MEASUREMENTS

THE AGILENT 4300 HANDHELD FTIR

This versatile instrument is ideally suited to at-site, mid-IR measurement of objects constructed from high-value materials. Its optimized design lets you quickly scan large surfaces or areas, and knowledgeably assess factors such as identity, quality, authenticity, and wear. In addition, the 4300 Handheld FTIR enables you to analyze objects directly – without removing a sample – so you can reduce your dependence on overworked or off-site labs.

The key features of the 4300 include:

- **In-situ measurements** – measure samples of any size or form. Weighing only 5 lbs (2.2 kg), the ergonomic 4300 FTIR can be used in any accessible location
- **Non destructive testing** – samples will be unchanged after measurement
- **Five different interchangeable, snap-on interfaces** allow you to collect the data you need. Choose from: Diamond ATR, Diffuse Reflectance, External Reflectance, Grazing Angle and Germanium ATR interfaces
- **Agilent MicroLab Mobile software** guides the user through the measurement process and includes application-specific functions such as spectral-matching for material identification.

The applications shown on the following pages provide guidance and typical results for common applications of handheld FTIR.

Rapid Quantification of the A:B mix-ratio of a 2K Industrial OEM PU paint prior to autoclave thermal activation

Authors

Leung Tang
Agilent Technologies

Introduction

Modern industrial paints are complex and highly engineered products. They typically contain a wide range of both organic and inorganic compounds with the cured organic polymeric binder often being the weakest link in the dry coating. These paints are applied in a multi-layered system, with each layer serving a particular primary function. Arguably the most important layer is the final clearcoat, sometimes referred to as the lacquer coat. In multi-coat systems (3-5 layer systems) it protects the lower layers from physical and environmental damage. This requires the clearcoat layer to have the supreme weather, chemical, abrasion and UV resistance, as well as high gloss.

Polyurethane(PU) formulations are often used as the clearcoat layer on a wide variety of transportation vehicles, structures and equipment. It is applied after mixing two components, labelled A & B, together. As with any two-part (2K) coating, the mix ratio of the two liquid components is critical to the final cure and performance of the coating. If the ratio is incorrect, surface wrinkling, tackiness,

and other physical defects can result, with the long-term performance potentially compromised. Remedial action/warranty claims are costly and their potential avoidance is discussed here using a hand-held 4300 FTIR and the external reflectance sample interface (45° specular).

In the industrial sector, automated or robotized spray guns are often used to apply paint prior to curing. Manufacturers need a quick and easy way to test whether the correct mix-ratio is being applied by the spray system to ensure the product passes subsequent QA/QC tests. An incorrect mix-ratio may result in remedial action at best and complete part scrappage at worst.

This study examined the use of a hand-held Agilent 4300 FTIR instrument (Figure 1) and a multi-variate calculation model to accurately and quickly quantify the component wet mix-ratio of a paint applied by a spray gun onto an aluminium coupon.

Figure 1. The Agilent 4300 FTIR instrument and the external reflectance sample interface, one of the many interchangeable interfaces available.

Experimental

The 2K PU used in this study was an industrial grade high-end OEM paint. It contains isocyanate blocking technology to ensure no appreciable reaction occurs in the mixed paint until the activation stoving temperature is reached or exceeded. Component B of the paint mainly contains the blocked isocyanate curative, designed to dissociate at a stoving temperature of 140 °C and then react with the polyol. Component A of the paint contains the aliphatic polyol formulation, additives and solvent. Aliphatic polyols are inherently more UV resistant than their aromatic counterparts.

As this particular paint formulation requires a stoving temperature of 140 °C, if the chassis of a vehicle is to be painted it must be free of all sundries that will not tolerate the elevated temperature. The stoving not only helps drive off the solvent but initiates a complex set of curing reactions.

A hand-held Agilent 4300 FTIR, fitted with the external reflectance sample interface (Figure 1), was used for all measurements. The interface allows the measurement of specular reflectance from the sample surface at 45° to normal. To prevent paint adhering to the instrument interface a small square of pierced sacrificial foil was placed over it. The foil was replaced for each measurement.

The external reflectance FTIR spectra of the samples were collected at 64 scans and 4 cm^{-1}, resulting in a spectral acquisition time of under 40 seconds.

First, the FTIR spectra of the two individual paint components, A and B, of the 2K PU paint were collected. Next, the spectra of the correctly mixed paint, applied to a coupon, was measured before and after the coupon received thermal stoving treatment.

Separately, the component mix ratio of the applied paint was quantified. Three more coupons were sprayed, each using a different ratio mix of the two paint components. FTIR spectra were measured at 10 sampling points per coupon. The paint component ratio mixes used are shown in Table 1. The ratios were calculated gravimetrically for higher accuracy rather than volumetrically.

Table 1. The two component paint ratio mixes that were applied to each plate.

Coupon No.	Part A	Part B
1 (Resin rich)	3.99	1
2 (Near correct ratio)	3.06	1
3 (Resin poor)	2.49	1

Results and Discussion

Measuring paint cure

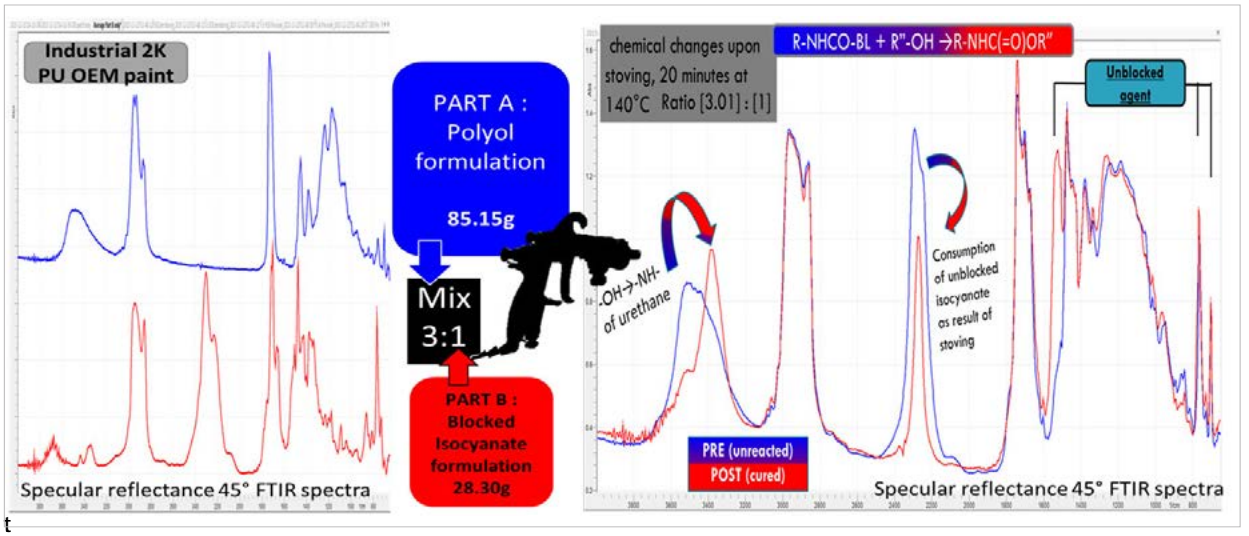

t

Figure 2. FTIR spectra of the samples. Left – component A (blue) of the 2K industrial PU paint and component B (red) curative of the 2K PU. Right – pre-stoving (blue-UNCURED) and post stoving (red-CURED).

The spectra, shown in Figure 2, were collected with the external reflectance sample interface, fitted to the Agilent 4300 FTIR instrument.

The two spectra on the left of Figure 2 identify the two component matrices of the 2K PU paint. The spectra are highly detailed with more than enough spectral information for the creation of a specular reflectance library. This could then be used to ensure the right paint mixture is allocated to the correct tank. The spectra could also be used as part of QA/QC to test for storage, delivery or composition changes.

The chemical changes during cure are both measurable and abundant, as shown in Figure 2, Right. The specified 20 minutes for the primary stoving period has introduced many spectral changes that are chemical changes directly related to the curing of the paint. The three main changes are highlighted in Figure 2. These changes have great potential to be used as part of QA/QC tests to determine the degree and quality of the paint cure.

Calculating component mix ratio

Using the spectra from the three sprayed coupons (shown in Figure 3, left), a model was created to calibrate the instrument in preparation to quantify the two paint components when mixed and applied. Using eight of the ten spectra from each sprayed coupon, the calibration model was created by applying a multivariate PLS1 (partial least squares) algorithm using Microlab Expert software. This model was then incorporated into the 4300 FTIR instrument. The remaining two spectra from each plate were used to independently validate the model.

The complexity of the spectra of the paint necessitated the use of the PLS1 chemometric technique. Its use has the advantage of greater robustness than empirical models as well as higher predictive ability. Warnings can be issued if a user attempts to apply the model to a different PU paint system than the one it was created for, preventing type 1 and type 2 errors. The model can also account for intra-sample variance. Earlier attempts at simple univariate- Beer-Lambert based models were unsuccessful.

The time taken to collect all 30 spectra in Figure 3 (left) was less than 20 minutes. Twenty-four of these spectra were used to create the quantitative model, with the remaining six used to validate the model post model finalization.

The average of each Mix-Ratio set of spectra per plate is shown in Figure 3 (Right). As shown in the figure, there are distinctive differences between the spectra of the different component ratios applied to the plates when averaged.

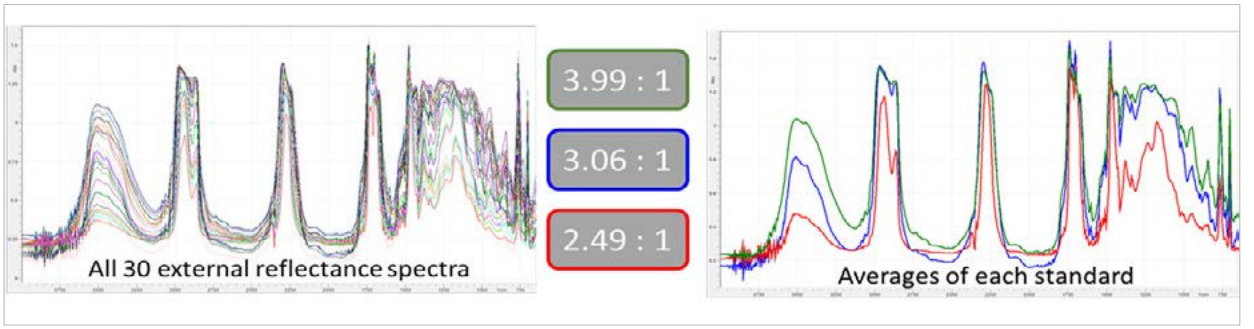

Figure 3. (Left) 3 x 10 external reflectance spectra of the three different ratios. (Right) The average of each 10 spectra, collected from the three coupons. The key to the color-coding of the spectra is shown to the left. Each individual spectra is the cumulation of 128 spectra ran at 4cm^{-1} resolution taking only 40 s per spectra.

The created PLS1 model was validated, using two randomly selected spectra of the ten obtained for each painted coupon. The model proved able to calculate the mix ratio of the applied paint to a high degree of accuracy. The actual mix ratio was plotted against the mix ratio calculated by the model, as shown on the left hand side of Figure 4. The graph shows impressive model statistics, with minimal pre-processing of a simple data mean centre resulting in excellent linearity, low calibration errors and low bias.

The right hand side of Figure 4 shows a visualisation of the model calculations. Spectra 1-10 were collected from the plate to which the paint component ratio 2.49:1 was applied. Spectra 11-20 were collected from the plate to which the paint component ratio 3.06:1 was applied and, finally spectra 21-30 were collected from the plate to which the paint component ratio 3.99:1 was applied. The ideal manufacturer's recommended ratio of this paint is 3:1 for A:B.

The PLS1 model demonstrated both excellent calibration statistics and validation statistics. Both the R and the R2 are better than 0.99 and the standard error of prediction (SEP) was very low at 0.036. This means the paint component ratio can be calculated by the model with 0.04 ratio confidence using a 6-factor PLS1 model.

The calculated paint component ratio value can be used to create a visual quality indicator to the user of the Agilent 4300 FTIR. Figure 5 shows three screen views. The one in the top left is an in-specification paint component ratio, coded green. The screen views in the top right and bottom are ratios that are critically out of specification and are displayed in red. The bottom screen view in Figure 5 also shows the critical low (low threshold) and high (high threshold) values, determined as the ideal component ratio ± 5%. These limits can be tightened or relaxed as per the paint manufacturer's recommendations or the user's specifications or experience with the product.

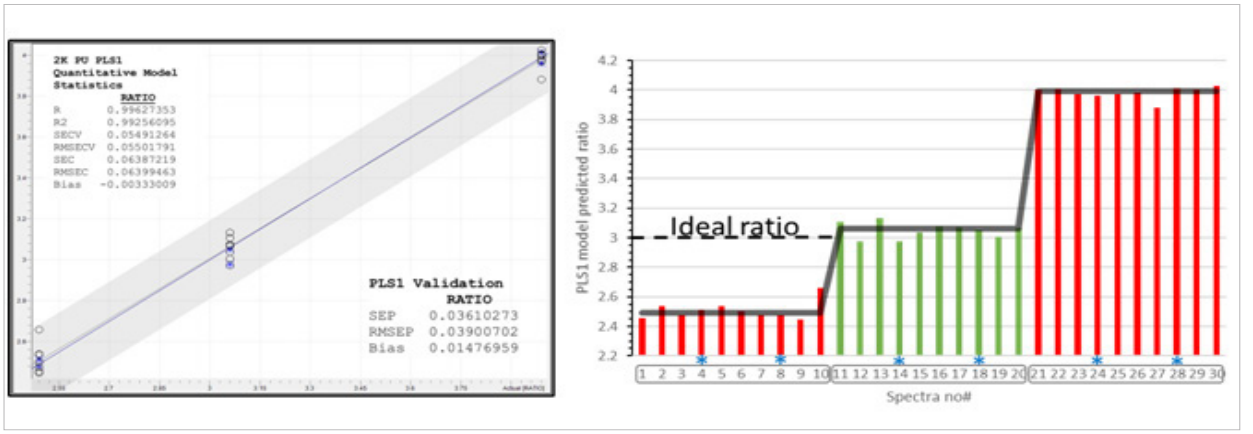

Figure 4. Left. Actual paint component ratios vs values calculated by the model. Right. The paint component ratio, calculated from 24 of the spectra collected. The asterisks (in both graphs) are the independent validation spectra that were not used to create the final model. The black dotted line indicates the ideal ratio of 3:1.

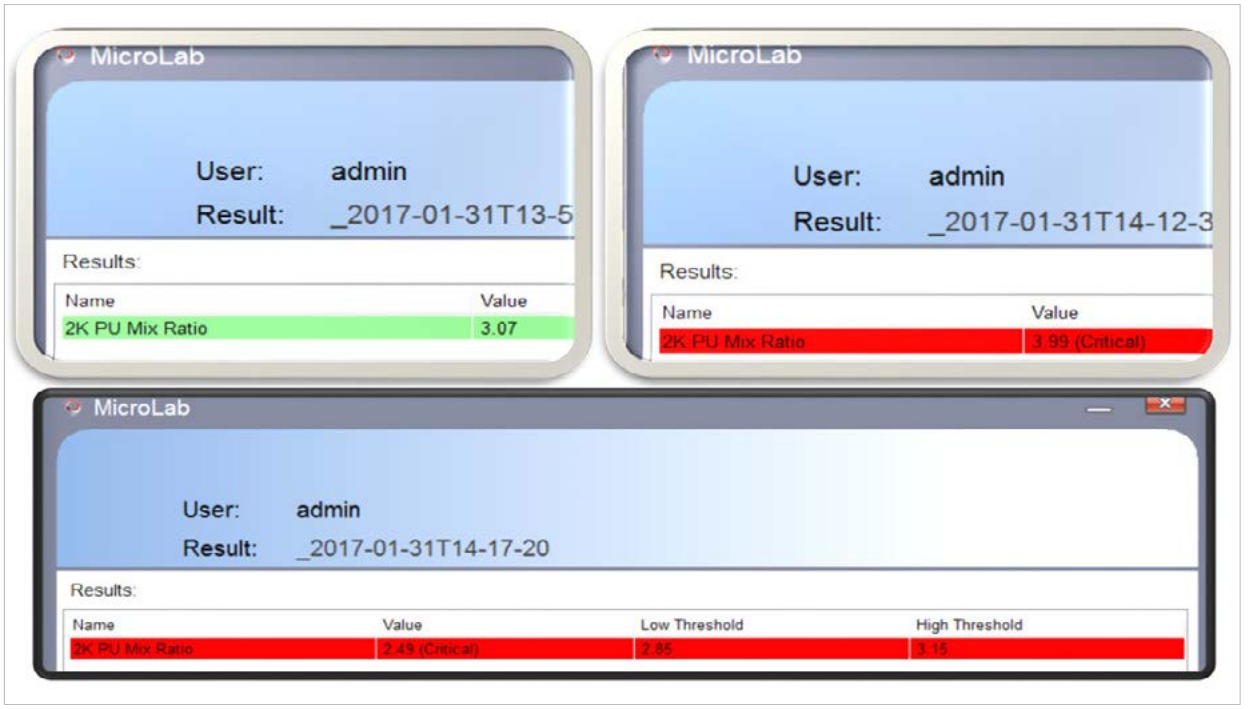

Figure 5. The visual display of the Agilent 4300 FTIR can display color-coded results, based on whether they are in or out of specification. Three example displays are shown here. (Top left). In-specification results are displayed in green. (Top right) Out of specification results highlighted in red (in this case, the resin rich sample). (Bottom) The specification limits can be adjusted in the method—this screens shows the upper and lower thresholds (flagging the resin poor sample).

Conclusion

FTIR spectra, collected with a hand-held Agilent 4300 FTIR instrument, have the potential to form the basis of a quick and accurate method of determining the cure level of a two component polyurethane paint. Spectra from the same instrument could also be used to identify paint component storage, delivery or compositional errors.

A multivariate partial least squares algorithm was used to develop a model for calculating the component ratios in a two component spray paint. Spectra collected from the paint, applied in three different ratio mixes to sample plates, was used to create and validate the model. Collection time for all the spectra needed to create the model was 20 minutes in total.

The model proved able to accurately calculate the ratio of the two paint components in the applied paint. The component ratio can be calculated by the model with 0.04 ratio confidence and has a predictive range of 2.5-4.0 for component A, where 3.0 is the ideal ratio.

The model can be incorporated into a method to be computed by the Agilent 4300 FTIR, combined with the Microlab PC software. Color-coding can be used to identify out of specification paint applications.

The combined instrument, method and user interface form a system that can quantify the as-sprayed paint component A:B ratio deposited onto a coupon in under 40 seconds. By testing the wet coating prior to painting an asset, incorrect mix-ratio application of the coating can be prevented at the point of delivery. This minimizes the risk of costly remedial action or warranty claims. The test can confirm that the paint is applied according to the manufacturer's design specification and that the spray equipment is correctly adjusted to apply the required component ratio. Models can also be created for manually mixed 2K paints and/or other chemical formulations using the same experimental protocol.

Comparison of Portable FTIR Interface Technologies for the Analysis of Paints, Minerals & Concrete

Application Note

Materials research and development

Author

Leung Tang
Agilent Technologies

Introduction

Fourier transform infrared (FTIR) spectroscopy is a well-established and powerful instrumental technique providing detailed spectra of a wide variety of samples. Even though FTIR is a mature technology, the best fit-for-purpose sampling interface can be often overlooked simply due to previous experiences and the ease of use of attenuated total reflectance (ATR).

Traditional benchtop FTIR measurement often requires some degree of sample preparation, moderate for transmission FTIR and often onerous for benchtop diffuse reflectance. In comparison, ATR FTIR measurements seem simple and quick.

Whilst ATR is a popular technique, it does have some drawbacks: Its short sampling depth means that spectral information is obtained only from the top few microns of the sample and the technique also requires intimate contact with the sample, meaning brittle and non-pliant samples may be damaged or break. ATR is really only suitable for flat, smooth, pliant samples.

An alternative to ATR measurements is diffuse reflectance. Agilent's 4300 hand-held FTIR instrument can be fitted with a range of different interchangeable interfaces, with a diffuse reflectance interface, a 45° specular reflectance interface and an ATR interface being three of the options. By simply changing the interface, the instrument can be used to study complex solids using multiple measurement modes.

The advantage of diffuse reflectance measurements is that they require no sample preparation requirements and are completely non-destructive to the sample. Diffuse reflectance spectra can be collected with or without direct contact with the sample surface. This is often requested for art and conservation projects where minimal contact is preferred. A diffuse spectra can in fact be collected with a 1-2 mm gap between the sample surface and the diffuse reflectance interface.

This study compares data obtained using three different FTIR measurement techniques: ATR, diffuse reflectance and specular reflectance (at 45°). Three different sample types: paint, geological samples and concrete were studied.

Experimental

An Agilent 4300 hand held FTIR (shown in Figure 1) was used for this study. It was fitted with one of three different interchangeable interfaces: an ATR interface, a 45° specular reflectance interface, and a diffuse reflectance interface. Sixty-four scans per spectrum were collected with each interface, using a resolution of 4 cm^{-1}. Each spectrum was acquired in under 40 seconds.

Figure 1. The Agilent 4300 hand held FTIR instrument, with the three interchangeable interfaces used in this study.

Three different sample materials were measured:

I. A dry modern white paint containing both inorganic (mainly pigment) and organic components (mainly binder),

II. A silicate based rock – 11 different locations on the surface of the rock were measured

III. Ordinary Portland cement based concrete, after a 60 day cure. It was made using a CEM I type binder with the requisite aggregate and admixture composition, resulting in a concrete with a minimum 30 day strength class of 42.5 N [5].

Results and Discussion

Analysis of paint with FTIR ATR & External Reflectance
Spectra of 14 different formulations of white acrylic paint on a cement fibre board substrate were collected with the ATR, 45° specular reflectance and diffuse reflectance sampling interfaces. The 14 formulations cover a wide price range, with varying quantities and types of additives and fillers in each formulation. The resultant spectra are shown in Figure 2. Only the diffuse reflectance spectrum contained enough detail to allow the discrimination of the different paint formulations [1]. The ATR spectrum (shown in red) did not contain enough detail to be used for this purpose.

Also shown in Figure 2 is the peak associated with the carbonate filler (at ~2500 cm^{-1}). This appears in the two external reflectance spectra, but is missing from the ATR spectrum.

During the measurements, the ATR technique required consistent sample contact for best results. This left a permanent depression in the paint samples. A high spectra-to-spectra variance was also observed across the ATR spectra.

Conversely, both the specular 45° reflectance and the diffuse reflectance measurements required a simple "point and shoot" method to be used. They could be used without applying force onto the sample, thereby enabling longer scan periods resulting in error-free data collection and preventing any damage to the sample surface. The spectra from the two external reflectance techniques were also highly reproducible, with minimal user-induced variance. A more detailed study describes the use of diffuse spectra to differentiate between coating formulations that differ only in additives and fillers [1].

As shown in Figure 2, there are many differences between the spectra collected with the different interfaces. The spectra have not been re-scaled or manipulated and it is obvious that the diffuse spectrum contains the most spectral information, followed closely by the 45° specular reflectance interface. The ATR spectrum contains the least detail.

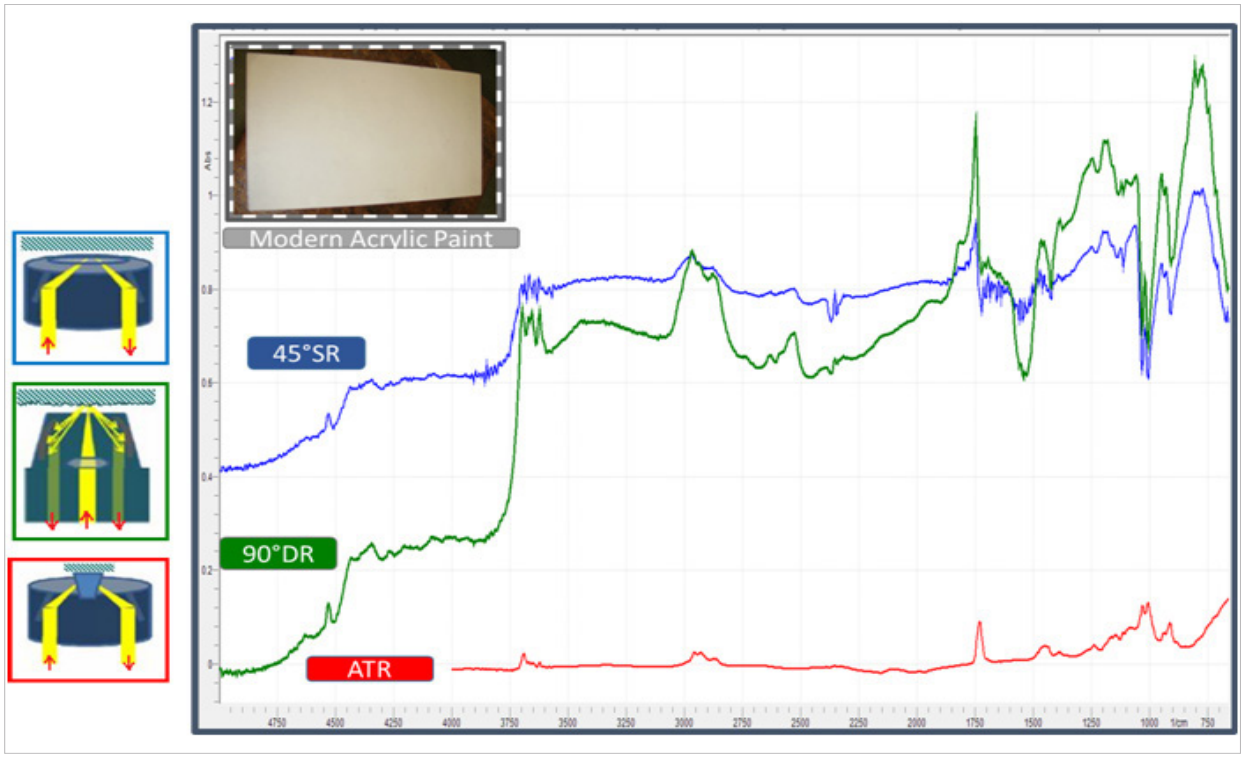

Figure 2. Spectra of a modern acrylic white paint collected by ATR (red), diffuse reflectance (green) and 45° specular reflectance (blue) interface FTIR measurement techniques. The left side bar illustrates the IR beam path of each interface type with color-coded box (red-ATR, green-diffuse reflectance & blue-45° specular reflectance)

The changes to paint that are induced by accelerated weathering has been studied non-destructively and in depth [2]. These changes are complex and the Agilent FTIR diffuse interface technique enables the same sample to be examined at intervals over the course of the ageing chamber regime. The portability of the instrument also potentially allows real-time studies of paint weathering. The more common ATR technique could be used but the requirement for surface contact could damage the sample, especially during the critical brittle failure stage of the coating's lifecycle.

Non-destructive FTIR analysis of geological samples

The sample three measurement techniques were also used to measure a geological monolithic silica based ore rock fragment, with the resultant spectra shown in Figure 3.

The ATR and specular reflectance techniques were unable to produce meaningful spectra. ATR failed due to the uneven surface of the rock sample. The rock sample had only a few point contacts for the ATR diamond, which was insufficient to collect meaningful data. An alternative would have been pulverisation of the rock prior to ATR measurements, but that would be expensive, time consuming and would have destroyed the sample. The 45° specular reflectance measurements failed due to the low reflectivity of the rock sample, which did not produce enough signal to be successfully measured by the instrument's detector.

As shown in Figure 3, the diffuse reflectance measurements of the rock sample were successful. The spectra show the primarily silicate nature of the mineral rock sample, with the peaks between 950 cm^{-1} to 1300 cm^{-1}. This is easily distinguishable from the smaller carbonate feature at 2500 cm^{-1}. There also detailed hydroxyl and resonant bands between 3,000 cm-1 – 4750 cm^{-1}.

The diffuse reflectance measurements required no sample preparation. All data was collected with an easy point and shoot manner using a Microlab PC method.

All eleven diffuse reflectance spectra of the rock sample were collected in under 10 minutes using standard instrumental conditions. Each spectrum was taken at a different location on the silicate-based rock sample. This provides information about the variation of the mineral

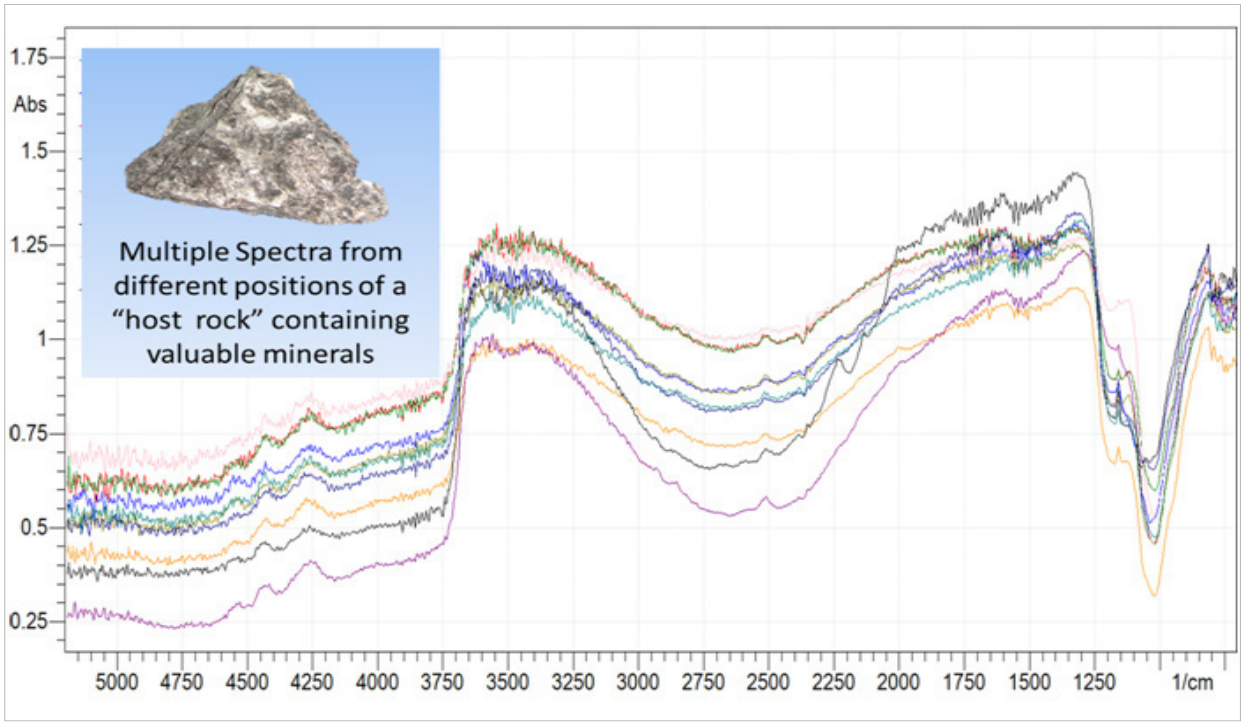

Figure 3. Diffuse reflectance spectra collected at 11 different locations on the surface of a geological monolithic ore rock fragment. Spectra were collected using an Agilent 4300 hand-held FTIR in conjunction with the diffuse reflectance interface option.

content across the rock's surface. The horizontal baseline shift is a result of the reflectivity differences across the sample, whereas the position of the peaks are directly related to the composition. The uneven, dull surface of the rock sample is ideal for diffuse reflectance measurements and incident light is widely scattered.

Hand held FTIR analysis of cured concrete

Modern concrete is by far the most commonly used construction material in the world today. It is available in a variety of grades and types, according to the presence or absence of specific additives, fillers and pozzolanic cement formulation used (the latter acts as the binder for the composite mixture). Handheld FTIR with a diffuse reflectance interface has successfully used for the non-destructive analysis of a geopolymer cement previously, effectively monitoring changes in composition and chemistry during cure [3].

The 4300 FTIR can also be used to differentiate between concrete blend types. It can even monitor the changes of these blends as a function of thermally induced chemical and physical changes and can correlate this to strength loss.

In this study, a concrete sample, cured for 60 days, was analyzed. The concrete consisted of a a composite mixture of a pozzolanic binder material and aggregates. After the addition of water, it cured to be a cross-networked solid structure interlocked with aggregates of various sizes. The complex pozzolanic cement reacts in an irreversible reaction with water forming a man-made rock. Modern concrete includes additives and aggregates, added to create various grades and types of concrete to suit specific building or engineering requirements [4].

The concrete's binder type was a CEM I type with the requisite aggregate and admixture composition resulting in a concrete with a 30 day strength class of 42.5 N [5].

We found that ATR measurements of the cured concrete sample were only possible if the sample was ground into a powder. This resulted in destruction of the sample, dilution of the concrete components and thermally induced changes. Measurements with the 45° external specular reflectance technique were not possible due to the very low reflectivity of the concrete sample.

To allow comparison of data collected with an ATR interface versus the diffuse reflectance interface, a sample of powdered concrete was measured with both. Figure 4 shows the resultant spectra. The diffuse reflectance spectrum was collected from the sample by simply pointing and shooting at the powdered sample. Collecting the ATR spectrum required drilling and subsequent ball-mill pulverisation of the drill

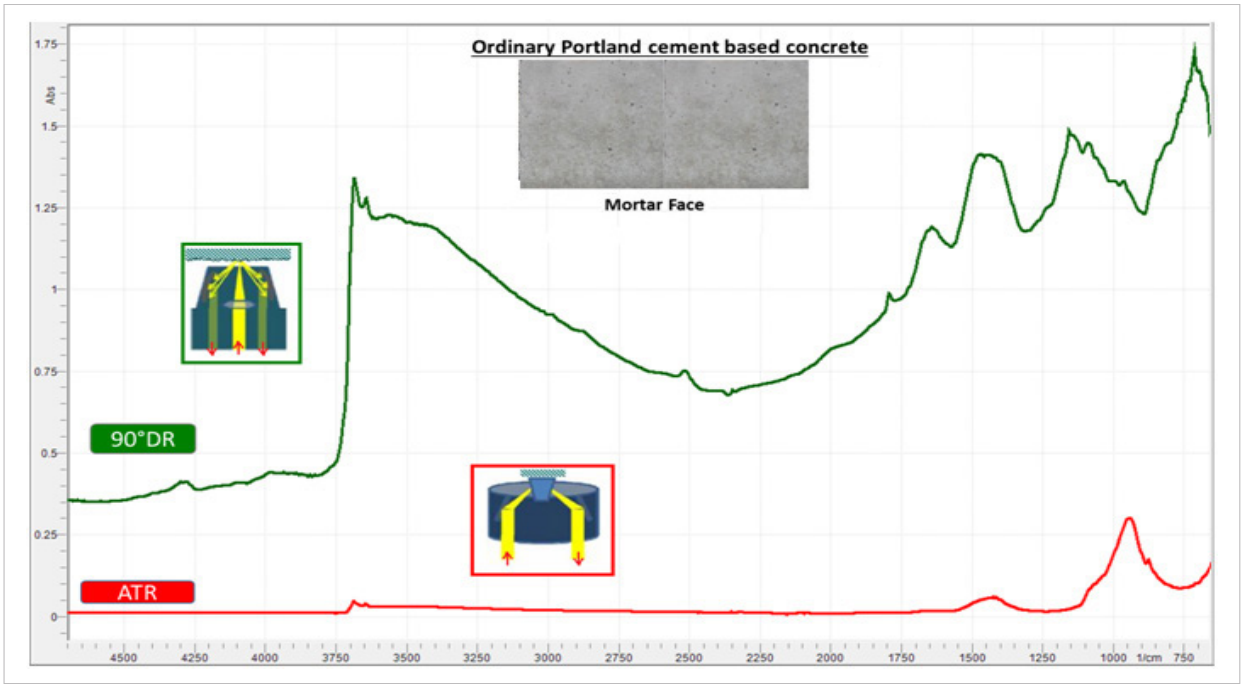

Figure 3. ATR spectra (red) of the powdered concrete and Diffuse Reflectance Spectra (green) of the mortar face of a concrete sample without any sample preparation.

debris semi-powder sample to achieve a particle size that would enable adequate intimate contact with the diamond ATR element. As shown in the figure, the diffuse reflectance spectrum contains more spectral information than the ATR spectrum. This is despite ATR measurements being the standard technique used for such analysis. The polished cross-section of the concrete samples shows visible aggregates as well as mortar (cured cement). The ingredient list of the concrete mixture is shown in Table 1.

Table 1. The material composition of the concrete block. By convention the 10/20 & 4/10 are called coarse aggregates and the 0/4 and 0/0.6 are termed the fines.

Ordinary Portland Cement (kg/m³)	Water (mL)	Aggregates—coarse & fines (mm)				Ad-mixture (mL)
		Sieved & sized Gabbro Rock (kg/m³)			Dune sand (kg/m³)	
		10/20	4/10	0/4	0/0.6	
380	152	702	378	630	297	2.66

A polished cross section contains mortar that acts as a binder for the aggregate fillers. The coarse fillers help bulk out and form a 3-dimensional network linked by cured cement, whilst the fines are designed to be void fillers. The aggregates are immutable in that during the cure they do not change at all, unlike the water, cement and ad-mixture which change markedly upon cure. The spectra of the light grey areas of the polished concrete are similar to those shown in Figure 4. Spectra of the aggregates and the dune sand show some marked differences due to their chemical and physical composition. The three sizes of gabbro aggregates were found on the polished section and their average spectra are shown in Figure 5, along with the dune sand. The collected reference dune sand spectra was not found in isolation on the polished cross section.

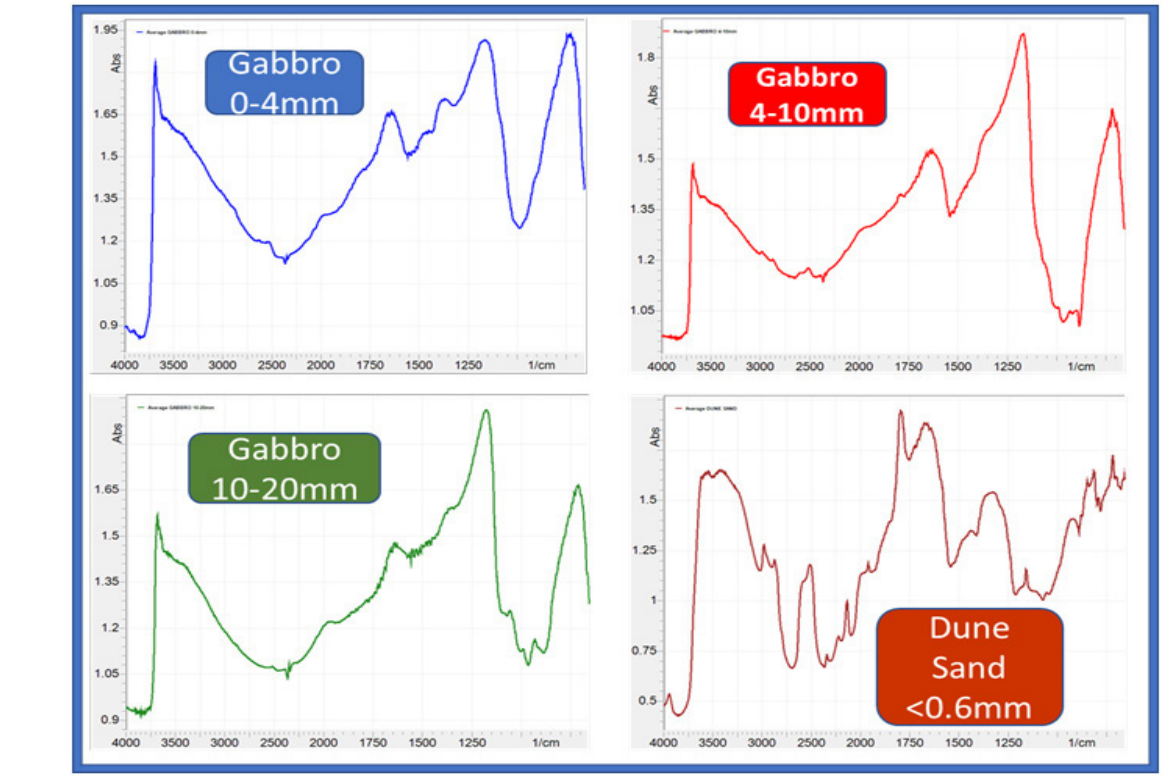

Figure 5. Diffuse FTIR spectra of the three different sized gabbro aggregates and the dune sand, all contained within a polished concrete sample.

Quantification of the thermally induced chemical and physical changes in concrete

In a separate set of measurements, diffuse reflectance spectra from 5 uncrushed/non-drilled concrete blocks were collected before and after thermal treatment. Non-destructive measurements were collected using the hand-held 4300 FTIR fitted with the diffuse reflectance interface option. Importantly, the measurements were done with no sample preparation or pre-treatment. The instrument was simply pointed at the face of the solid concrete samples.

Five concrete samples were created to investigate the changes that occur in the FTIR mid-infrared region. Each sample was cured for a full 60 days prior to being thermally treated at either 150 °C, 300 °C. 600 °C or 900 °C (one sample at each temperature). One of the samples was left untreated as a control. Full details of the study are available [4].

The diffuse reflectance spectra from the uncrushed concrete samples, collected after thermal treatment, are shown in Figure 6.

There are three notable changes shown in the spectra: First, the multiple peaks at 3600 cm^{-1} become one single peak after treatment at higher temperatures. Second, changes related to the carbonate in the sample can be seen to initially increase before complete removal at the highest temperature at 2500 cm^{-1}. This is in agreement with the decomposition temperature of calcium carbonate of ~840 °C. Thirdly, there are several structural changes related to the silicates and their forms, as evidenced by the shape changes in the fingerprint region ~1050-1300 cm^{-1} as well as region from 3,000-3750 cm^{-1}.

As the temperature changed, major differences in the spectra can be seen in the non-hydrogen bonded hydroxyl (~3600 cm^{-1} – several peaks), hydrogen bonded hydroxyl (3,000-3,400 cm^{-1}), carbonate (~2500 cm^{-1} & ~1750 cm^{-1}) and the reststrahlen inverted silicate regions (~1050-1300 cm^{-1}). These diffuse reflectance spectra correlate with TGA (thermal gravimetric analysis) and the thermograms are shown in the right. Note that the gabbro base aggregate fillers were highly carbonated with $CaCO_3$.

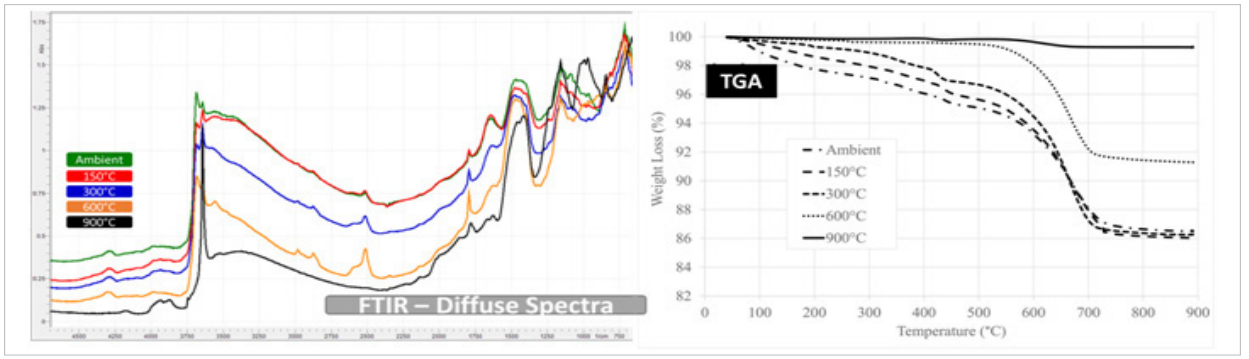

Figure 6. Left – diffuse spectra changes in a CEM I type concrete with gabbro rock aggregates at a variety of thermal treatments. Right the corresponding mass loss events for each concrete block post-thermal treatment.

Conclusion

The measurement of three different complex solids, using ATR, diffuse reflectance and specular reflectance measurement techniques revealed many differences in the data collection process and the resultant data:

- The Diffuse reflectance technique provided greater detail, higher repeatability and more in-depth information and sample penetration than ATR.
- Diffuse data collection was less prone to user error as there was no requirement for force against the sample surface.
- Thermal changes of a highly complex cement/aggregate network composite with thermal treatment revealed many measurable or quantifiable as well as identifiable changes that correspond directly with mass change events that could be elucidated without harming the sample in any way.

Contrary to popular belief and perception, the ATR technique performed poorly compared to the external reflectance techniques. The Agilent 4300 hand held FTIR instrument can be fitted with interchangeable interfaces, allowing the user to quickly change the measurement technique used. Diffuse Reflectance spectra can be collected with the instrument in-situ and without destruction of the sample and were found to have distinct advantages for paint, rocks and concrete studied here.

References

1. Positive and Non-destructive Identification of Acrylic Based Coatings – Agilent publication number 5991-5965EN
2. Coating Analysis: Non-Destructive Spectroscopic Modelling of an Industrial 2K Epoxy Resin Coated Panel Undergoing Accelerated Weathering as per ASTM G155 Protocol, Agilent publication number 5991-6976EN
3. M. Saafi, P. L. Tang, J. Fung, M. Rahman and J. Liggatt, Enhanced properties of graphene/flyash geopolymeric composite cement, *Cement and Concrete Research*, **2015**, 67, 292-299.
4. P. L. Tang, M. Alqassim, N. N. Daéid, L. Berlouis and J. Seelenbinder, Non-destructive Handheld Fourier Transform Infrared (FT-IR) Analysis of Spectroscopic Changes and Multivariate Modelling of Thermally Degraded Plain Portland Cement Concrete and its Slag and Fly Ash-Based Analogs, *Applied Spectroscopy*, **2016**, 70(5), 923-931
5. BS EN, 197-1: 2011. British Standard. Part I: Composition, Specifications and Conformity Criteria for Common Cements, 2011.

Mix Ratio Identification in Industrially Significant Two-Part Coating Systems Using the Agilent 4300 Handheld FTIR

Application Note

Quality Control in Coatings

Authors

Dipak Mainali and Alan Rein

Agilent Technologies, Inc.

Introduction

Protective coatings are commonly applied to automobiles, aircrafts, ships, railways, furniture, bridges, concretes, architectural constituents, industrial installations, and many other products that we encounter on a daily basis. Coating application in many of these products is primarily implemented to provide protection against harsh environments such as UV light, extreme temperatures, acid, alkali, salt, water, and so forth, and to improve the aesthetic appearance of finished products.

A wide variety of coating formulations exist in the market; their use depends on the performance requirement of the final product. Coatings may be applied to the products as a primer basecoat, a mid-coat, or as the topcoat. For example, polyurethane coating is applied on top of epoxy primer coating to prevent the discoloration of epoxy from UV and to provide the specified color and sheen.

Many of these coatings are packaged and supplied by the manufacturers as two-part systems, also known as two-pack or 2K. Coatings are also supplied as either single pack (1K) or even tri-pack (3K) systems. Two-part systems commonly consist of a reactive resin and a separate curing agent or hardener.

Manufacturers recommend proper mixing ratios of coating system components, either by volume or weight, before application to the product. To ensure the desired characteristics of the coating on the substrate, it is important to stay within the tolerated variability allowed by the mixing ratio. For some sensitive coating systems, small deviation from the recommended ratio will adversely affect performance.

Similarly, an incorrect mixing ratio can lead to product defects and irregularities. The effects of off-ratio mixing may not be readily apparent, but may show up after time, possibly leading to decreased coating performance or even premature coating failure depending on the degree of mixing error and the component. Cure agent-rich mixtures result in higher strength but also reduced impact resistance and higher probability of brittle failure, whereas resin-rich mixtures result in low strength. Both will affect the longevity of coatings on the product due to reduced performance, and can exhibit discoloration, inconsistent patchy gloss, blooming, cracking, and poor intercoat adhesion or stickiness.

This application note demonstrates that the Agilent 4300 Handheld FTIR system is highly effective for determining the mix ratio of two popular two-part coating systems: an epoxy primer and a polyurethane (PU) top coat. In addition, a simple two-coat system with epoxy as primer and PU as a top coat was also modeled. The mid-IR technique is ideal for monitoring the mix ratio because the components involved in each coating have their own distinctive spectra related to their chemical makeup and the degree of final cure. Furthermore, because of its exceptional portability and performance, the 4300 Handheld FTIR accomplishes this analysis wherever it is required. The method-driven, intuitive software and user interface enable users of widely varied experience to get rapid, highly accurate results.

Methods and Materials

Two-part marine grade epoxy and two-part polyester polyol saturated, aliphatic urethane coatings were obtained commercially. The recommended mixing ratio for the base (resin component) and the reactor (curing agent/hardener) was 1:1 by volume for epoxy and 2:1 by weight for polyurethane coating. A series of calibration and validation samples were generated by mixing the two-part coating system at the correct ratio as well as incorrectly (Table 1).

Table 1. Calibration and validation samples used for measuring mix ratio of two-part coating systems. The recommended mix ratio is highlighted in green.

	Polyurethane				Epoxy				Polyurethane on epoxy			
	Weight in grams								Weight in grams			
Steel panel	Part A	Part B	Actual ratio A/B	Target ratio A:B	Part A mL	Part B mL	Actual ratio A/B	Target ratio A:B	Part A	Part B	Actual ratio A/B	Target ratio A:B
Calibration sample												
1	10.50	2.22	4.72	2:0.40	17.05	8.83	1.93	1:0.5	11.93	2.82	4.24	2:0.45
2	10.20	2.70	3.78	2:0.55	14.95	11.23	1.33	1:0.75	10.00	3.36	2.98	2:0.65
3	10.21	3.34	3.06	2:0.65	15.28	15.33	1.00	1:1	10.85	3.96	2.74	2:0.75
4	11.06	5.63	1.96	2:1	17.40	21.61	0.80	1:1.25	7.59	3.78	2.01	2:1
5	10.15	5.86	1.73	2:1.15	9.56	14.47	0.66	1:1.50	11.03	6.74	1.64	2:1.20
6	10.23	7.07	1.45	2:1.35	14.33	25.19	0.57	1:1.75	9.17	6.58	1.39	2:1.45
7	10.38	9.36	1.11	2:1.80	11.74	23.38	0.50	1:2	7.22	6.78	1.06	2:1.9
Validation sample												
8	10.14	8.17	1.24	2:1.6	13.85	8.71	1.59	1:0.6	8.49	7.86	1.08	2:1.85
9	10.15	4.53	2.24	2:0.9	15.01	12.77	1.18	1:0.85	9.84	5.74	1.71	2:1.20
10	10.54	3.93	2.68	2:0.75	13.92	18.73	0.74	1:1.35	9.07	2.79	3.25	2:0.60

For both the polyurethane and epoxy coating systems, component B (curing agent) was varied to obtain different mix ratio compositions. The components were mixed and applied to the steel substrate within the pot life (working life) of the mixture. All other application conditions, such as induction time, temperature, substrate cleanliness, and dry time, were followed as specified by the manufacturer for each coating. Three types of coated coupons were prepared: polyurethane, epoxy, and polyurethane on top of epoxy.

The 4300 Handheld FTIR spectrometer with external and diffuse reflectance sampling interfaces was used for measuring the mix ratio of coating systems painted on a steel panel. The measurement was taken after the paint was left to air-dry overnight. Each spectrum was a result of 64 co-added scans at 4 cm^{-1} resolution, yielding a total measurement time of 26 seconds. The measured spectral range was 4,000–650 cm^{-1}. Five different spots were analyzed on each painted steel panel at each mix ratio. A calibration model based on Partial Least Squares (PLS) regression was developed using the mean centering and multiplicative scatter correction as the preprocessing algorithm.

Results and Discussion

Figure 1 shows the PLS calibration plots showing the actual versus predicated value for each coating mix ratio. The minimum number of factors yielding a correlation coefficient of R^2 greater than 0.99 was chosen for each calibration plot; 5, 6, and 4 factors were required for polyurethane, epoxy, and polyurethane on top of epoxy coatings, respectively. The number of factors used in each model also ensured the higher prediction accuracy on the validation sample, as shown in Table 2.

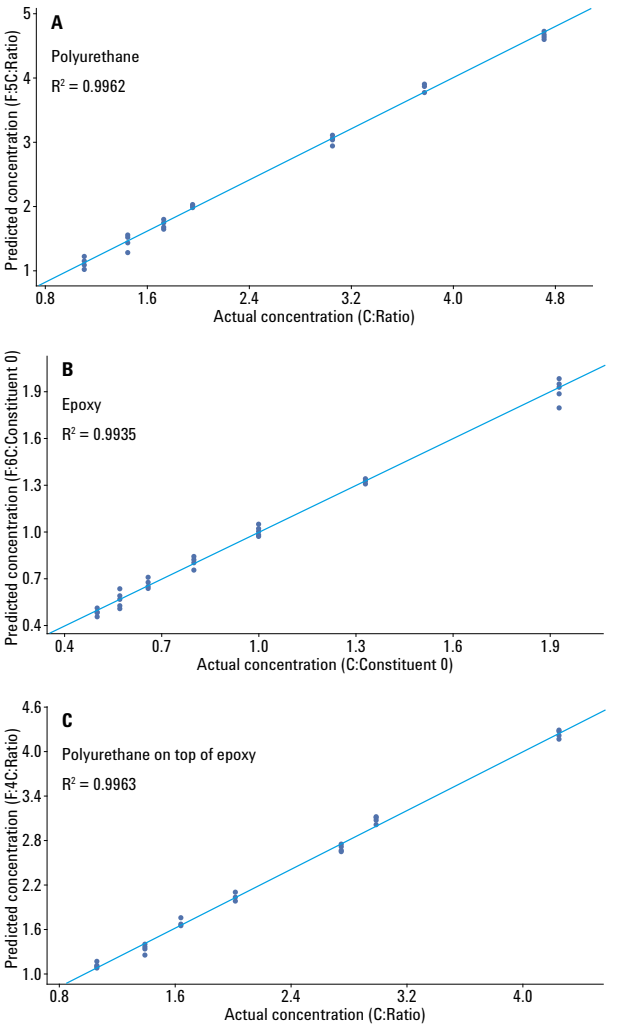

Figure 1. Calibration model obtained for different mix ratios of two-part coating systems (polyurethane, epoxy, and polyurethane on top of epoxy), developed using the PLS algorithm.

Table 2. Predicted mix ratio of validation samples using the PLS model for each coating.

Polyurethane			Epoxy			Polyurethane on Epoxy		
Actual	**Predicted[1]**	**% Difference**	**Actual**	**Predicted[1]**	**% Difference**	**Actual**	**Predicted[1]**	**% Difference**
1.24	1.24 ± 0.2	0.17	1.59	1.65 ± 0.16	3.77	1.71	1.65 ± 0.04	3.51
2.24	2.21 ± 0.04	1.34	1.18	1.21 ± 0.02	2.54	1.08	1.13 ± 0.04	4.63
2.68	2.46 ± 0.02	8.21	0.74	0.74 ± 0.02	0.41	3.25	3.24 ± 0.16	0.31
Average % error		3.24		2.24		2.82		

[1] Average value of five measurements taken on five different spots of the steel substrate panel ± two standard deviations.

Figure 2 shows the spectral region used to build the calibration model for the polyurethane coating system. Since the amount of component B (curing agent) was varied, the spectral band in the region ~2,100–2,400 cm^{-1} due to aliphatic polyisocyanate moiety was altered (Figure 2). The band intensity positively correlated with the increase in component B (that is, with the decrease in mix ratio).

Figure 3 shows the spectral region used to build the PLS calibration model for the epoxy coating system. Notable bands and spectral features that correlate with the mix ratio are in the 1,650–2,200 cm^{-1} and 1,600–800 cm^{-1} regions.

Although only measurements made using the external reflectance sampling interface are shown here, the diffuse reflectance interface yielded similar results. For example, the average percent error on mix ratio prediction of validation samples for polyurethane, epoxy, and polyurethane on top of epoxy were 3.24, 2.24, and 2.82, respectively (Table 2) using the external reflectance interface, whereas the average error was 4.83, 4.82, and 0.81, respectively, for the same samples when the diffuse reflectance interface was used.

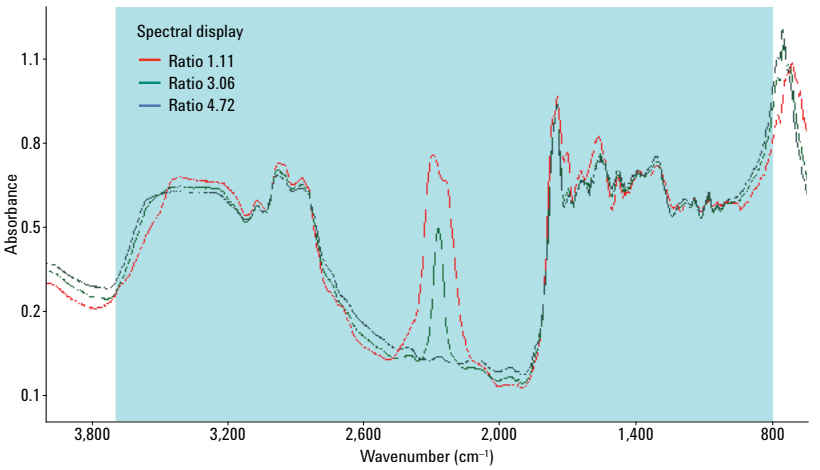

Figure 2. External reflectance IR spectra of three different mix ratios of polyurethane coating. The region highlighted in blue was used for the PLS calibration model.

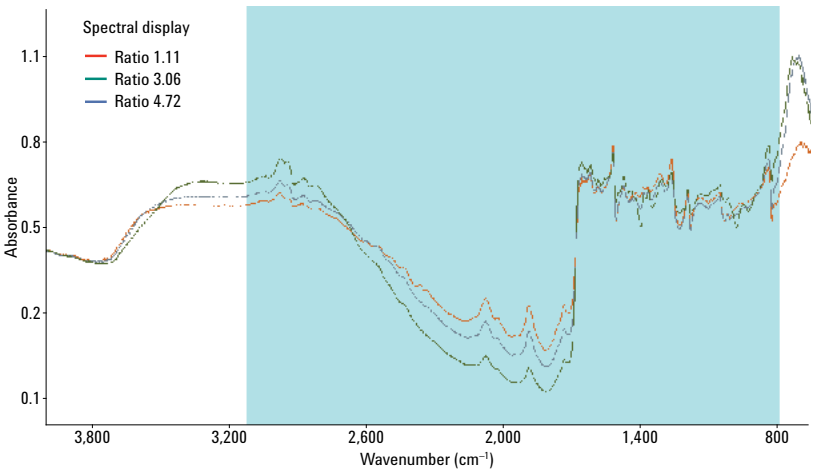

Figure 3. External reflectance IR spectra of three different mix ratios of epoxy coating. The region highlighted in blue was used for the PLS calibration model.

Conclusion

This project shows that the Agilent 4300 Handheld FTIR successfully identifies the mix ratio in 2K coatings and in a two-coat system. The instrument and accessory used here can be easily extended to identification of the mix ratio in other formulations, or the degree of cure for single- or two-component cure systems.

Excellent results are obtained using either the diffuse or external reflectance sample interfaces, depending on the coating system formulation and the painted substrate. For coating finishes on reflective metal surfaces such as steel or aluminum, the external reflectance sample interface is the better choice; for coatings with higher amounts of fillers or those applied to surfaces with minimal light reflection, the diffuse reflectance sample interface is the preferred approach.

The 4300 Handheld FTIR enables virtually instantaneous determination of the mixing ratio, helping to ensure that coatings meet their performance specifications and longevity requirements. Furthermore, the portable, handheld system enables these determinations where and when needed, whether in a laboratory environment or at the physical site where the coating is in use.

Agilent 4300 Handheld FTIR

Lightweight: At 2.2 kg (4.8 lb), the 4300 Handheld FTIR is ideal for mid-IR measurements in the lab, out of the lab, wherever and whenever needed.

Balanced: With a center of gravity located at the handle, the system is comfortable to use with less physical strain, allowing for more accurate and precise measurements.

Rapid scanning: Scan large surface areas in less time. With the optional MCT detector, the 4300 Handheld FTIR enables measurements to be made more rapidly.

Nondestructive: No need to excise a sample for later analysis in a lab—this handheld spectrometer is brought to the object or surface to be measured.

Immediate results: Focus on the measurement locations of greatest importance. At-site analysis lets you make decisions in real-time.

Intuitive: Easy-to-use software guides less experienced personnel to actionable results faster. Preprogrammed methods powered by advanced mathematical models, and advanced reporting features all function automatically behind the scenes.

The 4300 Handheld FTIR comes with the choice of interchangeable, permanently aligned sample interfaces. Two sampling interfaces are used in this application:

1. **External reflectance interface**
   - Allows the analysis of films and coatings on reflective metal surfaces such as aluminum or steel
   - Used for the analysis of smooth, opaque samples where infrared light reflects off the surface
2. **Diffuse reflectance interface**
   - Used when sample reflects little light
   - Provides excellent results for a wide variety of samples, including surface coatings with higher amount of fillers

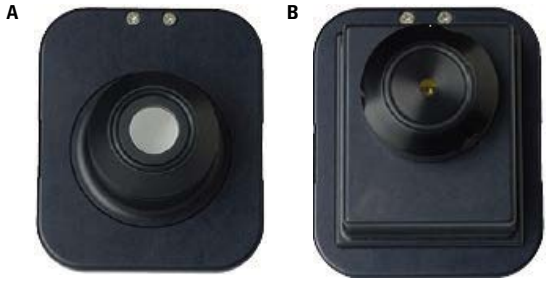

Figure 4. A) External reflectance interface and B) diffuse reflectance interface for the Agilent 4300 Handheld FTIR.

For More Information

These data represent typical results. For more information on our products and services, visit our Web site at www.agilent.com/chem.

Agilent 4300 Handheld Portable FTIR

Coatings Analysis: Non-Destructive Testing (NDT) of an Industrial 2K Epoxy Resin-coated panel undergoing accelerated weathering using the ASTM G155 protocol

Application Note

Authors

Leung Tang and Alan Rein

Introduction

It is crucial to understand the effect of environmental factors on the performance and lifecycle of paints, coatings, and protective films. One means of accomplishing this goal is to use aging chambers designed to accelerate and control the key parameters. This application note used the Agilent 4300 Handheld FTIR in conjunction with the most common class of aging chamber, called a weatherometer, to measure changes in an industrial 2K epoxy resin finish paint formulation coated onto an industry-standard Q-coupon. We show that the FTIR diffuse spectra effectively detect subtle chemical changes in the coatings as a factor of exposure time and conditions. To accomplish this work, a single Q-panel was weathered, and replicate diffuse reflectance spectra were recorded at intervals of 0, 3, 6, 10, 14, 21, 28, 35, 42, 49, and 56 days. The aging chamber was paused for 10 minutes to allow for multiple measurements of the panel before re-engagement of the weathering cycle.

Figure 1. Agilent 4300 Handheld Portable FTIR (Fourier Transform Infra-Red) spectrometer and the selection of available interfaces.

The 4300 Handheld FTIR coupled with the diffuse interface is particularly well-suited for this application since it enables the coated coupon to be Non-Destructively analyzed, thus enabling the remeasurement of a single coupon over the weathering period. The collected data can then be statistically analyzed using the multivariate analysis technique called partial least squares. Information gleaned from this work can be correlated to handheld FTIR measurements in a field-based, outdoor weathering farm with the potential to monitor batch performance or formulation potential.

Key benefits for paints and coatings analysis

Chemical information on coatings

The Agilent 4300 FTIR technology yields detailed chemical information on virtually all coating ingredients including binders, extenders, solvents, and additives, as well as the vast majority of organic or inorganic pigments and fillers. The diffuse IR spectra contain features directly related to changes in the coating as a function of weathering, both in the enclosed weathering chamber, or in an outdoor real-time weathering test facility. For this application, both ATR and diffuse interfaces were assessed. Only the diffuse interface was able to provide the data quality, data consistency, and true Non-Destructive analysis required. Therefore, only the diffuse interface results will be discussed in this application note.

Fast, Non-Destructive sample measurement

Each measurement takes <30 seconds (64 scans, 8 cm^{-1} resolution), and no sample preparation is required. Since the panel is measured directly and Non-Destructively, the same panel can be re-examined, thus eliminating the burdensome, costly need for a large set of samples to cover the testing intervals required by conventional destructive testing. This also eliminates errors introduced by using multiple panels.

Intuitive and readily field portable

The 4300 Handheld FTIR system weighs only 2 kg. The software and on-board methods allow less experienced users to get reliable results and rapidly become proficient. The ruggedness and ergonomics of the 4300 Handheld FTIR makes it ideal for supporting R&D and QA/QC efforts, as well as for on-site measurements of coated items regardless of size, including bridges, buildings, transportation vehicles, and so forth.

Figure 2. Two-part industrial epoxy resin finish coating sprayed onto a Q-panel, showing the visible effects of accelerated aging in a weatherometer before (unaged, top) and after 56 days (bottom: visible pin-holing).

Results and Discussion

Simulated weathering

An industrial-grade, 2K epoxy resin formulation coating was assessed in a weathering chamber. The conditions were adjusted according to ASTM G155.

Parameter	Value
Light intensity	55 W/m^2 at 340 nm
Black panel temperature	70 °C
Air temperature	47 °C
Humidity	50 %
Continuous 2-step cycle (see Figure 3)	

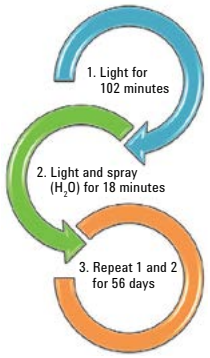

Figure 3. Two-step cycle used in the weathering process. The conditions are the environmental equivalent to sunlight at zenith at Florida's latitude and longitude. The acceleration of changes arises as the sun is not allowed to set for the whole test regime.

The chemical changes that occur during the accelerated weathering test regime (0–56 days, 11 intervals, A-K) are initially subtle, with little performance loss. With an increasing dose of light radiation and moisture, the changes are not only greater, but also begin to affect the performance of the material. For visual clarity, some of the complex changes on a reduced set of the data is shown; note there are numerous areas that change, and some of these are displayed in Figure 4.

- Induction period changes (mild, mainly chemical): 0–21 days
- Mid-term period changes (significant, both chemical and physical changes): 21–35 days
- End-of-life changes (extensive), where physical changes dominate and environmental stress cracking is evident: 35–56 days

Two individual multivariate partial least squares (PLS) models were developed to cover the induction-to-medium-term, and medium-to-long-term (Figure 5) cases.

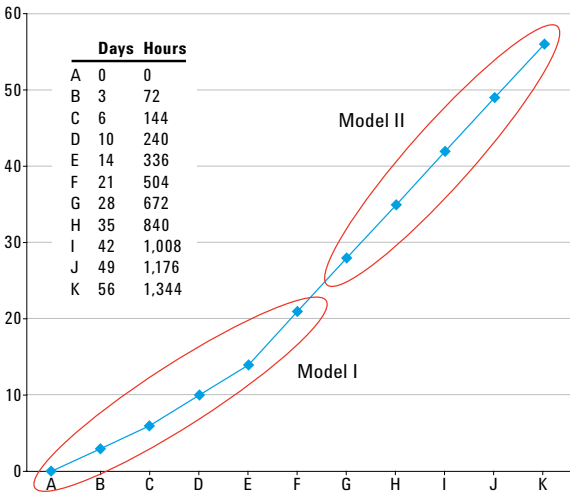

Figure 5. FTIR PLS Model I covers changes in the induction-to-middle exposure period. Model II covers the changes in the medium-to-end-of-life exposure period.

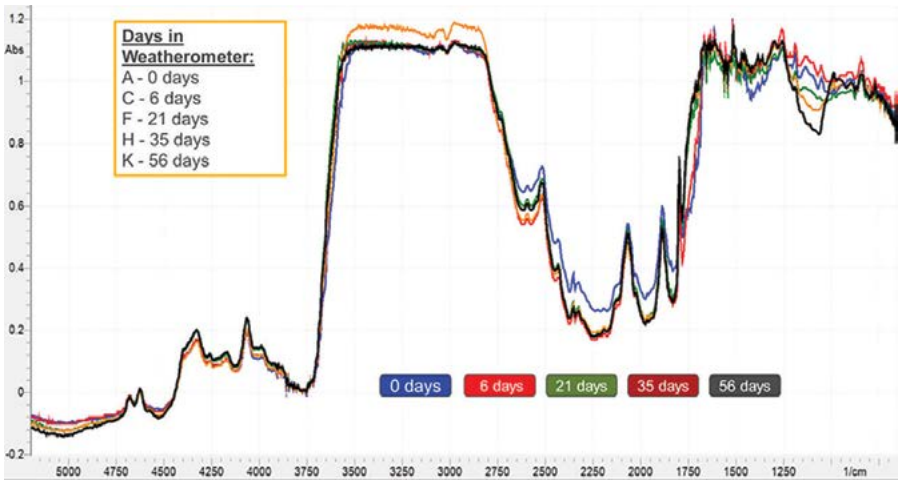

Figure 4. Selected diffuse spectra showing the different chronological changes.

The collected >100 spectra were split into calibration training data and validation data (80:20). The resultant PLS models for the industrial two-part epoxy paint finish (Figure 6) demonstrate high linearity and predictive ability.

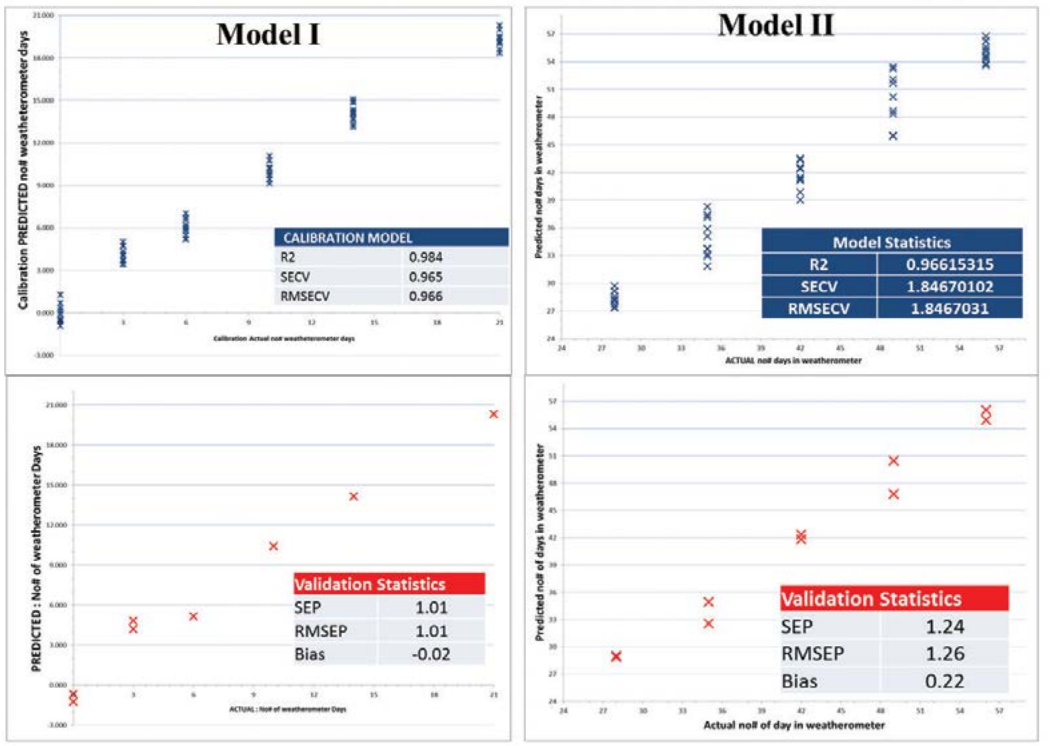

Figure 6. Model I, 0–28 days, and Model II, 28–56 days calibration (top left and right), and independent validation (bottom left and right) actual versus predicted plots.

Conclusion

We used a weatherometer-class aging cabinet and an Agilent 4300 Handheld FTIR in a 56-day accelerated aging study of an industrial 2K epoxy paint finish. This work provides an understanding of the IR spectral response to weathering a baseline coating formulation. Both chemical and physical changes invisible to the naked eye were elucidated by means of analysis of the spectra. By changing various constituents of the coatings matrix, the performance of different formulations were tested, or individual additives and their effects targeted. As a consequence of our Non-Destructive sample analysis using the handheld FTIR, only one coupon was needed for each formulation. Therefore, the performance of many different formulations were ascertained in one complete aging cycle, within the confines of a single cabinet. Moreover, other types of aging chambers specifically designed for high temperatures, outer space, aggressive chemicals, corrosive environments, salt water, and their combination would equally benefit from this type of Non-Destructive spectroscopic information-rich analysis and modeling.

In summary, we have shown:

- Successful model creation and validation using an Agilent Cary 4300 Handheld FTIR system for the accelerated aging of an industrial grade epoxy coating (Model I: 0–28 ±1.01 days, Model II: 28–56 ±1.25 days)
- Changes in the diffuse reflectance IR spectra that cover the 0–56 (accelerated) days aging regime. Similar changes can be applied to other coating types, glossy or matt
- A means for practical condition monitoring of in-service paint to end-of-life state, which can aid in prolonging performance of the underlying asset
- The opportunity to quickly examine whole sets of potential formulations in a standard weathering cabinet to ascertain the composition most resistant to chemical change
- The ability to discern subtle, initial chemical changes that can improve test cycle times for in-lab weathering studies or in-field, real-time testing
- The ability to monitor long-term real-time aging studies *in-situ* Non-Destructively with the choice of increasing the sampling intervals to suit the spectral, chemical, and physical changes without sacrificing actual painted coupons

For More Information

These data represent typical results. For more information on our products and services, visit our Web site at www.agilent.com/chem.

Positive and Nondestructive Identification of Acrylic-Based Coatings

Using Partial Least Squares Discriminant Analysis with the Agilent 4300 Handheld FTIR

Application Note

Materials Testing and Research

Authors

Dipak Mainali and Leung Tang

Agilent Technologies, Inc.

Introduction

Acrylic-based coatings are produced in formulations to suit all the major markets within the coatings industry. Industrial, decorative, printing inks, powder, and wall coverings are some of the market areas where acrylic-based coatings are widely used. Water emulsion and film-forming acrylic-based coatings are of particular importance due to their relative high performance and extremely low volatile organic compound (VOC) emissions.

To ensure performance and longevity, it is critical to properly apply the correct acrylic coating in the substrate. Equally important is the ability to assess changes in the chemical composition of the coating under actual use. For this reason, a portable analyzer is of great interest to engineers who are responsible for ensuring that coatings meet their performance claims.

In this application note, we used the Agilent 4300 Handheld FTIR (Figure 1) to analyze 14 industrial acrylic coatings that have the same binder type and similar chemical composition. First, we used an extended library method to identify the acrylic coatings. However, the library search method was not sensitive enough to clearly distinguish between similar coatings. To clearly separate these we used a partial least squares discriminant analysis (PLS-DA) multivariate classification method for more sensitive discrimination of the coatings, since they have similar binder types. We combined the PLS-DA algorithm with unique Agilent MicroLab PC Component Reporting to provide precise identification of each acrylic coating.

Figure 1. Agilent 4300 Handheld FTIR spectrometer with external reflectance (diffuse and specular) and internal reflectance (ATR) sampling interfaces. Interfaces can be changed in seconds, with no realignment required.

Experimental

The acrylic coatings were individually spray-coated onto separate 4 × 9 inch Q panels (~10 × 23 cm), and 10 spectra were collected randomly from each panel. Acquisition of multiple spectra across the coating was important to account for paint inhomogeneity and paint application variance. To develop the library for each acrylic coating, eight of these randomly collected spectra were used to populate the library, and the remaining two spectra were used as the test unknowns.

The 4300 Handheld FTIR spectrometer, coupled with a diffuse reflectance interface, was used to measure the 14 proprietary acrylic coatings (labeled A to N) using spectral acquisition conditions of 128 co-added interferograms at 8 cm^{-1} resolution from 5,200 to 650 cm^{-1}. The total spectral measurement time was less than 40 seconds per spectrum. Similar measurements were collected using the 4300 FTIR equipped with the attenuated total reflectance (ATR) sample interface for comparison.

Library searches were carried out using the software similarity match algorithm of the 4300 FTIR MicroLab PC. PLS-DA calibration models were developed using eight spectra for each acrylic coating out of 10 collected spectra. The two spectra that were not included in building the PLS-DA model were used as test spectra to assess the final MicroLab method for coating identification. For each calibration model development, spectra were preprocessed using mean centering, multiplicative scatter correction, and a nine-point Savitzky-Golay first derivative.

Results and Discussion

The diffuse reflectance spectra of 14 acrylic coatings were used to build the library of coatings, and also to perform PLS-DA classification. Diffuse reflectance measurement is preferred since more spectral information related to binder, pigment, and additives is obtained as a result of the higher penetration of the IR beam into the coating, as compared to surface-sensitive ATR measurement (Figure 2). In addition, diffuse reflectance measurement of coatings is nondestructive and highly reproducible, compared to ATR measurement.

The library method for coating identification was developed using a similarity search algorithm in the MicroLab PC software. The library search results for the test spectra for each coating are shown in Table 1. The library was constructed by multiple entries of spectra per coating. The primary hit group (1st, best matching, A) and the secondary hit group (2nd, best matching, E) are listed in the library hit column. Figure 3 displays the advantages of having multiple entries where the hit quality value for the primary group and the secondary group ranges from 0.99986 to 0.99952 and 0.99134 to 0.99045, respectively.

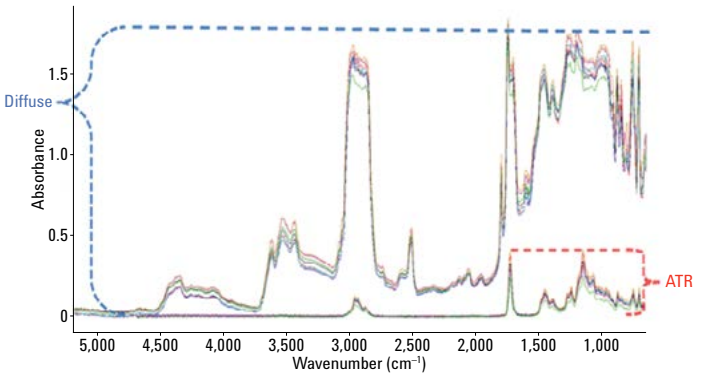

Figure 2. ATR and diffuse reflectance spectra of the same acrylic-based paint A. The diffuse reflectance spectra provide more information from overall stronger absorbance bands, as well as the ability to record bands that are too weak to observe by ATR. The maximum absorbance for the diffuse reflectance and ATR are indicated by the blue and red lines, respectively.

Table 1. Fourteen Acrylic-based Coatings, A to N, and Their Primary and Secondary Hit Sets

Coating	ID	Library hit	Coating	ID	Library hit
A	✓	1st = A, 2nd = E	H	✓	1st = H, 2nd = D
B	✓	1st = B, 2nd = A spectra 8, C	I	✓	1st = I, 2nd = F
C	✓	1st = C, 2nd = A spectra 8, E	J	✓	1st = J, 2nd = D
D	✓	1st = D, 2nd = J	K	✓	1st = K, 2nd = I
E	✓	1st = E, 2nd = A	L	✓	1st = L, 2nd = C
F	✓	1st = F, 2nd = I	M	✓	1st = M, 2nd = A
G	✓	1st = G, 2nd = A	N	✓	1st = N, 2nd = G

Note that a green tick was attributed only if both test spectra gave correct positive identification of coating type. For coatings B and C, a single spectrum (A, spectra 8) separated the groups.

The individual spectral primary hit quality value in all cases was better than >0.998 for both test spectra when checked against all 14 acrylic-based coatings in the library. The top eight library search results for two test spectra for each coating formulation A to N indicated the correct match. In all cases, the next best hit (that is, the 9th ranked hit) was not the correct coating, and the hit quality value ranged from 0.892 to 0.997. In some cases, the secondary hit quality value was as high as 0.997, indicating that the library search result may not be sufficient for the proper identification of the coatings with high confidence, especially when the hit quality values differ very slightly between the correct and incorrect match-coating results. Therefore, for the coatings with similar chemical formulations, a more rigorous statistical analysis method is needed to gain confidence on identification of the correct coating.

Multivariate discriminant analysis techniques, which capture more spectral variance than library search algorithms, are needed to provide confidence on coating identification of similar formulations. Multivariate analysis methods (MVA) are used both to discriminate (qualitative analysis), and to measure the extent of processes (quantitative analysis) such as degree of cure, days in a weatherometer, or even amount of trapped solvent remaining in an analysis of coating-plus-mixture ratios.

We have examined both the PCA and PLS-DA approaches and, though both are effective, we implemented the latter method in the 4300 FTIR MicroLab PC software. PLS-DA is considered a more sensitive discriminant analysis technique compared to PCA when separating spectra that are nearly identical. PLS-DA is a supervised classification technique where the analyst assigns an arbitrary membership value to each group of spectra, which are used for classification. Once values are assigned to define a class, the calibration model is developed in a similar manner to building a PLS quantitative calibration model. Finally, after a calibration plot is obtained, a threshold y-value is chosen from the PLS plot to classify the groups based on their distribution profile. The calibrated classification model can then predict the identity of the unknown samples relative to one of the defined classes.

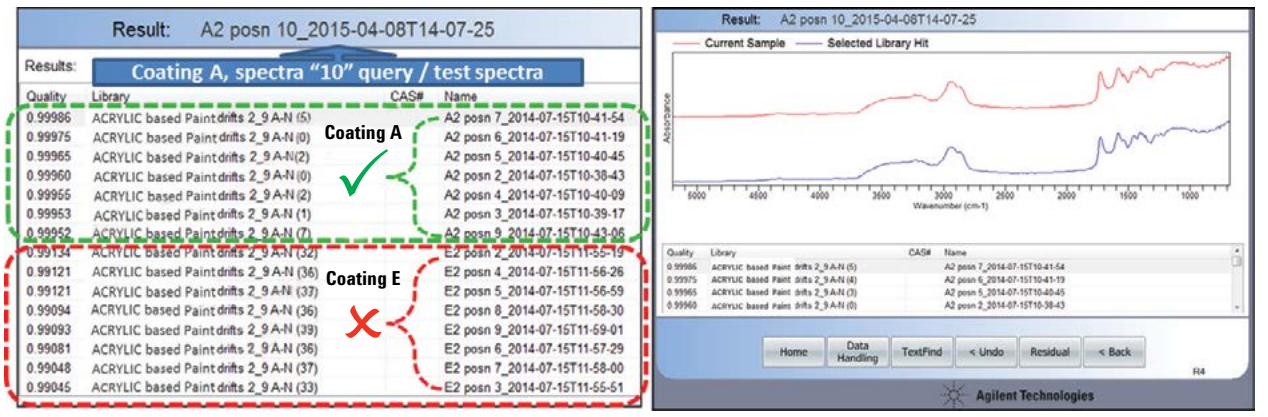

Figure 3. Library search results with hit quality value of acrylic coating type A test spectra (left); spectrum of test sample (red) and best match from the spectral library (blue) (right). Note: A2 = coating A by diffuse and posn. 10 = 10th position on Q-panel.

Eight spectra, collected from eight different spots of the painted Q panel, were used to represent the individual acrylic-based coatings while building the PLS-DA models. Five PLS-DA calibration models were needed to obtain proper classification between the 14 coatings. The calibration models were developed sequentially to have well-defined separation between the groups of spectra for each coating. The calibration parameters obtained for each calibration model are shown in Table 2. Based on the visual spectral similarity, the 14 acrylic coatings were first divided into three groups. The first group consisted of spectra representing D, H, J, and M coatings, the second group of spectra of A, B, C, E, F, G, I, K, and L coatings, and third group of spectra of coating N (Figure 4). As an example (Figure 4), the first calibration model was able to classify coating N from the rest of coatings.

Table 2. PLS-DA Calibration Model Parameters

Calibration model	R^2	No. of factors required	Arbitrary value assigned for each coating group	Coatings separated
1	0.984	6	[D, H, J, M] = "0" [A, B, C, E, F, G, I, K, L] = "1" [N] = "2"	N
2	0.997	3	D = "0", H = "1", J = "2", M = "3"	D, H, J, and M
3	0.994	5	[A, B, C, E] = "0" [F, G, I, K, L] = "1"	[A, B, C, E] and [F, G, I, K L]
4	0.999	3	A = "0", B = "1", C = "2", E = "3"	A, B, C, and E
5	0.998	4	F = "0", G = "1", I = "2", K = "3", L = "4"	F, G, I, K, and L

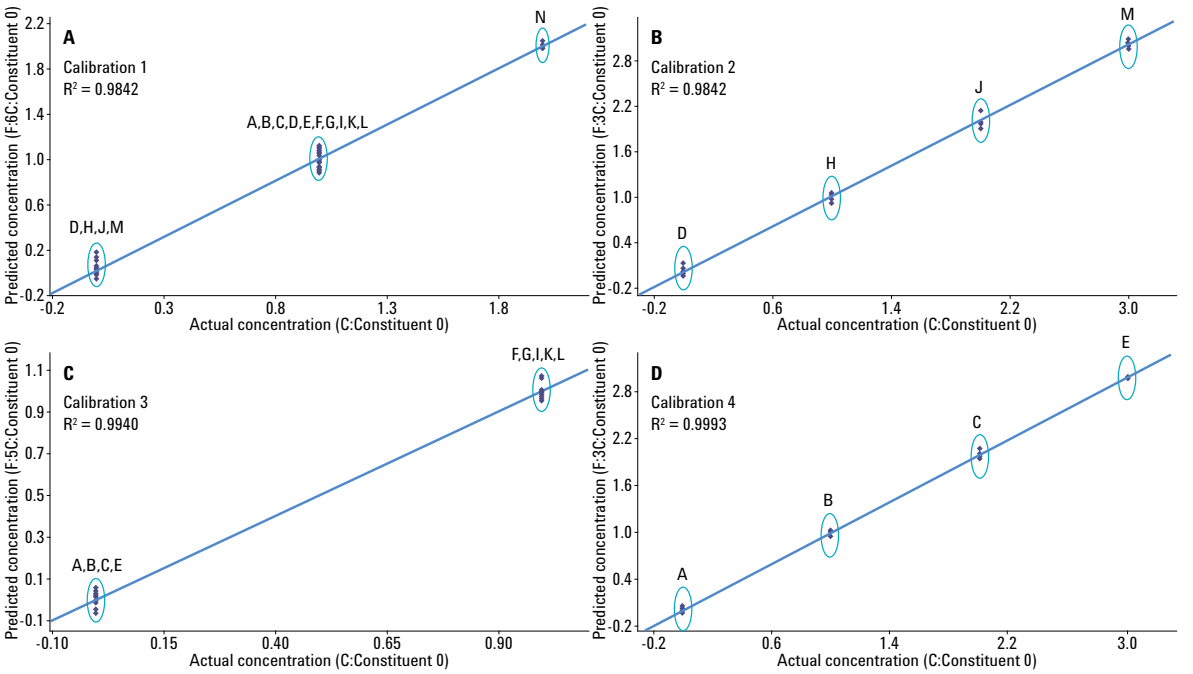

Figure 4. Four PLS-DA calibration plots (the fifth calibration plot looked similar to Calibration 4).

The second calibration plot was able to classify between four coatings D, H, J, and M. The third calibration plot classified between two groups, [A, B, C, E] and [F, G, I, K, L]. The fourth calibration plot classified between four coatings A, B, C, and E. Similarly, the fifth calibration plot classified between the remaining five coatings F, G, I, K, and L. Therefore, with five separate PLS-DA calibration plots, the classification of all 14 acrylic-based coatings was successfully obtained. However, and most importantly, the next step combined all calibration models into one method for the identification of an unknown sample.

The innovative Agilent MicroLab PC Software, with a unique Component Reporting feature, is able to incorporate five calibration models into one single method. The final method can positively identify all 14 acrylic coating test spectra successfully. In Component Reporting, the threshold y-value from each calibration plot was used to set the logic so that the appropriate calibration models were executed as necessary to predict the unknown spectra (Figure 5). Several conditions can be placed on each component using logic statements. For example, coating N uses the Mahalanobis distance (MDistance) to determine if the sample is statistically within the calibration set. Component Reporting allows several pieces of information taken from the five distinct calibrations to be combined to yield a single informative result (Figure 6). In effect, the specialty knowledge usually required to differentiate closely related coatings can be built into the method, making an advanced analysis automatic and field deployable.

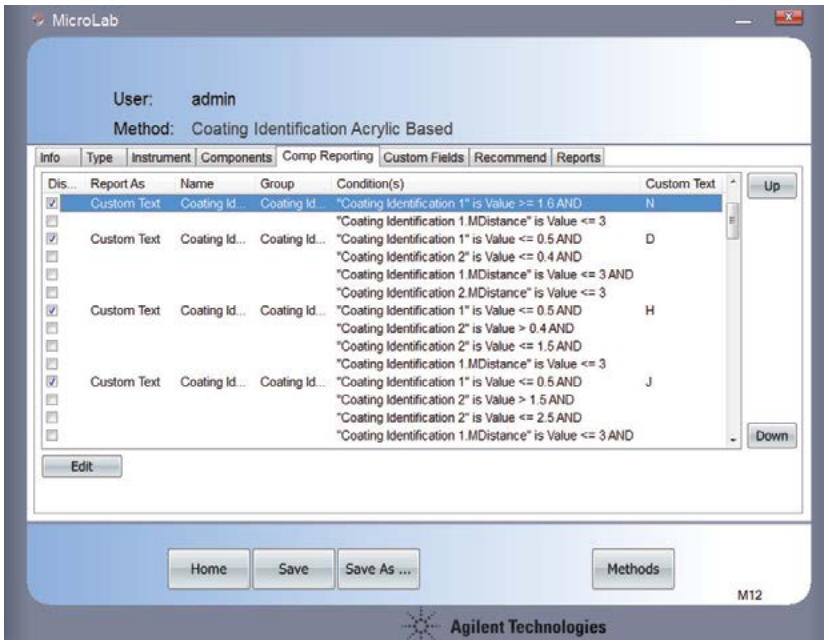

Figure 5. The Component Reporting feature of Agilent MicroLab PC Software allows conditions to be set to select the correct calibration model, and to choose the component to be reported in the final result.

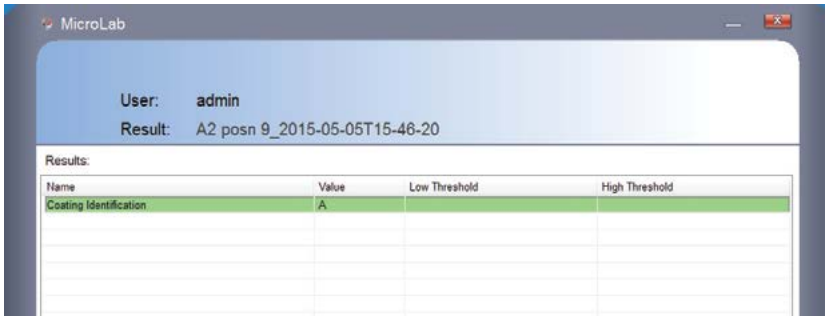

Figure 6. Final result display screen where the coating spectrum is identified as coating A.

Conclusions

The identification of specific acrylic coatings was performed using two different methods of discrimination. A similarity match algorithm was used to correctly identify specific acrylic coatings. Although they were correctly identified, the limited statistical basis of the library search did not provide the means to positively identify closely related coatings. Discriminant techniques, such as PLS-DA are statistically based, providing greater confidence in the match found. A series of PLS-DA calibration models were combined into one method using the Agilent 4300 MicroLab PC Component Reporting capability. This method quickly and successfully differentiated and identified these very similar coatings. The PLS-DA methods provide an extra layer of security and confidence in the identification of closely matched acrylic coatings.

We have shown that the Agilent 4300 Handheld FTIR, equipped with the diffuse sample interface, is well suited for positive material identification of coatings. The spectrometer is particularly useful because of its portability and available sample interfaces, which enable the analysis and identification of specific formulations on a coated article regardless of location, size, and shape. Since the spectrometer is taken to the sample, we have a truly nondestructive method for analyzing coatings. In addition, a sample does not need to be excised for measurement in a lab. We have shown that the diffuse reflectance measurement is preferable since more spectral information is gained, and the measurement is truly nondestructive because the coating surface is not marred or stressed in any way during spectral analysis.

Analysis of Artificially Weathered PET and a Separate PET Hydrolysis Evaluation Using the 4300 Handheld FTIR

Application Note

Authors

Frank Higgins

Pik Leung Tang

Alan Rein

Agilent Technologies, Inc.

Danbury, CT 06810

Introduction

Elucidating chemical changes in carbon fiber composites prior to physical degradation has been effectively demonstrated using handheld FTIR analyzers [1]. This application note shows that a handheld infrared spectrometer is equally effective at measuring early onset chemical changes in environmentally stressed PET polymer, which precede cracking and other physical degradation processes. This is an important issue in applications where polymers (as well as other materials such as paints and coatings) are exposed to environmental conditions varying from climatic conditions that depend on their geographic locale to complete submersion, as in the case of marine paints. The commercial availability of handheld FTIR spectrometers affords the capability of nondestructively measuring areas of large polymer sheets, as well as other coatings.

A wide variety of polymer types are used in the photovoltaic industry as encapsulants, substrates, backsheets, adhesives, sealants, packaging, cabling, fasteners, frames, and junction boxes. PET is one of the most widely used commodity thermoplastics, and is frequently employed for the frames and junction boxes used to fit photovoltaic cells to buildings. In recent years, formulated PET has been considered for use in photovoltaic devices to replace other more expensive backsheet materials such as glass, PEN, or PVF. This requires that in-service PET has the correct additive(s) incorporated to enhance the weather resistance of the base polymer and thereby meet the expected lifetime of the solar panel.

The polymer materials used in solar cells are exposed to a host of environmental and weather related stresses including light, temperature, moisture, and electric fields. This exposure initially leads to subtle chemical changes on the polymer surface. As the environmental stress continues, chemical and compositional changes become more severe, and there is deeper and more prevalent damage. At some point, the severity of the degradation leads to stress cracking, mass loss, and physical shrinkage of the material (Figure 1). Additive chemicals mixed in the base polymer can help delay these changes, but the wrong additive may have no effect, or worse, actually speed up the degradation.

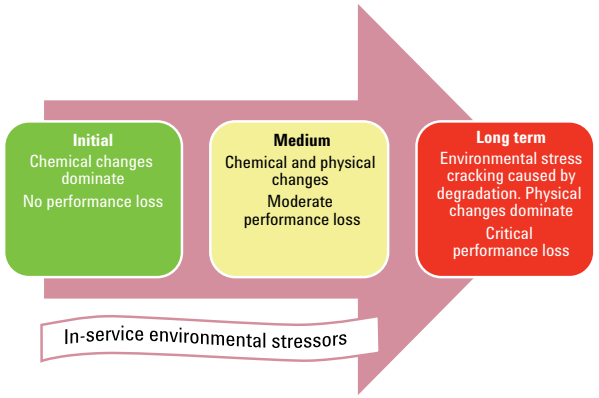

Figure 1. The common degradation pathway of polymers is shown, an arrow indicates increasing time/dosage.

An Agilent 4300 Handheld FTIR was used to measure chemical changes in PET polymer samples. The spectral data measured the effects of weathering in a controlled weatherometer (WOM) chamber, and separately, the effects of hydrolysis on fully submerged polymer samples. The spectroscopic changes were monitored as a function of time to elucidate the chemical changes related to each stress environment. The onset of these chemical changes provided an excellent benchmark performance for additive-free PET film. Subsequent proprietary formulations can be examined to gauge the effectiveness of degradation-resistant additives, compared to the benchmarked PET results, as well as a function of the additives costs. The conditions used to stress these films were selected to provide spectral results from incipient changes, that is, in the initial-medium range where the physical changes are less dominant and not visibly observable. The complexity of the chemical changes suit the use of multivariate based models, which were created and implemented into the Agilent 4300 Microlab PC Software and combined with conditional reporting. Traditional univariate analysis was performed but correlated worse, as it could not account for the number and complexity of the changes.

Infrared spectroscopy for monitoring environmentally induced changes in polymers

There are major advantages in applying a rapid, nondestructive method to detect and analyze the onset of environment related stressors:

- Enables the selection of optimized additive formulations to the base polymer.

  Determining the early onset of chemical changes reduces the cost of testing programs by rapidly eliminating those formulations likely to fail or not reach the expected performance criteria. Using the infrared analyzer, in combination with an accelerated environmental chamber, enables more rapid decisions to optimize the additive formulation. Handheld FTIR, which does not require the excision of a sample for lab analysis, means that the test protocol does not need to be disturbed for analysis, and the analysis can be carried out on-site, in actual weathering field locations.

- Enables nondestructive on-site analysis of in-service products containing polymers (for example, solar panels and so forth).

  Extensive knowledge of the spectroscopic changes in polymers as a function of environmental stresses is gained during the development phase, leading to the selection of the proper additive formulation. This information provides maintenance and upkeep personnel a powerful nondestructive testing method capable of determining the condition of installed systems with respect to these stressors.

Method and Instrumentation

Mitsubishi Hostaphan RNK 50 poly (ethylene terephthalate) 50-µm films were used in this project. This specific PET product has no extra performance additives, and the films were aged for 0, 5, and 10 days in an Atlas XLS+ xenon arc lamp WOM. The films were aged at 700 watts/m^2 irradiance with filter set A. This filter alters the chamber's xenon arc lamp to mimic the distribution of spectral frequencies in sunlight. The temperature of the chamber was set to 40 °C, the minimum achievable without external cooling apparatus. This light intensity was roughly equivalent to the power of the sun at the equator. The weathering chamber was set to constantly irradiate at this calibrated energy onto the thin PET films. Therefore, there was no night/day or radiant/irradiance cycling that results in only moderate rates of accelerated degradation.

A 4300 Handheld FTIR (Figure 2), equipped with either a diamond ATR or an external reflectance interface, was used to measure the 50-µm PET films. The weathered surface of the films (top, that is, facing the xenon lamp) and the lesser-exposed bottom surface of the films were both analyzed by FTIR. All FTIR spectra were collected at 4 cm^{-1} resolution, and consisted of 64 co-added interferograms resulting in a spectral acquisition time of ~35 seconds. The measured spectral range was 4,000–650 cm^{-1}. Films were placed flat to the bottom plate at the same horizontal plane as the irradiance calibration standard.

Figure 2. Agilent 4300 Handheld FTIR with diamond ATR and external reflectance sample interfaces used for measurement of PET. Sample interfaces are instantly interchangeable with no realignment necessary.

For the accelerated hydrolysis experiments, PET samples were refluxed in distilled water over a period of 0 to 14 days while fully submerged in water. The samples were measured *ex-situ* after drying, using the 4300 Handheld FTIR equipped with a spherical diamond ATR interface. The spectra were recorded at 4 cm^{-1} resolution, 64 co-added interferograms, and a spectral range of 4,000–650 cm^{-1}.

Results and Discussion

Simulated weathering of PET using a weatherometer

As expected, the infrared spectra of the top face of the thin film surface exhibited the greatest level of change, and only very slight differences were observed on the bottom side of the PET thin films. Since the PET material is free of additives, the light, heat, and moisture present in the chamber induces chemical and physical changes in the industry-standard base polymer. Results from infrared measurements of these samples were useful as a control benchmark. The results from similar measurements of PET, with additive formulations, can be compared to determine the best-in-class formulations.

The spectra of the top-side exposed films exhibit oxidation absorbance at 1,773 cm^{-1} and 1,690 cm^{-1}, consistent with typical oxidation products of hydrocarbons (Figure 3). The ISO 10640:2011(E) [2] standard also notes these same absorbance frequencies to measure the critical photoproducts in PET or polybutylene terephthalate (PBT). The 1,773 cm^{-1} band is typically assigned to the formation of peresters (R-C(=O)-O-O-R), however, other oxidation products may also give rise to this band. The strong oxidation band at 1,690 cm^{-1} is consistent with an aromatic carboxylic acid functional group, such as benzoic or terephthalic acids, which are common reaction products from photo-initialized hydrolysis. The broader absorbance observed in the 1,450–1,150 cm^{-1} region is also consistent with OH deformation and C-O stretch absorbance from carboxylic acid groups. In addition to the above specific vibrational changes, some general indicators of aging such as band broadening and baseline shifting were observed.

After 10 days of exposure, some oxidative damage was observed on the bottom side of the film. The photo-degradation of PET forms two types of radicals; an alkoxy type radical and a hydroxyl radical. The latter is highly mobile [3] and can diffuse through the polymer matrix from the top side to the bottom face of the film. This may be one possible source of the degradation measured on the bottom sides of the exposed films; secondary reflected light or thermal oxidation may also contribute to the degradation observed on the bottom surface.

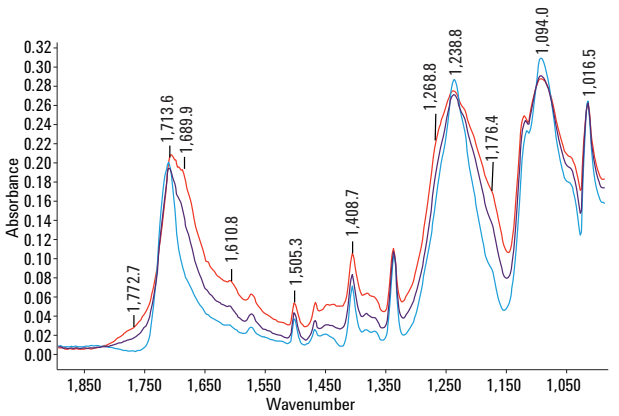

Figure 3. ATR spectra of weathered PET at 0 days (blue), 5 days (purple), and 10 days (red) of WOM chamber exposure.

Multiple discrete spectra from the top surface of the PET films were used to create a partial least squares (PLS) calibration for oxidative PET degradation. PLS calibrations are used to create multivariate correlations and allow multiple IR regions in the spectra to be used to build a calibration model. The PLS calibration (Figure 4) employed a gap 2nd derivative (nine points smoothing) and multiplicative scatter correction (MSC) preprocessing. The calibration with five factors (latent variables) resulted in a correlation coefficient of $R^2 = 0.9871$. This correlation coefficient is somewhat lower than a traditional FTIR calibration with a single analyte in a uniform polymer matrix, in which one might expect an R2 of >0.99. However, polymer oxidation is a complex mechanism with both chemical and physical variables which hinder direct polymer analysis correlations such as those described in this application note. The ISO 10640:2011 [2] (Section 3, 4 and annex A) standard describes the variables inherent in photo ageing measurements of polymers.

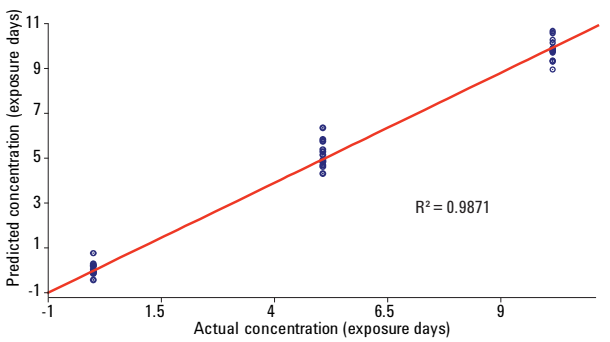

Figure 4. PLS actual versus predicted calibration plot for 0, 5, and 10 days of WOM-exposed PET (top side). This PLS calibration model uses mean centering, 2nd derivative (9 points), MSC, and 5 factors.

Spectra from the bottom side of the PET films were tested against this calibration. The results indicate little or no oxidative damage in the 0 and 5-day exposure coupons, but the bottom surface spectra of the 10-day exposure coupons exhibit oxidative exposure equivalent to 1 day of top surface exposure. Since the bottom side of the PET film spectra are not used in the PLS model, their results can be used to validate the models performance. The degree of damage in the bottom side of an exposed polymer film, relative to the damage on the exposed side, is a useful measurement for ascertaining the optimum film thickness with regard to weather-resistance.

The external reflectance (ER) infrared data also provide a similar performing correlation with amount of exposure. The ER PLS calibration model indicates an $R^2 = 0.987$ with two factors, using mean centering and gap 2nd derivative (5 points) for the preprocessing. Either sample measurement technique can be used to correlate the weathering damage of PET. The ATR spectra are more convenient to interpret and evaluate since they are more frequently described in literature, and more often contained in spectral libraries. The penetration depth of ATR is typically 2–3 µm, yielding results that are particularly surface-sensitive and ideally suited to monitor and evaluate chemical changes at or near the surface. The ER interface allows very easy sampling and minimal contact with the PET sample, but the spectra are less familiar in appearance (Figure 5) and cannot be analyzed with an ATR library or data set. ER spectra contain primarily first-surface reflected IR light, specular reflectance, and some degree of diffusely reflected IR light. The rougher the surface, the more diffuse reflectance will occur and, thus, a higher depth of penetration. Since highly photo-damaged polymers develop a rough surface, the ER measurement may have an advantage in this condition.

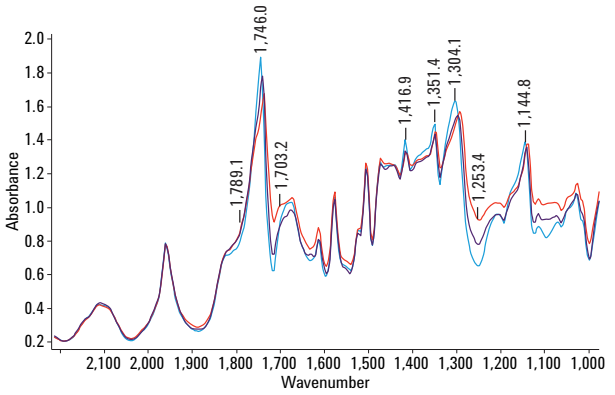

Figure 5. External reflectance (ER) infrared spectra of WOM-exposed PET: 0 days (blue), 5 days (maroon), 10 days (red).

The PLS calibration models can be incorporated into the 4300 MicroLab Software to predict the equivalent weathering of an unknown sample. The exposed PET sample shown in Figure 6 indicates a high degree of oxidation, equivalent to 10 days of accelerated WOM exposure. The software also evaluates the Mahalanobis distance, as a secondary check, to gauge whether the sample spectrum is appropriate for the model. High values indicate the sample is different from the calibration set.

Marginal (yellow) and critical (red) thresholds are set in the method to provide actionable limits for unknown damaged samples. The Mahalanobis distance (M-distance) field in Figure 6 indicates the sample is matching or fits the calibration set, within an acceptable range. Samples with M-distances greater than six are considered statistically different from the calibration set. Samples that are not PET will also be flagged with high M-distance warnings. Comparison of the PET data from these experiments to those of levels of polymer oxidation from natural and artificial aging in the literature [4], indicate that 1 day of WOM exposure in nonstabilized PET is approximately equivalent to 2 years of ambient weather exposure in fully stabilized PET. This calculation is based on the conditions expected in a photovoltaic cell application, and takes into account the indirect exposure to sunlight.

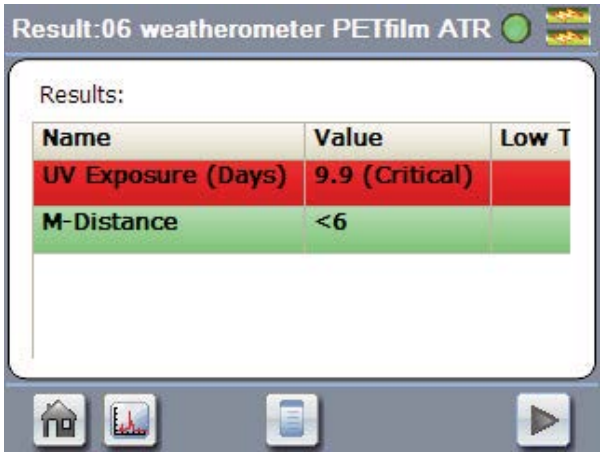

Figure 6. Results from this sample of PET indicate a significant degree of oxidation and alerts the user through a color coded (red) warning. The level for the warning, red critical value, can be tailored to suit.

Hydrolysis of PET

The backsheet of solar panels are typically exposed to above-ambient temperatures, which are especially higher in tropical climates. The following experiment was designed to mimic these conditions and provide information regarding the effectiveness of antihydrolysis additives in PET, without photo-induced events.

PET samples, having been immersed in refluxing distilled water for 0, 3, 7, 10, and 14 days to accelerate hydrolysis, were measured with the 4300 Handheld FTIR equipped with the spherical diamond ATR sample interface. The differences in spectral features of PET exposed to these conditions are weaker, less visible, and mainly involve changes in the aromatic ring vibration bands. This is consistent with published research indicating hydroxyl free radical reactions as the sole source of chemical change in the samples. This polymer system was exposed to two major stressors; temperature, the boiling point of water, along with full submersion of the PET samples. The full sample submersion virtually removes any photo-degradation or oxygen-based changes, as oxygen and light are excluded from the experiment. PLS regression was used to correlate the spectra with the time-based degree of hydrolysis (Figure 7). The model used 2nd derivative (12 points) and standard normal variate (SNV) preprocessing to produce an acceptable grouping of replicates, resulting in a correlation coefficient of $R^2 = 0.9131$. Only two PLS factors were necessary to produce the best performing calibration with the ATR data. Some of the samples became brittle, making sampling more difficult. However, the method and calibration was sufficient to categorize the hydrolysis into low (0–3 days), medium (3–7 days), and high (> 7 days) ranges.

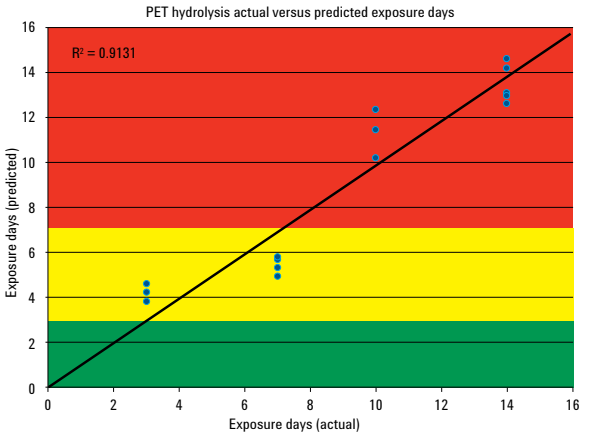

Figure 7. The ATR 4300 PLS actual versus predicted calibration plot for 0, 3, 7, 10, and 14 days of hydrolysis-exposed PET.

These hydrolysis ranges can be incorporated in the Microlab PC software using the conditional reporting feature, and used to report an appropriate text message depending on the model's prediction (Figure 8).

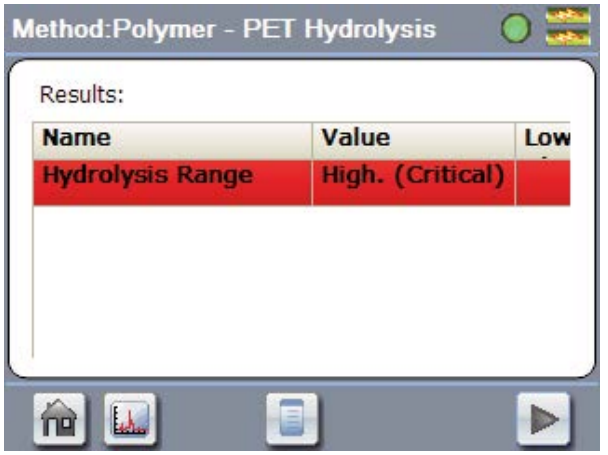

Figure 8. This PET sample indicates a critical level of hydrolysis. The method shown is incorporated in the Agilent 4300 MicroLab Software and warns the user through a color-coded message. The level can be chosen and changed by the user.

Conclusions

We have shown that a handheld FTIR analyzer, the Agilent 4300 Handheld FTIR spectrometer, can rapidly elucidate early changes in PET polymer after exposure to simulated constant irradiance sunlight, 40 °C temperatures, and air. The PET film that had been exposed in the weatherometer exhibited predominantly chemical changes, with the actual weight and physical dimensions of the sample remaining unchanged. A separate hydrolysis experiment enabled the chemical changes in submerged samples to be modeled in isolation of the oxidative or photo-degradative events.

The 4300 Handheld FTIR can rapidly determine the equivalent aging time of PET formulations with regard to hydrolysis and photo-degradation. This enables more efficient determination of additive effectiveness in less time. The system can alert the user if the polymeric material is exhibiting signs of significant change through color-coded warnings.

The information from these testing protocols results in a new nondestructive, on-site method for measuring the aging of polymers used in solar panels, or in other industrial applications. The ruggedness, performance, and ease-of-use of the 4300 Handheld FTIR system maximizes the value of the technology for field use, and represents a new means for on-site determination of deleterious changes in a wide range of organic-based materials. This capability is especially applicable to on-site testing in weathering fields, where samples are aged in real time, under actual ambient conditions.

Acknowledgments

The authors wish to thank Ms. Kimberley Miller for her numerous contributions to this work.

References

1. F. Higgins, “Non-Destructive Evaluation of Composite Thermal Damage with Agilent’s New Handheld 4300 FTIR” March 2, 2014 Retrieved from http://www.chem.agilent.com/Library/applications/5991-4037EN.pdf
2. ISO 10640:2011(E), Plastics – Methodology for assessing polymer photoageing by FTIR and UV/Visible spectroscopy, Section 4.2, Table 1 – Critical photoproducts and modified properties.
3. S. Junkichi, “Radical Migration as an elementary process in degradation”, *Pure & Appl. Chem.*, Vol. **55**, No. 10, pp. 1595-1601, 1983.
4. W.J. Brennan, S.J. Sheperd, “Developments in weatherable Polyester Films For Photovoltaic Applications” DuPont Teijin Films, http://www1.eere.energy.gov/solar/pdfs/pvmrw2011_p62_csi_brennan.pdf

For More Information

These data represent typical results. For more information on our products and services, visit our Web site at www.agilent.com/chem.

Epoxy primer thickness on aluminum measured with the handheld Agilent 4100 ExoScan FTIR

Reliable analysis, even on thin coatings

Application Note

Author

John Seelenbinder

Agilent Technologies,
Connecticut, USA

Abstract

The handheld Agilent 4100 ExoScan FTIR can be used to effectively measure epoxy primer thickness on aluminum. The calibration technique facilitates accurate predictions. Sensitive enough to detect even small discrepancies in thickness, the system is ideal for use in aircraft applications.

Introduction

Determination of primer thickness is key to the quality control of many painting processes. Ultrasonic and Eddy Current probes can be used to measure coating thicknesses; however, they often lack the resolution required for thin primer coats.

The Agilent 4100 ExoScan FTIR is a handheld infrared (IR) spectrometer. It enables easy measurement of both chemical composition and thickness of organic and oxide layers on metallic surfaces. The absorbance of IR spectral bands is directly related to the concentration of a chemical substance, and the pathlength of the light through that substance. The 4100 ExoScan external reflectance sample interface used in these studies transmits the light completed through thin coatings and collects the reflected light. Since the pathlength is defined by the coating thickness, the IR absorbance is directly proportional to the coating thickness. Additionally, since IR absorbance bands are specific to chemical functionality, the method can be designed to look at bands solely due to the epoxy resin in the primer, making it unaffected by additives and fillers. Unlike other lab based IR spectrometers, the handheld 4100 ExoScan enables non destructive analysis of large parts.

This study demonstrates the use of the 4100 ExoScan FTIR for determining epoxy based primer thickness on aluminum panels. A series of calibration standards were measured by the 4100 ExoScan; their IR absorbance was correlated to the thickness as measured by destructive physical testing methods. A second set of 'unknown' samples were tested, showing that the thickness could be accurately measured.

Samples and experiment

All samples consisted of an aircraft grade epoxy primer coated on aluminum panels. In the calibration set, the primer thicknesses were 0.06, 0.09, 0.17, 0.30 and 0.39 mils (1.5, 2.3, 4.3, 7.6 and 9.9 µm). All samples were measured using a 4100 ExoScan FTIR with an external reflectance sample interface; a picture of the 4100 ExoScan in use is shown in Figure 1. The measurements consisted of 32 co-added scans at 8 cm^{-1} resolution, yielding a sample measurement time of about 8 seconds. Backgrounds were measured off a bare aluminum sample for each sample, also taking 8 seconds each.

Figure 1. The handheld Agilent 4100 ExoScan FTIR with the external reflectance sample interface being used for quality inspection of an aircraft coating

Results

Spectra collected from the calibration samples are shown in Figure 2. These spectra, shown from 2000 to 650 cm^{-1} display many bands, which are due to the epoxy coating.

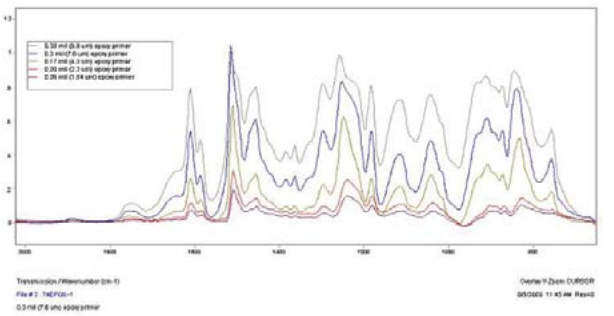

Figure 2. IR spectra collected with the Agilent 4100 ExoScan FTIR using the external reflectance sample interface of epoxy primer on aluminum sheet ranging in thickness from 0.06 mils (1.54 microns) to 0.39 mils (9.9 microns)

For the range of thickness measured, several bands could be used to determine the primer thickness. In this calibration, the band centered at 1610 cm^{-1} was used. This band had an absorbance of approximately 0.07 absorbance units for the thinnest sample and 0.7 absorbance units for the thickest sample. This falls within the linear range of IR absorbance (typically 0.05 to 1 absorbance units). It should be noted that both stronger bands (that is, 1510 cm^{-1}) and weaker bands (that is, 1285 cm^{-1}) exist, which could be used for thicker or thinner calibration ranges respectively. Figure 3 shows the calibration curve for epoxy thickness as measured by the band area for the epoxy band at 1610 cm^{-1}. The calibration shows an excellent linear fit between the IR data and the actual epoxy thickness.

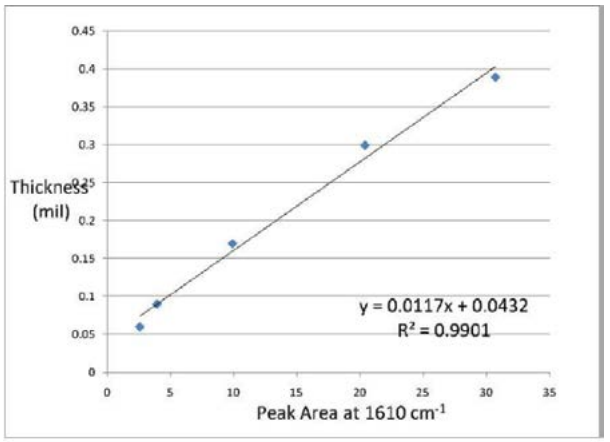

Figure 3. Calibration plot of epoxy primer thickness as measured with the Agilent 4100 ExoScan FTIR. Calibration thicknesses were 0.06, 0.09, 0.17, 0.30 and 0.39 mils

Conclusion

This study shows that the handheld Agilent 4100 ExoScan FTIR spectrometer can be used to measure the thickness of aircraft epoxy primers on aluminum. The excellent linear agreement of the calibration shows that an accurate prediction can be made using this technique. Additionally, the system is sensitive to small changes in primer thickness, even at thin coatings typically used in aircraft applications.

In addition to the 4100 ExoScan FTIR, Agilent also offers the 4200 FlexScan FTIR. The 4100 ExoScan and 4200 FlexScan both provide easy, handheld FTIR analysis, but with slightly different form factors. The 4200 FlexScan has the same optical components as the 4100 ExoScan, but the optics and electronics are separated by a cable. This make the handheld component smaller, while still providing the spectroscopic performance needed for a wide variety of applications. The 4200 FlexScan has a 3 pound optical head attached to a 4 pound battery and electronics pack. Although the form factor is different, use of the two systems, including the software, is identical. While the 4100 ExoScan provides an integrated, compact package, the 4200 FlexScan has a smaller size to fit into spaces with tight clearances.

Metal coatings analysis using the handheld Agilent 4100 ExoScan FTIR

In situ anozidation thickness measurement

Application Note

Author

John Seelenbinder

Agilent Technologies,
Connecticut, USA

Abstract

Infrared (IR) spectroscopy provides a non-destructive means of identifying and quantifying anodized coatings, as well as detecting if parts have been powder or Teflon coated. The anodized aluminum oxide surface provides a strong IR signature that can be easily quantified and, depending on the anodization process employed, the IR spectrum of the aluminum oxide coating changes significantly.

Since FTIR spectroscopy is typically carried out in a laboratory, measurement of the anodized layer by reflection IR spectroscopy has not provided a significant advantage over other analysis techniques for articles that are very large. These oversized samples need to be destructively cut up.

But Agilent has developed the portable, handheld 4100 ExoScan FTIR, capable of measuring anodization thickness and type on large parts in situ. The handheld nature of the 4100 ExoScan enables even large parts to be measured in any orientation. Customized optics are designed to obtain an optimum focus when the 4100 ExoScan is placed in contact with the sample, facilitating easy measurements.

With the 4100 ExoScan, large parts can be easily, non-destructively qualified, ensuring that they meet their design criteria in critical applications.

Introduction

Nearly all metal surfaces are coated in order to increase corrosion resistance, improve bonding to other surfaces or improve hardness. As the use of new alloys grow, the need to protect those materials from oxidation using the correct type and thickness of coating gains increasing importance. Anodization is a process that is used to protect metal surfaces. By increasing the thickness of a natural oxide layer, the anodizing process increases corrosion resistance and wear resistance of a metal surface. It is often used on aluminum parts; the aluminum oxide formed by the electrostatic passivation provides a smooth, durable layer. This is especially important for high strength aluminum alloys, due to the increased corrosion caused by the other metals present. Other metals such as titanium, zinc and magnesium are also anodized to improve specific properties.

Anodized metals have very different properties than the un-oxidized base metal. These properties are crucial for the metal part to meet its design criteria, especially when used in a high performance application. One factor that determines these properties is the thickness of the oxide layer. The current applied and the time over which it was applied determines the thickness of the resulting coating; therefore, it is important to determine that the correct coating thickness has been obtained on critical parts. Additionally, there are several different types of anodization based mostly on differences in the electrode baths in which the processes take place. Examples include chromic acid anodization, sulfuric acid anodization or borate sulfuric acid anodization. Each process produces slightly different properties, but may not result in a visible difference between parts. Additionally, parts are often post-treated after anodization. They may be powder coated, Teflon coated or hardened to achieve specific properties. Many of these post-anodization processes are not detectable by visible inspection only. There is a need to verify that the anodization process has been carried out correctly and that any further modification of the surface has been properly completed before using a part in a critical application.

Typically parts are destructively analyzed in order to identify and determine the thickness of an anodized coating. Atomic spectroscopy is the primary method used to determine whether parts were sulfuric acid or chromic acid anodized. This is done by looking for peaks due to contaminants from the acid bath remaining in the coating. Unfortunately, alloys contain small amounts of chrome and sulfur unrelated to the passivation process, making this technique non-definitive. Various techniques are available to determine the thickness of the anodization. One popular method is a gravimetric technique. The coating is first dissolved in acid, and then the amount of coating is determined by weighing the part before and after the coating has been dissolved. This analysis is time consuming, error prone and uses hazardous chemicals. Due to the destructive nature of these tests, they are often not carried out even though the wrong thickness or process could greatly reduce the serviceability of the metal part.

Anodized surface measurement by the Agilent 4100 ExoScan FTIR

The small size and portability of the 4100 ExoScan FTIR enables measurement of the sample directly in the field. The 4100 ExoScan has two available sample interfaces. The internal reflectance interface (ATR) is used for highly absorbing or non-reflective samples. For analysis of anodized coatings, the external reflectance sample interface is used. The IR light from the 4100 ExoScan is reflected from the sample at an angle of 45 degrees and then collected by the sampling optics. Samples can be measured over the full mid-infrared range from 4000 to 650 cm^{-1} at a maximum resolution of 4 cm^{-1}. For the anodization coating measurements in this study, 8 cm^{-1} resolution was used.

The 4100 ExoScan software provides multiple levels of user interaction. The Administrator level allows full use of the system to develop methods, including advanced data processing. The system is designed to wirelessly communicate with either a PDA for data collection, or a laptop computer. Method development personnel can collect the data on either the PDA or laptop. If data was collected with the PDA, it can be wirelessly transferred to the laptop for advanced processing. Once the method has been developed, the Operator level of software allows simple data collection, automated data analysis and presents easy to understand results that are displayed on the PDA. This allows the system to be used with very little training. The methods can be set up to give users a simple yes/no answer when looking for a specific type of coating or thickness.

Aluminum anodization thickness

Five samples of 2024 aluminum that were treated with borate sulfuric acid anodization (BSAA) were measured with the 4100 ExoScan FTIR. The aluminum oxide surface concentration ranged from 66 to 374 mg/ft^2. The overlaid spectra of the five samples are shown in Figure 1. The strong aluminum-oxygen stretching band is observed at 1128 cm^{-1}. Both the height of this band and the area of this band using local baseline points at 1390 and 995 cm^{-1} were plotted with respect to aluminum oxide concentration. Both plots are easily fit with quadratic equations, each producing a correlation of 0.995. The calibration plots are shown in Figure 2.

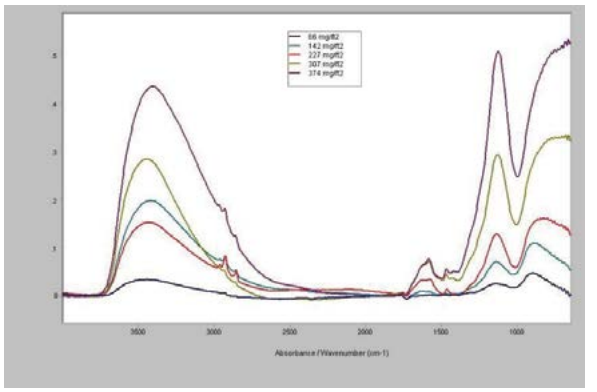

Figure 1. Spectral overlay of BSAA on 2024 aluminum calibration standards. Spectra were measured with 32 scans at 8 cm^{-1} resolution with the Agilent 4100 ExoScan FTIR using external reflectance

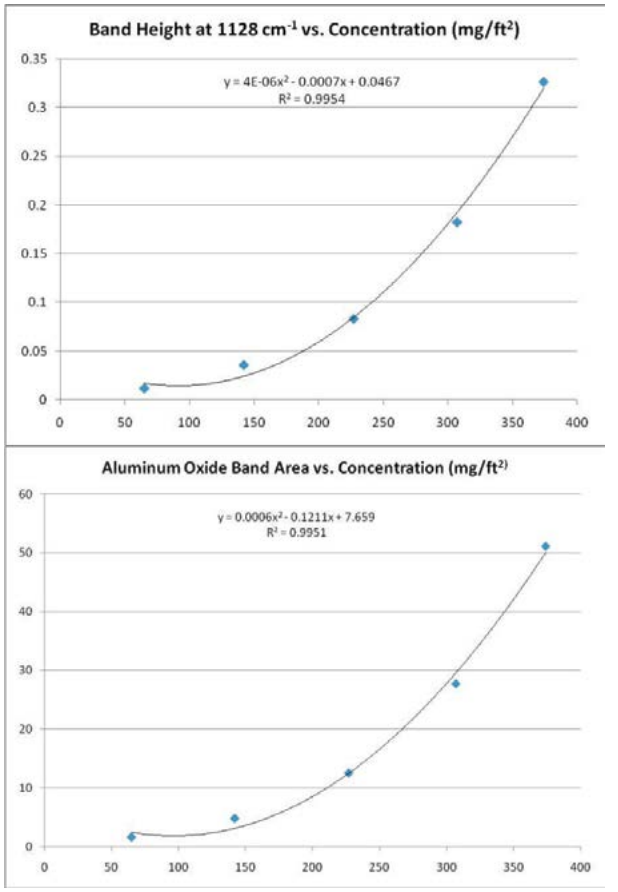

Figure 2. Calibration curves showing the aluminum oxide band height at 1128 cm^{-1} versus concentration (top) and the aluminum oxide band area from 1390 cm^{-1} to 995 cm^{-1} versus concentration (bottom). Both calibration curves are fit by a quadratic equation with an excellent correlation coefficient.

IR spectra of the anodized coating are independent of the aluminum alloy. Figure 3 shows samples of 7075 aluminum that have been treated with the same BSAA process as the 2024 samples above. The calibration in Figure 2 was used to predict the concentration of aluminum oxide; the results are shown in the legend of Figure 3.

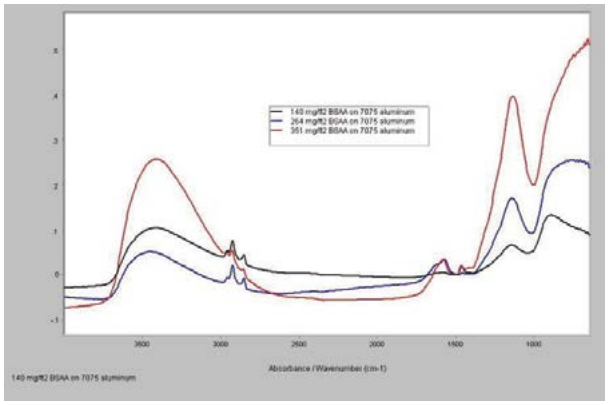

Figure 3. IR spectra of BSAA on 7075 aluminum measured with the Agilent 4100 ExoScan FTIR. Concentrations of anodized coating calculated from the spectra are shown in the legend

Coating type identification

The IR spectrum of the anodized coating is not characteristic of the alloy to which it is applied; rather, the spectrum is characteristic to the coating process. Each coating process produces a slightly different crystal size and shape. These slight differences produce changes in the IR spectra, which can be correlated to the coating type. Using a library search approach, one can determine the anodization process used on a particular part from the IR spectrum. With the 4100 ExoScan FTIR, this can be done on large parts without the need for disassembly or destruction of the part.

Figure 4 shows the spectra of three different aluminum samples that were treated with BSAA. The first sample is 2024 aluminum alloy sheet, the second is 7075 aluminum alloy sheet and the third is a cast aluminum part. It should be noted that the two aluminum alloy sheets had a very smooth surface, but the cast part had high amount of surface roughness. This shows that spectra of the anodization coating can be obtained even from low reflecting surfaces.

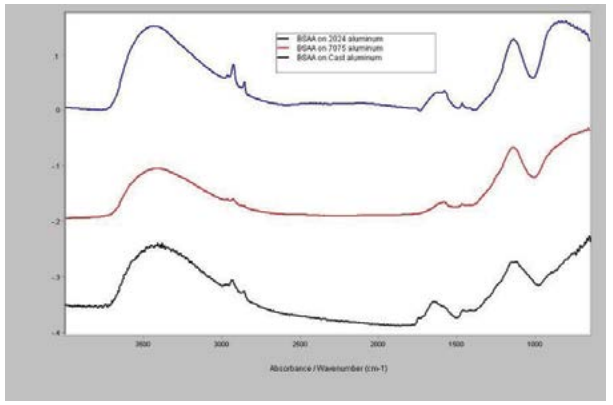

Figure 4. Comparison between spectra of BSAA on 2024 aluminum (blue), 7075 aluminum (red) and rough cast aluminum (black)

Spectra of samples from three different types of aluminum anodization processes were measured. Each process produces slightly different properties in the metal part. The processes used were BSAA, sulfuric acid anodization, and chromic acid anodization. Each anodization produced a distinctly different spectrum as is shown in Figure 4. Figure 5 shows a library search carried out in the 4100 ExoScan FTIR software identifying a BSAA anodization type on a cast aluminum part.

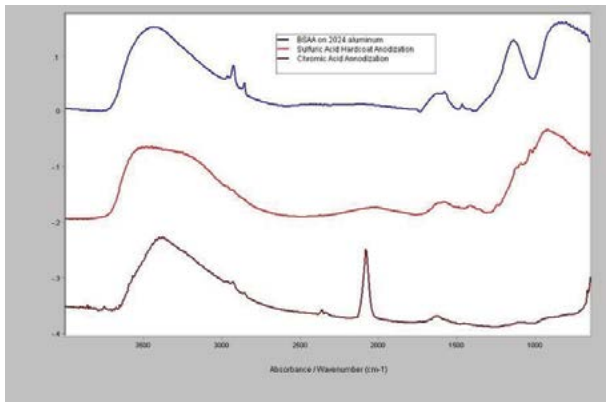

Figure 5. IR spectra of BSAA anodization (blue), sulfuric acid hardcoat (red) and chromic acid anodization (brown)

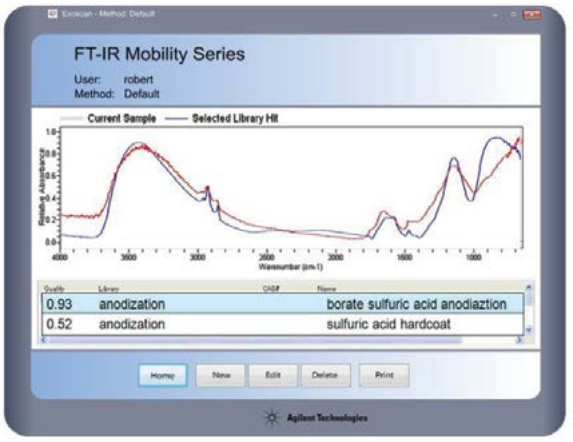

Figure 6. Library search in the AgileInt 4100 ExoScan FTIR software showing a positive match for the BSAA process

Conclusion

A variety of coatings are used in order to ensure corrosion resistance and durability of metals for high performance applications. In order to ensure that the metal parts will perform as designed, it is important to verify both the type of coating used, and the thickness of that coating. IR spectroscopy can identify many coatings used on aluminum and other metals. Even thin anodized coatings, as shown here, can be both identified and quantified using the 4100 ExoScan FTIR. The 4100 ExoScan can also be used to identify paint and primer coatings[1]. Since the 4100 ExoScan is handheld, portable and designed to be used directly where the article of interest is located, it permits measurement of coatings on these large complex parts without disassembling or destroying the parts. The 4100 ExoScan is a very useful quality control device for ensuring that incoming parts have the proper type of coating with the correct thickness for the intended application.

For more details on paints and primers, see Agilent application note 'First article and incoming product inspection of paints and plastics using the handheld Agilent 4100 ExoScan FTIR'.

In addition to the 4100 ExoScan FTIR, Agilent also offers the 4200 FlexScan. The 4100 ExoScan and 4200 FlexScan both provide easy, handheld FTIR analysis, but with slightly different form factors. The 4200 FlexScan has the same optical components as the 4100 ExoScan, but the optics and electronics are separated by a cable. This makes the handheld component smaller while still providing the spectroscopic performance needed for a wide variety of applications. The 4200 FlexScan has a 3 pound optical head attached to a 4 pound battery and electronics pack. Although the form factor is different, use of the two systems, including the software, is identical. While the 4100 ExoScan provides an integrated, compact package, the 4200 FlexScan has a smaller size to fit into spaces with tight clearances

Detection of trace contamination on metal surfaces using the handheld Agilent 4100 ExoScan FTIR

Ensuring ultimate cleanliness for maximum adhesion

Application Note

Author

John Seelenbinder

Agilent Technologies,
Connecticut, USA

Abstract

Efficient adhesive bonding of metal surfaces requires a high level of cleanliness of the surfaces. The 4100 ExoScan FTIR with a grazing angle sample interface enables identification and quantification of metal surface cleanliness in the field. After the metal has been cleaned, the analyzer can be used to detect the presence of organic and some inorganic contaminants. Even very low amounts of contamination can severely decrease the ultimate bond strength; the highly sensitive 4100 ExoScan can detect trace levels of contaminants.

Introduction

Adhesive bonding provides strong, reliable attachment between similar and dissimilar materials. Often, adhesive bonds can provide greater breaking strength than the materials which are being bonded together. Additionally, the use of bonding can produce stronger, lighter components through the elimination of heavy mechanical fasteners and the holes which are required to use such fasteners.

Although adhesives can produce a very strong bond, the ultimate strength is often determined by the cleanliness of the two surfaces that are being bonded. Adhesives applied to a contaminated surface will only bond to the contaminant, leaving only a weak bond between the two substrates. For some applications, even trace amounts of contaminants can severely decrease the ultimate bond strength.

In order to ensure that bonding surfaces are free of contaminants, extensive cleaning procedures have been developed for critical bonding applications. It has been shown that even small deviations in these cleaning procedures can produce substandard bonds. To guarantee strong bonding, surfaces should be analytically tested to confirm their cleanliness before application of adhesives. A good testing technique should be non-destructive, identify and quantify contamination, and ideally be field deployable. The technique must also have the sensitivity required to see low levels of contamination on bonding surfaces.

Infrared (IR) spectroscopy is a non-destructive method, which can both quantify and identify many contaminants on metal surfaces. All organic chemicals and many inorganic chemicals can be measured by IR. Using a grazing angle sample interface, IR is sensitive enough to measure contaminants at very low levels. These are all positive properties; however, grazing angle IR reflectance has typically been measured on small test samples using traditional benchtop FTIR spectrometers in laboratory environments. The Agilent 4100 ExoScan FTIR overcomes this limitation by offering a sensitive, handheld IR spectrometer that can be applied to the analysis of components of virtually any size in manufacturing or maintenance facilities. This application demonstrates the use of the 4100 ExoScan with a grazing angle sample interface to measure small amounts of contaminants on metal surfaces.

Grazing angle infrared reflectance

There are many ways to measure samples using IR spectroscopy. In all cases, the IR light from the spectrometer must interact with the sample, and then be directed to the detector. The simplest example of this is a transmission measurement, where the light passes straight through the sample. For samples on reflective surfaces, the typical measurement configuration is known as infrared reflection-absorption spectroscopy (IRRAS). Using IRRAS, the light from the spectrometer passes once through the sample, reflects off the metallic surfaces, and then passes through the sample a second time before being collected on the detector. A diagram describing the sample IRRAS is shown in Figure 1.

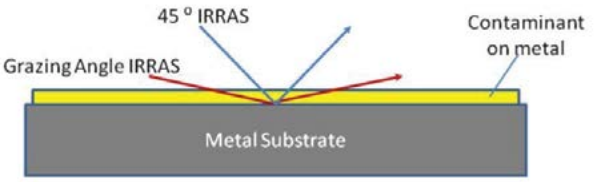

Figure 1. Diagram showing the sample interface of infrared reflection absorption spectroscopy (IRRAS) in both the grazing angle (red) and specular reflectance (blue) geometries. The grazing angle geometry has an increased pathlength through the contaminant

The intensity of an IR absorbance measurement is directly proportional to both the concentration of the sample and the pathlength of the light traveling through the sample according to Beer's Law (Absorbance = Concentration * Pathlength * Molar absorptivity). In an IRRAS experiment, the pathlength can be increased by using a very shallow angle with respect to the substrate surface. If the angle of incident light is greater than 75 degrees from normal, the experiment is typically referred to as a grazing angle measurement. Figure 1 also shows pictorially the difference in pathlength

comparing reflection at 45 degrees (typical specular reflectance measurement) to a grazing angle reflectance at 80 degrees to normal. In addition to the increased pathlength, grazing angle reflectance shows additional sensitivity compared to a typical specular reflectance measurement. The increase in sensitivity is due to enhancement of the electric field of the p-polarized light at the surface. One can visualize the p-polarize light as creating a standing wave on the surface thus greatly increasing the effective path length. The greatest enhancement in the field strength for smooth metallic surfaces is near 88 degrees from normal; this is instrumentally unpractical, so grazing angle sample optics typically have a average angle near 80 degrees.

The 4100 ExoScan FTIR is a portable, handheld IR spectrometer for surface analysis. It has been designed specifically for reflection techniques; one if the three available sampling interfaces is a grazing angle geometry. The 4100 ExoScan grazing angle has a nominal angle of 82 degrees. The high throughput optic system yields over 80% throughput, producing excellent signal-to-noise even on short measurements. The 4100 ExoScan is also available with specular reflectance (45°) and attenuated total reflectance (ATR) sample interfaces making it a versatile instrument for many sample types. The 4100 ExoScan is fully portable, requiring no power or computer connections. The data is collected and results are displayed on a PDA computer; the results can also be transferred to a PC for further evaluation. Additionally, the 4100 ExoScan measures the full IR spectral range for identification and quantification of most contaminants, and it is impervious to atmospheric conditions.

Contaminant measurement using the Agilent 4100 ExoScan FTIR

All IR spectrometers, including the 4100 ExoScan FTIR, are sensitive to many different organic and inorganic contaminants. Figure 2 shows spectra obtained with the 4100 ExoScan of a thin layer of hydrocarbon oil and a thin layer of silicone, each on an aluminum surface.

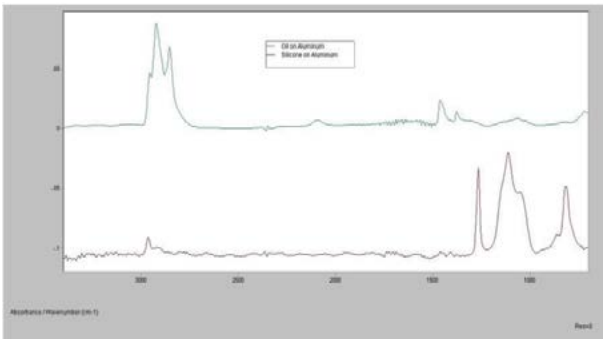

Figure 2. Hydrocarbon oil (blue) and silicone oil (red) on an aluminum substrate measured with the Agilent 4100 ExoScan FTIR.

As can be seen from the spectra, the 4100 ExoScan FTIR can easily distinguish different types of contaminants, enabling the user to select the proper cleaning procedure to remove the contaminant.

The 4100 ExoScan FTIR was designed to provide easy to understand answers for both skilled and unskilled users. The spectra shown above and below are informative for a skilled user to determine the amount and type of signal present, but the successful use of the 4100 ExoScan in field applications requires that the results be presented in a simplified form. Methods can be generated in the 4100 ExoScan to produce numeric results related to the amount of sample on the surface. Limits are provided, allowing the results to be displayed as red, yellow or green if the sample is in a critical, marginal or safe range respectively. Figure 3 shows the results screen for a measurement of oil contamination. In this case the amount of silicone was above the marginal but below the critical limit, so the result is display in yellow. This indicates to the user that the area should be cleaned and re-measured before proceeding.

Figure 3. 4100 ExoScan FTIR Results screen showing a marginal oil contamination on a metal surface

Limit of detection of surface contamination

To determine the limit of detection for contaminants on smooth metal, a series of test samples were made by spray coating a silicone mold release (Frekote) on sheet metal aluminum plates. The silicone was applied by spraying a precise amount of material on the surface in two sweeps. The concentrations were verified by measurement on a laboratory IR spectrometer with an established method. The average concentration of six measurements for each panel was calculated; the concentrations ranged from 1.6 to 8.8 µg/cm^2. Table 1 shows the average concentrations of each sample in this test set.

Table 1. Surface concentrations of silicone mold release agent on aluminum

Sample	Concentration (µg/cm^2)
1	1.6
4	3.2
6	6.1
10	8.8

Several spectra of each panel were measured using the 4100 ExoScan FTIR. Spectra were measured using 8 cm^{-1} spectral resolution; 32 scans were co-added yielding a 10 second data collection time. Representative spectra from this sample set are shown in Figure 4. The three prominent bands of silicone at 1265, 1112 and 820 cm^{-1} are easily distinguished, even at the lowest concentration measured.

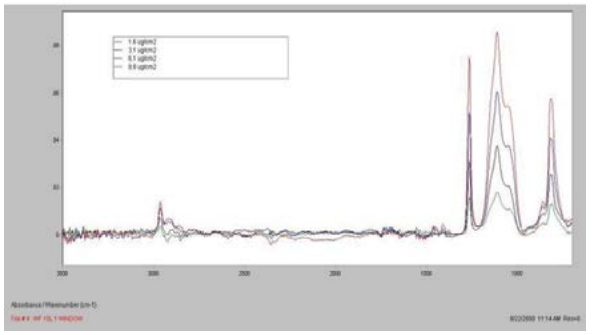

Figure 4. Spectra of silicone mold release agent on aluminum measured with the Agilent 4100 ExoScan FTIR using the grazing angle sample interface. Spectra were collected at 8 cm^{-1} resolution with a 10 second collection time.

A calibration curve was plotted using the area of the silicone band at 1265 cm^{-1}. The calibration is shown in Figure 5. The calibration is linear with an excellent correlation of 0.997. The limit of detection was calculated by measuring baseline area from 2210 to 2120 cm^{-1}. This area was multiplied by 3 (3x the baseline noise) to give the limit of detection of 0.17 µg/cm^2. It should be noted this LOD is a worst case prediction; the measurement of entire silicone band area or measurement over a longer period of time would produce a lower LOD.

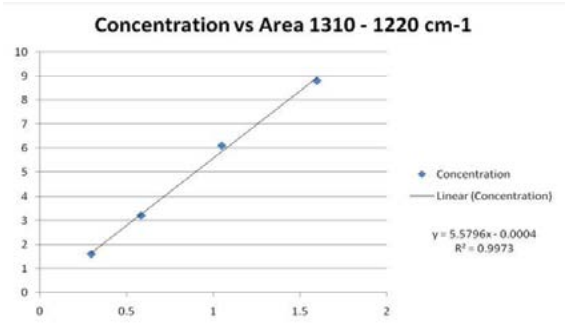

Figure 5. Calibration curve for silicone mold release agent on aluminum from 1.6 to 8.8 µg/cm^2

Conclusion

The quality and strength of an adhesive bond is directly proportional to the cleanliness of the surface being bonded. In addition to stringent cleaning procedures, measurement of bonding surfaces post-cleaning can provide a needed quality control step. The 4100 ExoScan FTIR system, equipped with grazing angle sample optics, can provide the level of sensitivity required for the detection and identification of a large number of organic and inorganic contaminants on metal surfaces. Even with a quick 10 second measurement, a limit of detection of 0.17 µg/cm^2 was obtained for a silicone mold release agent on aluminum surfaces. Methods can be created to present the measurement results in easy to understand categories for use by field personnel. The 4100 ExoScan FTIR enables field measurement of surface cleanliness at detection levels required for efficient bonding.

In addition to the 4100 ExoScan FTIR, Agilent offers the 4200 FlexScan FTIR. The 4100 ExoScan and 4200 FlexScan both provide easy, handheld FTIR analysis, but with slightly different form factors. The 4200 FlexScan has the same optical components as the 4100 ExoScan, but the optics and electronics are separated by a cable. This makes the handheld component smaller, while still providing the spectroscopic performance needed for a variety of applications.

The 4200 FlexScan has a 3 pound optical head attached to a 4 pound battery and electronics pack. Although the form factor is different, use of the two systems, including the software, is identical. While the 4100 ExoScan provides an integrated, compact package, the 4200 FlexScan has a smaller size to fit into spaces with tight clearances.

Identification and Evaluation of Coatings Using Hand-held FTIR

Application Note

Authors

Shannon M. Richard,
Pik Leung Tang PhD

Agilent Technologies,
Connecticut, USA

Introduction

Coatings serve a variety of purposes. Some of those are purely aesthetic in nature, but the majority of coatings are added for their physical properties whether it is to protect by inhibiting oxidation or wear due to weathering of the product, or to enable two materials to be bonded that ordinarily would not bond well as is the case for a primer coating. These protective coatings are typically multi-layered industrial coatings that consist of a process involving the substrate materials, pre-treatment of the substrate, primer/adhesive application and a topcoat or film laminate to seal the coating. In order to ensure that the coating has been applied and cured effectively, process engineers have had to rely on a standard waiting time before proceeding to the next process in manufacturing. However, times could vary depending on conditions surrounding the process causing the wait period to maximize to ensure that the product was complete in order for the process to move forward.

FTIR has been used in the coating process in the past, but mainly for research and development applications. This was due to fact that the instruments had to be maintained in a laboratory environment and that small samples or pieces of large samples would have to be brought to the lab and could not be measured at the point of concern or production. Agilent's hand-held portable FTIR systems with innovative sampling technologies have taken the FTIR out of the lab and enabled its use on the production floor or wherever the sample happens to be operational. This is essential for measurements that need to be made at the point of concern or for samples that are just too large to be able to measure in a laboratory setting. This can be critical, since not all samples allow for taking a small enough piece to the laboratory for measurement when issues or concerns arise.

Examples using FTIR technology

The identification of coatings on materials can prove to be a cumbersome task, especially when samples look identical to the eye. At times, it is important to identify various materials in real time. Coatings are an excellent example of the materials that can be identified as most coatings, primers and bonding materials are made of organic compounds. In Figure 1, we show an example of using the Agilent 4100 ExoScan FTIR with the Diffuse Reflectance sampling interface to determine the difference between Polyvinyl Chloride (PVC), Polyurethane (PU), and Polyvinylidene Fluoride (PVDF). The spectra show that these are easily distinguishable from one another.

In this particular instance, the PVDF coating is used for situations where weather, UV and solvent resistance are critical to the end product's offering. It is important to note that it is also the most expensive of the three coatings. Choosing the wrong coating for the appropriate application or situation by merely viewing the visually identical samples could result in choosing the wrong coating for the customer. Depending on the usage, it could cause the substrate to weather exponentially and lead to failure. In turn, choosing a sample that has PVDF when it is not required costs the supplier due to the expensive nature of this coating versus the others.

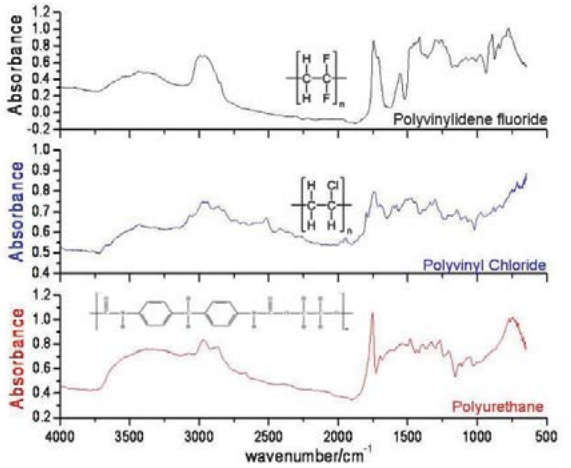

Figure 1. Diffuse FTIR Spectra of Polyvinylidene Fluoride, Polyvinyl Chloride, and Polyurethane

Another instance where FTIR can prove to be beneficial is during the cure process for coatings. Determining whether the cure process has completed or what the optimal cure rate and temperature should be can be a tricky task. Using the ExoScan, also with the Diffuse Reflectance sampling interface, a two part epoxy primer cure profile was established. The cure times ranged from 0 to 308 minutes at specified intervals. The sample was cured at room temperature to establish baseline data. Figure 2 shows representative data and specific regions of the spectra where changes are evident. These changes can be used to establish the level of cure of the epoxy/hardener mixture. Establishing cure level versus curing time is easily done and can be used to set pass/fail criteria for cure completion when sampling the material.

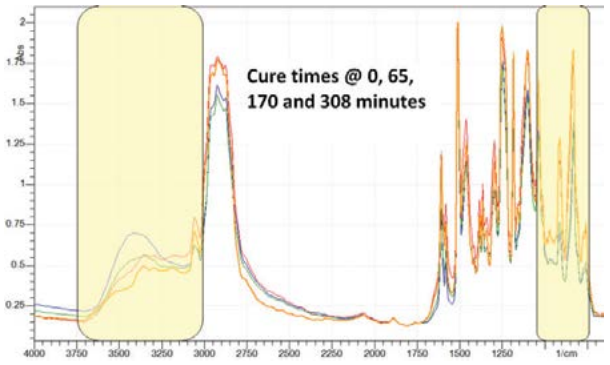

Figure 2. Room temperature cure of Epoxy/Hardener coating at 0 (orange), 65 (red), 170 (green) and 308 (blue) minutes. Highlighted areas show changes as the mixture cures and can be used to measure cure level directly once a correlation has been set up

Examples using FTIR technology

These examples show that FTIR can easily be used for simply identifying coatings as well as the more complicated task of evaluating cure completion. Hand-held FTIR has also been used to determine contamination on the actual coating, coating thicknesses, anodization thickness levels and even accelerated weathering studies to determine long term performance of high-end coatings. These other examples show the versatility of Agilent's portable 4100 Exoscan FTIR in the coatings industry and the diversity applicable samples that are expanding each day.

Measurement of composite surface contamination using the Agilent 4100 ExoScan FTIR with diffuse reflectance sampling interface

Application note

Materials testing

Author

John Seelenbinder

Agilent Technologies
Danbury, CT, USA

Introduction

Contamination of composite surfaces is a large problem in the composites industry. Contamination is obviously a problem for adhesive bonds used in manufacturing, but it can also cause problems with composite repairs. In most cases, composites are contaminated either by a hydrocarbon or silicone based contaminant. Detection of these materials on carbon epoxy composites has always been difficult. Strong background signals present in composites along with the desire to attain low levels of detection have typically presented problems with these measurements.

Infrared spectroscopy provides a means of measuring contamination on composite surfaces. The unique infrared signature of both hydrocarbons and silicones allows them to be differentiated from the underlying epoxy substrate. One issue preventing the use of infrared, however, was the size of laboratory instruments. Until now, laboratory instruments were only practical for measuring small samples. The handheld Agilent 4100 ExoScan FTIR spectrometer allows direct measurement of components without bringing them to the lab. Advancements in the design and production of the 4100 ExoScan allow for a small instrument size without affecting the analytical performance. This allows one to take the instrument to the production part instead of taking the part to the instrument. FTIR can now be used as a true nondestructive technique for evaluation of composite parts.

The 4100 ExoScan FTIR provides the full performance and frequency range of a standard laboratory FTIR. Additionally, the diffuse reflectance sampling interface produces high signal-to-noise measurements of low reflectance surfaces, such as carbon composites. This interface brings the light normal to the sample surface and collects the scattered, diffusely reflected light. The design provides an easy to perform measurement, which can typically be made in 30 seconds.

Silicone

Silicone is pervasive in lubrication and mold release products. Contamination of bond surface by silicone can be difficult to detect; additionally, silicone is difficult to remove and can significantly reduce the effectiveness of a bond. Silicone has a distinctive infrared spectrum, making it easy to identify; it has a characteristic doublet at 1095 and 1018 cm^{-1} accompanied by two sharp bands at 1260 and 800 cm^{-1}.

Three contaminated samples were prepared by solvent evaporation onto a single composite coupon. The three contaminated locations were prepared at separate locations. A solution of silicone in chloroform was dried onto the coupon covering an area of approximately 10 cm^2. The coupon was weighed to the nearest 0.1 mg before and after measurement to determine the surface concentration of each application. Samples had the following approximate concentrations: 0 ug/cm^2, 40 $\mu g/cm^2$, 78 $\mu g/cm^2$, and 300 $\mu g/cm^2$. Each sample and a blank was measured by co-adding 128 scans at 8 cm^{-1} resolution, producing a total measurement time of about 30 seconds per sample.

Figure 1 shows the spectra collected with the 4100 ExoScan FTIR on each of the samples and the blank. The silicone bands at 1260, 1095, 1018 and 800 cm^{-1} are clearly present. Interestingly, the bands are negative on the absorbance scale. This often occurs in reflectance spectroscopy when the samples become strongly absorbing. The spectra shown in Figure 1 have been baseline corrected, but the true absorbance of the blank is near 1.2 absorbance units in the silicone region. The negative silicone bands still correlate with concentration; they just have a negative correlation.

A band area was calculated using the 800 cm^{-1} band of the silicone contaminant. This band is relatively free of baseline interferences. Figure 2 shows a calibration curve plotting the negative band area versus the approximate concentration. The concentration response becomes non-linear, fitting a second order curve; however, the low concentrations can be easily fit with a straight line. Although additional samples at low concentration are needed to accurately determine the limit of detection, this data indicates that a LOD near 10 $\mu g/cm^2$ could be obtained.

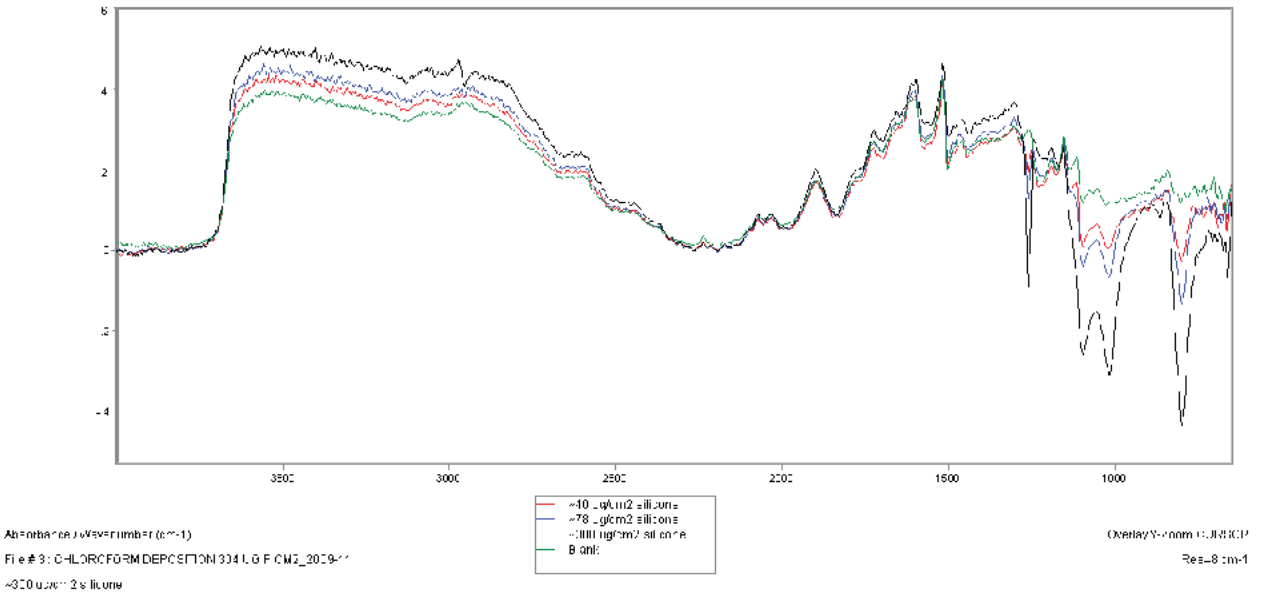

Figure 1. FTIR spectra of three composite coupon samples contaminated with silicone, and a blank

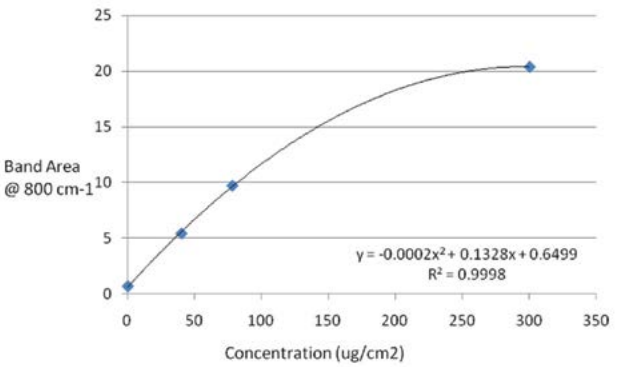

Figure 2. Calibration curve of negative band area versus approximate concentration of silicone

Hydraulic fluid

Contamination of composites by hydraulic fluid is a large concern for aircraft repair. Hydraulic leaks can cause the composite to be saturated. Although hydraulic fluid can be removed from the surface by a simple solvent wipe, fluid present in micro-cracks may be pulled into the bond layer by heat and vacuum used to effect the repair. Plasma cleaning can be used to remove residual hydraulic fluid from a saturated sample. Care must be taken, however, to ensure that the plasma is strong enough to remove the fluid, but not too strong as to damage the composite.

A set of three samples was saturated with a hydrocarbon based hydraulic fluid. The samples were cleaned with a standard acetone wipe. One half of each sample was then cleaned with a plasma cleaner. A different plasma cleaner was used on each sample, each imparting different amounts of energy to clean the surface. Figure 3 shows spectra collected on both the contaminated and clean side of one sample compared to a reference spectrum of the hydraulic fluid. The fluid in the contaminated sample can be clearly seen by the sharp CH stretching band at 2930 cm^{-1} and the C=O shoulder at 1730 cm^{-1}. These bands are clearly absent from the plasma cleaned sample.

Of the three plasma cleaning techniques, Sample 3 (shown in Figure 3) clearly provides the best cleaning without damaging the surface. The plasma cleaned side of Sample 1 still shows a small amount of hydraulic fluid as is shown in Figure 4. On the other extreme, the plasma used on Sample 2 used too much power. Figure 5 shows the hydraulic fluid contaminated sample and the plasma cleaned sample; no epoxy signature is evident in the plasma cleaned sample, indicating that it has been damaged by the plasma.

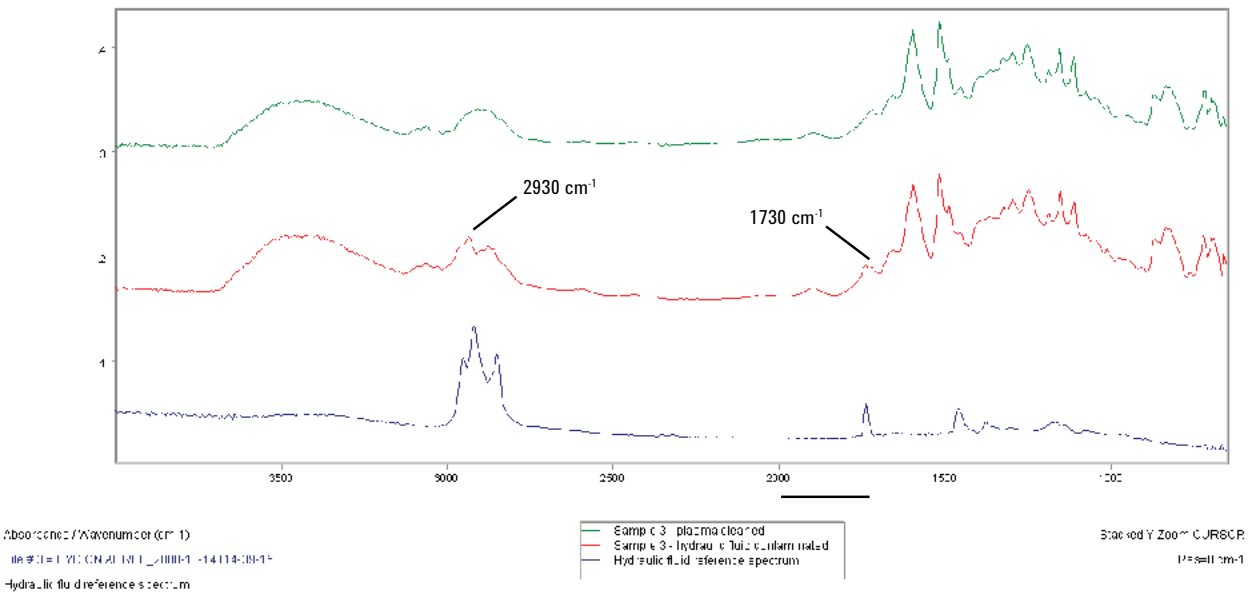

Figure 3. FTIR spectra of composite 'Sample 3' contaminated with hydraulic fluid, and cleaned composite, compared to a hydraulic fluid reference spectrum

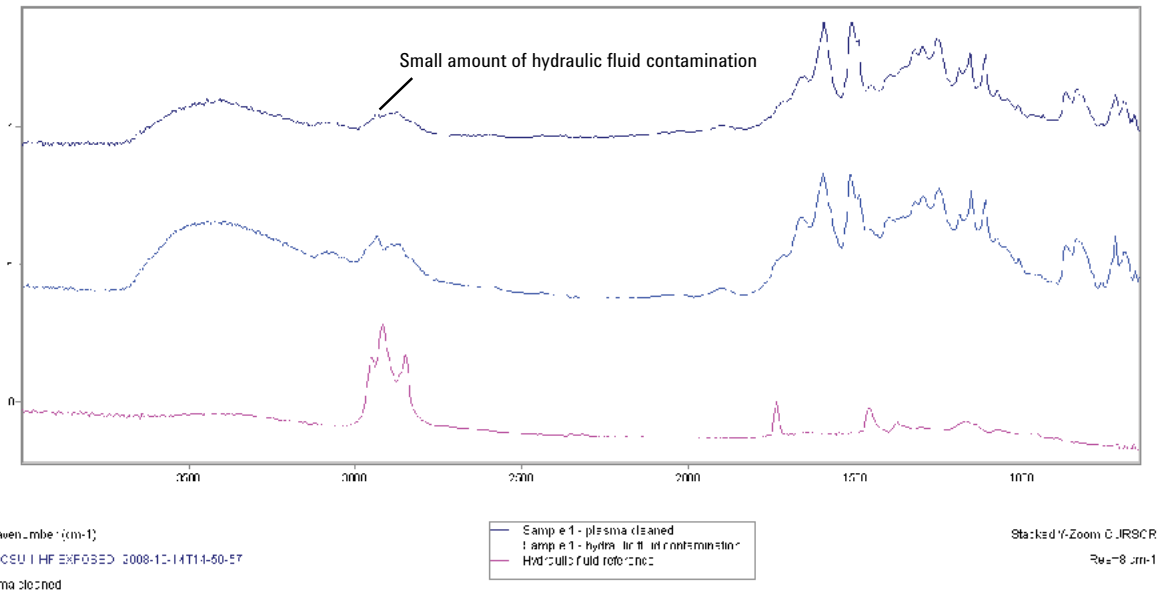

Figure 4. FTIR spectra of composite 'Sample 1' contaminated with hydraulic fluid, and cleaned composite, compared to a hydraulic fluid reference spectrum. It is evident that the cleaned sample still contains a small amount of hydraulic fluid.

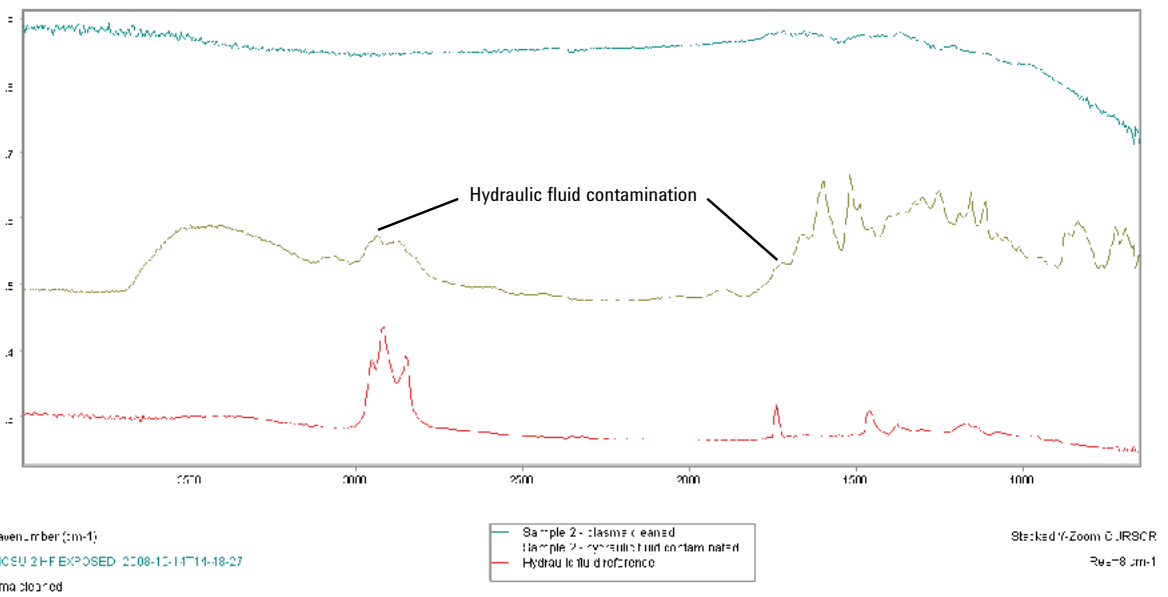

Figure 5. FTIR spectra of composite 'Sample 2' contaminated with hydraulic fluid, and cleaned composite, compared to a hydraulic fluid reference spectrum. It is evident that the cleaned sample was damaged by the plasma.

Conclusion

The Agilent 4100 ExoScan FTIR with diffuse reflectance sampling interface can measure contaminants on composite surfaces. Both silicone and hydraulic fluid were measured on epoxy carbon composites. Hydraulic fluid could still be detected on composite surfaces even after they were cleaned with solvent. Additionally, the 4100 ExoScan was used to determine the efficacy of plasma cleaning on composites; cases were displayed of cleaning, over-cleaning and under-cleaning the surface.

Analysis of plasma treated carbon fiber reinforced polymer (CFRP) composites by portable Fourier Transform Infrared Spectroscopy (FTIR)

Application note

Materials testing

Authors

Alan Rein, Ph.D.
Pik Leung Tang, Ph.D.
Agilent Technologies, Inc., USA

Introduction

Engineering grade CFRP is widely used in commercial and military aerospace applications due to its unique combination of light weight, strength and impact resistance. Since it is an organic based material, it is susceptible to physical and chemical stresses that are different than those that affect metals used in aircraft manufacture. The Agilent 4100 ExoScan FTIR system is known to be a highly useful non-destructive analyzer for measuring the deleterious chemical changes in CFRP that occur from oxidation resulting from elevated thermal exposure. In this application note, we show that the 4100 ExoScan is equally effective in measuring how well the surface of a peel ply released CFRP structure is treated and activated via plasma treatment to support optimal bonding of CFRP parts.

Composite parts are commonly formed using pre-preg that is cured in place around molds to form the desired shape. The process consists of placing the pre-preg between layers of other materials and then subjecting the entire system to a vacuum. A peel ply (release fabric) layer is used to prevent the composite laminate from adhering to the other layers. This layer contains a chemical release agent, typically a polydimethyl silicone (PDMS) formulation or a hydrocarbon based formulation (wax). After the peel ply layer is removed from the formed CFRP part, inevitably some of the release agent is left on the part and this must be treated and the surface activated to achieve optimal bonding. Surface treatment and activation is conducted using radio frequency generated plasma. If the CFRP part is either under treated or over treated during the plasma cleaning process, the result will be an sub-optimal surface for bonding. Under treatment does not cause enough changes in the release agent while over treatment will change the release agent but additionally causes thermal damage to the CFRP. Under treatment causes the more severe adhesive failure with greatly reduced strength whereas over-treatment results in CFRP damage, but only moderate peel strength decrease. Therefore a fine balance of treatment is required to ensure that the surface is properly prepared and the degree of thermal damage in the CFRP is minimized.

The effectiveness of the plasma treatment is highly dependent on the speed at which the plasma nozzle traverses the CFRP surface as well as the distance the nozzle is from the surface. Small changes in either variable can lead to a significant diminishment in the effectiveness of the treatment. The intention of this study is to demonstrate that a handheld FTIR can non-destructively detect and measure chemical changes in CFRP surfaces induced by plasma treatment and subsequently provide an objective measurement of the effectiveness of the plasma treatment via a multivariate prediction algorithm.

Experimental

Materials, methods and instrumentation

To test the ability of portable FTIR systems such as the 4100 ExoScan and the recently introduced 4300 Handheld FTIR (see sidebar) to measure the effectiveness of the plasma treatment, an experimental protocol has been employed which uses the measured G1c values from the adhesive peel-strength testing of CFRP bonded to CFRP. Changes in the FTIR spectrum of the CFRP test strip were measured as a function of the distance of the plasma nozzle from the surface, as it traversed the coupon at a constant horizontal velocity and progressively changing vertical distance. In this manner, the full range of over-treated, optimally treated and under-treated surface was available for measurement by the FTIR system. CFRP treated surfaces contained PDMS or wax release agents and were tested with the 4100 ExoScan FTIR after the above plasma cleaning protocol. The FTIR system was equipped with the high collection efficiency diffuse reflectance sample interface (Figure 1). All FTIR spectra consist of 128 co-added interferograms, which took approximately 1 minute to acquire at 8 cm^{-1} resolution.

Figure 1. Agilent 4100 ExoScan FTIR spectrometer equipped with diffuse reflectance sample interface for measurement of composites

CFRP samples were plasma treated after removal from the mold. Several CFRP coupons were prepared that had both residual PDMS or wax based release agents on the surface. The plasma nozzle traversed each CRFP coupon at a constant speed (6 cm/sec) and the full sweep of the surface took approximately 4.5 sec. The distance of the nozzle from the coupon surface was pre-programmed to change from 20.5 mm to 5 mm (Figure 2). The largest vertical distance (greatest gap size) creates a condition in which the surface is under treated and remains well under 100 °C in temperature. The smaller gap sizes, for which the nozzle is close to the surface, creates an over-treated condition, and the transient temperature at the surface exceeds 260 °C. Twenty infrared measurements were made along the coupon and these spectra were representative of the different temperature conditions experienced at the surface. Several adhesive peel strength measurements were made on a number of sections of the coupons that were exposed to various nozzle heights.

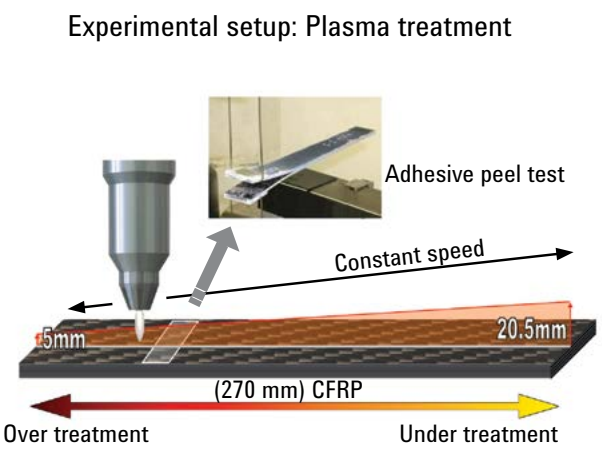

Figure 2. Plasma nozzle traverses CFRP coupon at fixed speed at continually decreasing distance from surface to induce temperature variation. Smallest plasma gap from surface creates highest temperature conditions. G1c value is collected from the adhesion peel measurements that were made with an Instron 5566 Universal Testing Machine. The CFRP laminate is 270 mm long. Two sections are bonded together with adhesive for the peel test.

Optimized Handheld FTIR Developed for Composite Analysis

Agilent has introduced the next generation handheld FTIR for the measurement of composite based products. The 4300 Handheld FTIR is a result of extensive R&D efforts in the area of non-destructive, material analysis by mid infrared spectroscopy.

Light weight. At 4.8 lbs (2.2 kg), the 4300 FTIR is the lightest handheld FTIR in existence. Make measurements for longer periods with less physical strain.

Balanced. With a center of gravity located at the handle, the system is comfortable to use. Take more accurate and precise measurements.

Rapid Scanning. With the optional MCT detector, the 4300 FTIR enables measurements to be made rapidly. Scan large surface areas in less time.

Non-destructive. The handheld spectrometer is brought to the object or surface to be measured. No need to excise a sample to be analyzed in a lab.

Immediate results. At-site analysis lets you make decisions in real-time. Focus on the measurement locations of greatest importance.

Versatile. A selection of interchangeable, no alignment sampling interfaces are available to analyze a wide range of materials and surface types.

Intuitive. Easy-to-use software guides all users to obtain great data. Preprogrammed methods, powered by advanced mathematical models, and reporting features all function automatically behind the scenes.

Temperature was independently measured as a function of the distance from the nozzle tip to the surface of the CRFP using a thermal camera with recording sensors measuring time and temperature. The measured flux is influenced both by the horizontal velocity and the nozzle height therefore as the plasma gets nearer to the surface, the temperature increases (Figure 3).

Results and discussion

The spectra of residual release agent, recorded when the plasma nozzle was at minimum and maximum distance from the coupon surface, exhibit subtle changes (Figure 4). In analyzing these spectra, certain regions are informative. For example, the broad vibrations at 3400 cm^{-1} arise from the O-H stretching modes; 3100 cm^{-1} bands are related to aromatic – H stretch; 2900 cm^{-1} from methyl/methylene stretch (alkyl), 1720 cm^{-1} from the carbonyl stretch; 1580 cm^{-1} and 1340 cm^{-1} are associated with secondary alcohols — the height of the former bands diminish with increasing temperature (i.e., bond/functional group destruction or changes) while the carbonyl band increases with rising temperatures, resulting from plasma-induced thermal damage.

These spectra indicate that for CFRP treated with either PDMS and wax release agent, there are signs of oxidative damage when the nozzle is closest to the surface (highest temperature condition) as evidenced by the increased intensity of a carbonyl peak at ca. 1720 cm^{-1}. Also, there is a noticeable drop in the O-H stretching vibration at 3300 cm^{-1} in both the PDMS and wax based release agent treated samples.

Fully cross-validated multivariate partial least squares was used to analyze the relationship between measurement position on the coupon (which in turn relates to nozzle gap and temperature to which the

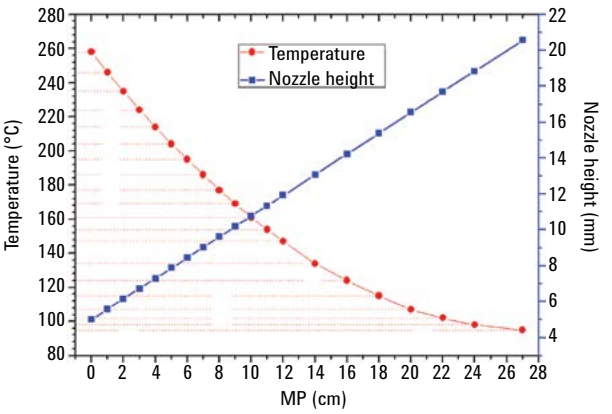

Figure 3. Nozzle height position and corresponding temperature as a function of measured positions (MP) on CFRP coupon.

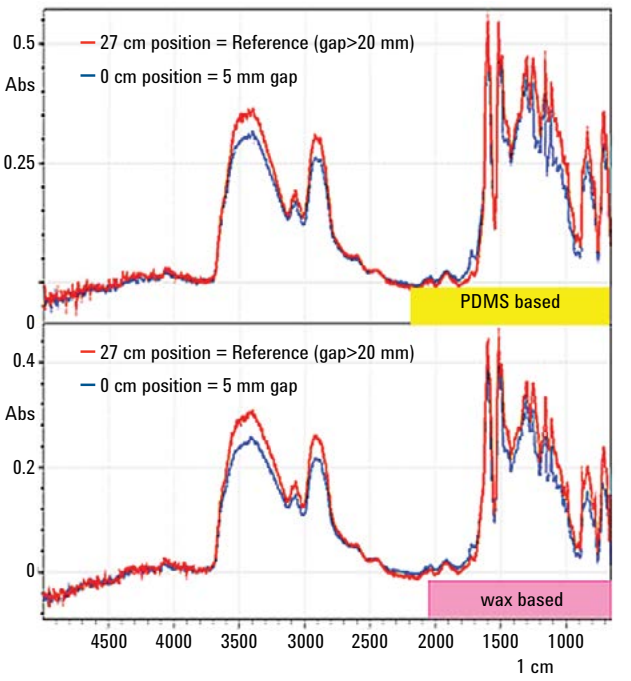

Figure 4. Infrared spectra of residual PDMS and wax release agent atop CFRP. The PDMS and wax formulations share some similarities spectrally since the PDMS formulation contains many wax-based compounds as well as PDMS.

surface is exposed) and changes in the spectra. To develop this model, 560 wavenumber points in the 780–1850 cm^{-1} region and the 2715–3700 cm^{-1} region were used. In order to optimize the model, the position on the coupon was measured via a ruler. The spectral files were recorded with the smallest nozzle gap (5 mm) corresponding to 00 cm on the coupon and the largest nozzle gap (20.5 mm) corresponding to 27 cm from the starting point. The actual versus predicted plot (Figure 5) demonstrates very good agreement and the model is able to predict within +/- 1 cm of the position on the coupon (i.e. amount of treatment) for the PDMS based release agent, as an example.

Adhesive peel strength measurements, combined with % silicon values from XPS analysis, were used to determine the under, optimal and over treatment regions of the test coupons. This information was then applied to the predicted values generated from the PLS model. The result (Figure 6) is an effective representation of the optimum plasma treatment zone, which contains only cohesive failure modes and therefore superior strength. The other zones, which demonstrate mixed or adhesive failure, were correspondingly colored yellow or red to signify warning or critical levels. The over treated region yields mixed mode failure as well as thermal oxidation of the CFRP, and is therefore in the critical zone.

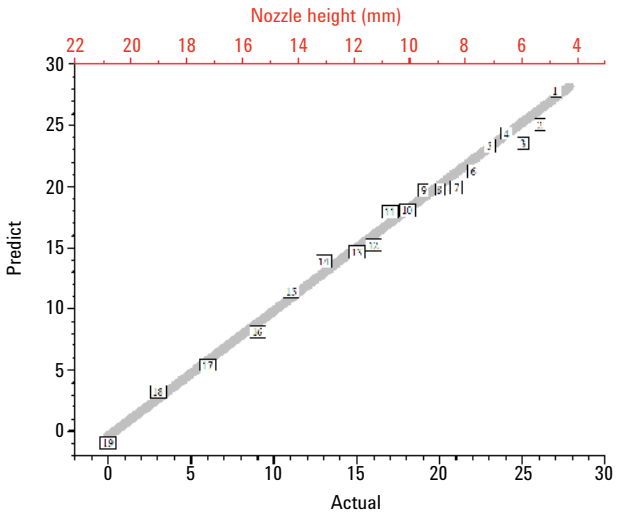

Figure 5. PLS multivariate analysis correlating infrared spectra as a function of position (i.e., nozzle height and temperature) on CFRP coupon for the PDMS based release agent. The cross-validated PLS model used three factors in the final optimized prediction model.

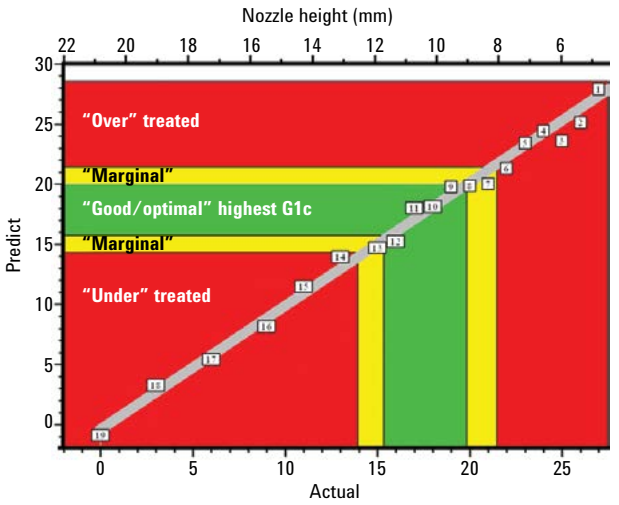

Figure 6. Independent adhesion peel tests and % silicon data were used to define the different regions of treatment and the spectra based PLS model was overlaid on these zones. The zones are readily differentiated by the PLS model, which reflect a number of subtle spectral changes. In the narrow green band, the G1c from the adhesive peel measurements is optimal for the nozzle height, velocity and type of plasma employed, as well as the region where the temperature reached does not degrade the CFRP substrate.

Conclusion

Portable FTIR systems, such as the 4100 ExoScan and the recently introduced 4300 Handheld FTIR, equipped with a diffuse reflectance interface provide valuable information for monitoring plasma treatment to ensure removal of CFRP peel layer release agent. We have demonstrated that plasma treatment of CFRP surfaces containing PDMS or wax based release agents result in spectral changes associated with partial removal of the agent, as well as chemical bond changes. A multivariate PLS model was developed that correlates spectral changes with nozzle position on the CFRP surface. Thus, this model relates to the temperature flux that the surface is experiencing and the chemical changes that result. The PLS model for plasma nozzle position (i.e., corresponding heat flux) compares quite well with the results from adhesive peel ply measurements. The information from this work also compares favorably to XPS measurements, which show the effect of increasing and decreasing silicon concentration on experimentally determined adhesive peel strength G1c values.

Acknowledgement

Agilent Technologies, Inc. gratefully acknowledges the contributions of the scientists and engineers at Airbus Group Innovations for data, information and discussion associated with this project.

Measure Release Agent on a Polymer Reinforced with Carbon Fiber

The Agilent 4100 ExoScan Handheld FTIR

Application Note

Materials Testing and Research

Authors

Pik Leung Tang, Alan Rein

Agilent Technologies, Inc.

Introduction

Release agents are applied as a liquid that forms a thin film coating to aid removal of carbon-fiber-reinforced polymer (CFRP) parts from a mold or peel ply. This process, however, leads to inevitable contact transfer, causing release agent to remain on the part or repair. Before painting or bonding of the CFRP component to other structures, proper post-treatment to remove vaporizable components of the release agent is required. Improper or inadequate post-treatment leads directly to reduction of bond strength of joined parts or topcoat paint adhesion.

The complexity of CFRP systems requires the use of new nondestructive analysis technologies such as FTIR spectroscopy, for the analysis of the surface matrix of the material. The primary objective of this application note is to demonstrate that FTIR spectroscopy can nondestructively measure the level of release agent on a carbon fiber epoxy system before bonding. The analysis uses an Agilent 4100 ExoScan FTIR. This handheld spectrometer enables *in-situ* inspection during manufacturing, in-service, or repair environments, or *ex-situ* in a laboratory. The analysis is accomplished in less than 1 minute and does not require any sample pretreatment.

This work was part of a joint project commissioned by the European Union entitled ENCOMB (extended nondestructive testing of composite bonds) [1].

Materials and Methods

The CFRP system was a T700 carbon fiber incorporating M21 epoxy with resultant coupons of six unidirectional layers. This fiber/polymer combination is an advanced formulation designed for extreme aeronautical performance. The release agent was a Henkel Frekote 700NC formulation. The release agent formulation contains 1 to 3% polydimethylsiloxane (PDMS) with the remaining consisting of various volatile and nonvolatile hydrocarbons.

Further details of the treatment scheme and the mechanical testing of bond strength are reported in research articles by ENCOMB consortium members [2,3,4]. The project examined the effects of four contamination scenarios on bonding CFRP with Cytec FM300 K.05 film adhesive by mechanical and instrumental measurement. The contamination scenarios were release agent [5], moisture uptake, aqueous acidic extract of a fire-resistant, phosphate-ester hydraulic fluid, and thermal damage. Bonded CFRP coupons were mechanically tested for bond strength by calculation of the critical strain-energy release rate (Glc). This parameter was calculated from analysis of the stress-strain curve. The Glc is directly related to the energy required to fracture the bonded CFRP, and is, therefore, often seen informally as the bond strength. Mechanical tests were performed using an MTS Universal Testing Machine in compliance with ISO 15024 and 25217.

For FTIR measurements, an Agilent 4100 Handheld ExoScan equipped with a diffuse reflectance sample interface was used. The 4100 ExoScan is the Agilent first-generation handheld FTIR spectrometer, and has been used extensively for the measurement of composites and polymers, as well as in surface analysis applications. More recently, Agilent introduced the Agilent 4300 Handheld FTIR, which has the superior performance characteristics of the earlier system, but is lighter in weight and ergonomically improved.

Each CFRP coupon was measured at a minimum of 16 discrete sampling points resulting in 71 spectra. The spectra consisted of 128 coadded interferograms measured at 8 cm^{-1} resolution giving a measurement time of 40 seconds for each point. The complexity of the release agent formulation [5], treatment, and CFRP system required the use of multivariate analysis (MVA) to develop a model based on the FTIR spectra. FTIR spectra of the release agent on the CFRP coupons' spectra were split into two groupings for processing by MVA. Fifty-five spectra were used to develop a cross validated model, and 16 were used as validation spectra. The results of the FTIR analysis were compared to measurement of percentage silicon present on the surface, as determined by X-ray photoelectron spectroscopy, the accepted consortia reference method.

Results and Discussion

The ENCOMB project measured the effect of four treatment scenarios with various levels on the Glc critical energy of fracture. These included the amount of residual release agent, water/moisture uptake, pH of acidic extract, and thermal damage. Figure 1 is a graph of Glc versus treatment severity for the four contamination scenarios. Treatment severity is defined by increasing levels of the respective treatment scenario. For release agent, the increasing severity value reflects increasing levels of surface contamination, from 1 (2.2% silicon) lowest, to 4 (10.5% silicon) highest. The highest severity level has a resultant Glc value of 40 J/m^2. This represents a significant drop of the Glc value at the lowest severity level 1 of 1,036 J/m^2. Of the four different treatments, the graph clearly shows that bond strength is most affected by the level of residual release agent present. The color-coding in Figure 1 is based on current best practice for acceptable strength ranges and includes mechanical error and guideline bond strength.

A

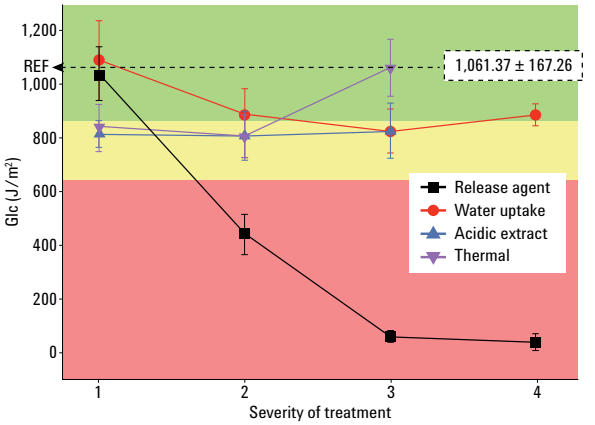

B

Treatment scenario	Treatment severity level 1	2	3	4
Release agent (% Si)	2.2 ± 0.3	6.7 ± 0.2	8.4 ± 0.8	10.5 ± 0.3
H_2O uptake (% mass increase)	0.46	1.84	1.19	1.29
Acidic extract of FRHF (pH)	4	3	2	
Thermal degradation (°C)	190	200	210	

Figure 1. Glc bond strength versus release agent, water/moisture uptake, pH of acidic extract, thermal damage, and treatment severity, where 1 is the lowest severity and 4 is the highest severity (A). The dotted line represents a Glc value of 1,061.37 J/m^2, which is the reference bond strength of an optimally treated bonded carbon-fiber-reinforced polymer. The table (B) shows the four treatment scenarios versus their severity levels and the individual treatment values.

The measurement of the percentage silicon present on the surface of CFRP by X-ray photon spectroscopy (XPS) is a commonly used method for determining the amount of residual PDMS release agent. The relationship between that value and the GIc is well characterized and, as the percentage silicon increases on the composite surface, the mechanical strength of the bond decreases (Figure 2B). In this study, four levels of treatment were applied to provide a range of residual percentage silicon on the CFRP coupon, from 2.2 to 10.5%, as determined by XPS. Figure 2 shows the average FTIR spectra that result from the four treatment levels, and the effect on bond strength with increasing residual release agent on the CFRP surface.

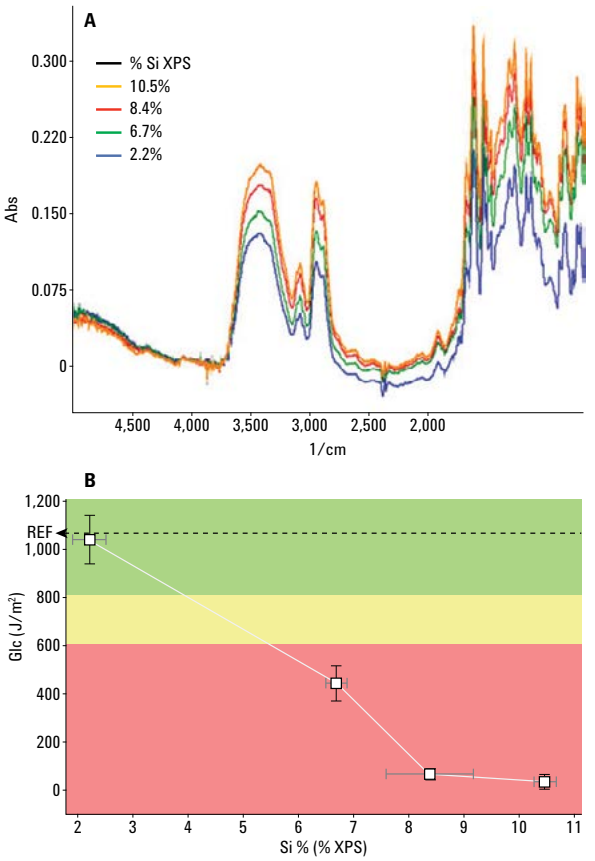

Figure 2. Averaged FTIR spectra of four release agent treatment levels (A) and the percentage silicon determined by X-ray photoelectron spectroscopy. The resultant effect on the (GIc) bond strength and the associated errors from multiple measurements are shown in B.

To correlate the FTIR spectra for the different levels of treatment with the percentage silicon, as determined by XPS, a partial least squares (PLS) model was implemented that required several preprocessing steps. Multivariate modeling of FTIR [6,7] spectra was effective for measuring several CFRP-related chemical changes, such as those resulting from thermal damage, and proving the efficacy of plasma treatment for surface preparation of CFRP before bonding. In this release agent study, the resultant cross-cross validated PLS model was optimal using four factors, as shown in a graph of the standard error of cross validation versus number of factors (Figure 3A). The percentage silicon predicted by the PLS model calibration and validation spectra for the four treatment levels is shown in Figure 3B at approximately ¾:¼.

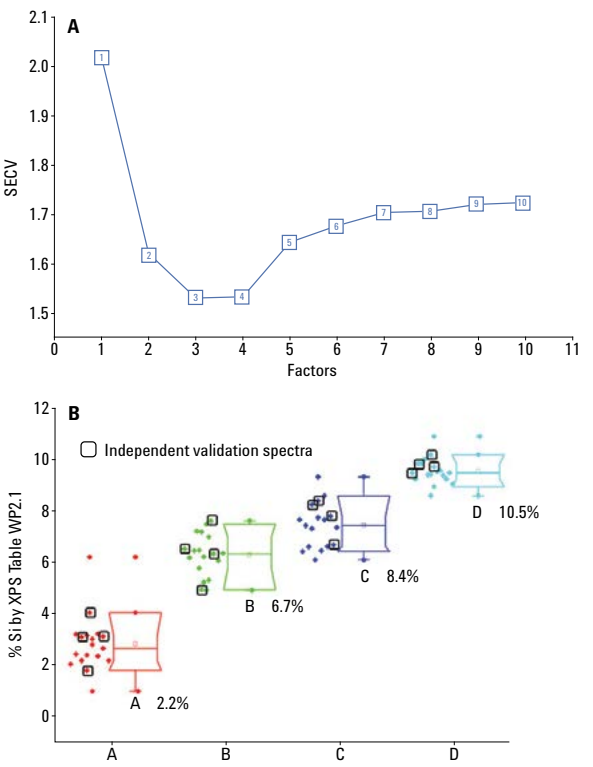

Figure 3. Standard error of cross validation versus number of factors (A), four treatment levels, and their partial least squares predicted values (B). The boxed black values are the validation spectra set aside to independently test the partial least squares model.

The MVA model PLS regression has an R = 0.96, which is very encouraging for such a complex system. The 4100 ExoScan results yielded a strong correlation between multivariate spectral changes and the percentage of silicon, when cross referenced with XPS results (Table 1).

Table 1. Percentage silicon on a carbon-fiber-reinforced polymer coupon as determined by X-ray photoelectron spectroscopy and percentage silicon as predicted from FTIR spectra using a multivariate method with the Agilent 4100 ExoScan Handheld FTIR.

Treatment level/severity	% Si XPS	% Si XPS and Agilent 4100 ExoScan Handheld FTIR
1 (A)	2.2 ± 0.3	2.5 ± 1.07
2 (B)	6.7 ± 0.2	6.3 ± 0.81
3 (C)	8.4 ± 0.8	8.3 ± 0.87
4 (D)	10.5 ± 0.3	10.1 ± 0.51

Conclusions

Of the identified treatment scenarios, the residual release agent had the most deleterious effect on bonding strength. If CFRP components are left untreated, or partially/poorly treated and then bonded, there is often a drastic loss in the tensile strength of the bond. If the CFRP part is coated, rather than bonded, then the peel strength/adhesion strength of the coating will be adversely affected. The importance of ensuring that surfaces are properly prepared before further manufacturing operations cannot be overstated, as witnessed by the dramatic drop in GIc bond strength caused by increasing amounts of remnant release agent.

In this application note, we successfully demonstrated the ability of an Agilent 4100 ExoScan Handheld FTIR analyzer to measure accurately the amount of release agent remaining on the surface of a CFRP panel in a fully nondestructive manner. We have 'trained' the FTIR analyzer with a model to predict the percentage Frekote 700NC on an advanced CFRP T700/M21 system to within 1 to 2% silicon as correlated to XPS results. The PLS-calibrated model can be incorporated into a "pass/fail" method that quantifies and categorizes the result to indicate the severity level in a color-coded manner. This enables the direct determination of whether the removal of release agent from the surface of a CFRP component is complete, independent of other physical, chemical, or mechanical criteria.

The 4100 ExoScan Handheld FTIR analyzer is useful for this measurement since it is portable and requires no sample preparation. In addition, due to the onboard method, it can be used by individuals with varied experience levels to get accurate results. This allows the system to be used in manufacturing quality assurance and maintenance applications for rapid, direct measurement of a CFRP component. In addition, as demonstrated in previous studies, the FTIR analyzer can ascertain that surface areas are properly treated by plasma cleaning, and detect and measure thermal damage in CFRP.

New and appropriate methods of nondestructive quality assurance, such as the portable FTIR and interface system, are vital as carbon fiber composite technology becomes more common in vehicles of all types, aerospace, and consumer products.

Acknowledgement

This research received funding from the European Union's Seventh Framework Programme for research, technological development, and demonstration under grant 266226.

References

1. www.encomb.eu
2. Markatos, D. N; Tserpes, K. I; Rau, E; Ehrhart, B; Pantelakis, S. The effects of manufacturing-induced and in-service related bonding quality reduction on the mode-I fracture toughness of composite bonded joints for aeronautical use. *Compos. Part B: Eng*. **2013**, *45 (1)*, pp 556-564.
3. Markatos, D. N; Tserpes, K. I; Rau, E; Pantelakis, S. Degradation of mode I fracture toughness of CFRP bonded joints due to release agent and moisture pre bond contamination. *J. Adhesion* **2014**, *90 (2)*, pp 156-173.
4. Markatos, D. N; Tserpes, K. I; Chamos, A; Pantelakis, S. The combined effects of pre-bond contamination accelerated aging and high temperature on the mode-I fracture toughness of CFRP bonded joints. In *Proceedings of the 3rd International Conference of Engineering Against Failure (ICEAF III)*, Kos, Greece, 26-28 June, **2013**.
5. http://mymsds.henkel.com/mymsds/Search.do?BUSAREA=0006&DOCTYPE=MSDS&COUNTRY=GB&LANG=EN&MATNR=380957
6. Higgins, F. Non-Destructive Evaluation of Composite Thermal Damage with Agilent's New Handheld 4300 FTIR; *Agilent Technologies Application Note*, publication number 5991-4037EN, **2014**. http://www.chem.agilent.com/Library/applications/5991-4037EN.pdf
7. Rein, A; Tang, P. L. Analysis of plasma treated carbon fiber reinforced polymer (CFRP) composites by portable Fourier Transform Infrared Spectroscopy (FTIR); *Agilent Technologies Application Note*, publication number 5991-4033EN, **2014**. http://www.chem.agilent.com/Library/applications/5991-4033EN.pdf

For More Information

These data represent typical results. For more information on our products and services, visit our Web site at www.agilent.com/chem.

UV-VIS-NIR MEASUREMENTS

THE AGILENT CARY 7000 UMS

The Agilent Cary 7000 UMS allows you to measure virtually any sample; measure absolute reflectance and transmission at any angle; and measure them all unattended.

This includes:

- **Achieve complete sample characterization**, measuring both absolute reflection and transmission in a single sequence — at variable angles and polarization — without moving or disturbing the sample.
- **Achieve fast data collection times** — reducing your analysis from days to hours or hours to minutes — with direct-view detection and single baseline productivity.
- **Obtain new insights** into advanced materials with an unprecedented 10 Abs range.

The Cary 7000 UMS offers the following six modes of measurement – all automated and performed unattended.

1 **Specular (direct) reflectance**
Measuring the mirror-like reflection (or gloss) from a surface, usually at 90° to the incident beam.

2 **Diffuse Reflectance**
Measuring the light reflected from a surface at many angles to the incident beam.

3 **Glossy scattering**
Measuring the light reflected from a surface across a narrow band of angles around 90° to the incident beam.

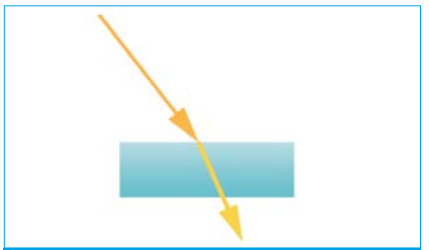

4 **Transmission**
Measuring how much of an incident beam passes directly through the sample.

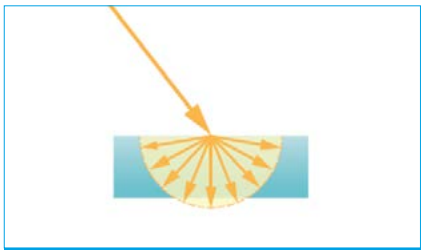

5 **Scattered transmission**
Measuring how much light passes through a sample, at all angles to the incident beam.

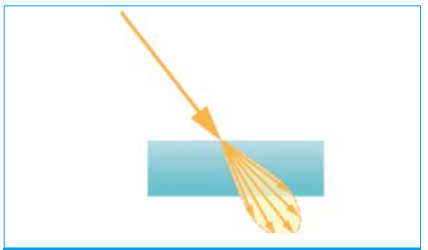

6 **Partially scattered transmission**
Measuring the light transmitted through a sample across a narrow band of angles to the incident beam.

Automated Spectrophotometric Spatial Profiling of Coated Optical Wafers

Application note

Materials testing and research

Authors

Travis Burt
Fabian Zieschang
Agilent Technologies, Inc.

Parts of this work have already been published in:
Burt, T., Zieschang, F. "Optical Coating Uniformity of 200 mm (8'') Diameter Precut Wafers", Optical Interference Coatings (OIC) OSA Meeting, USA (2016).

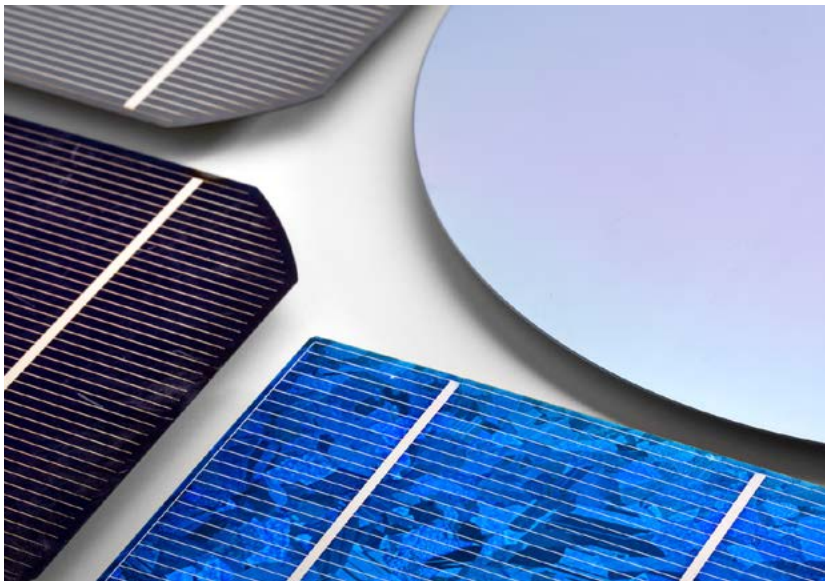

Introduction

Frequent and cost effective spectroscopic characterization is important in the development of competitive optical thin film coatings. Fully automated and unattended spectroscopic measurements can help reduce cost-per-analysis, increase productivity, and help expand quality assurance programs. In the manufacturing process, large, usually circular substrate wafers are coated in deposition chambers that usually operate at full capacity. An efficient and productive optical characterization tool needs to deliver accurate and meaningful information at user-defined points across the surface of the wafer before it is cut. The Agilent Solids Autosampler,

designed for the Cary 7000 Universal Measurement Spectrophotometer (UMS) and Universal Measurement Accessory (UMA), can mount samples up to 200 mm (8'') in diameter and provide angular absolute reflection and transmission data in the UV-Vis and NIR spectral range.

The capabilities of the Cary 7000 UMS, together with the autosampler, have been previously demonstrated for the automated and unattended analysis of multiple samples mounted in a 32x sample holder [1] and spatial mapping of a linear energy band gap gradient of a zinc tin oxide (ZTO) layer [2]. This study examines the use of the Cary 7000 UMS with autosampler for automated, angular resolved mapping, of the coating uniformity across a 200 mm diameter wafer.

Instrumentation and sample

Cary 7000 UMS UV-Vis/NIR spectrophotometers (Figure 1) are designed to perform multi-angle photometric spectroscopy (MPS) measurements over a wavelength range of 250 nm to 2500 nm. In MPS applications, the absolute reflectance and/or transmittance of a sample is measured over a wide range of angles of incidence from near normal to oblique [3]. Recently, MPS data has proved helpful for reverse engineering complex thin films [4], gaining deeper insights into oscillations in the total losses in thin dielectric films [5], and improving reverse engineering strategies applied during coating production steps [6].

The simple but versatile design of the UMA allows it to position the sample and the detector at any angle, independently of each other, without operator intervention. In a single sequence, the UMA acquires both transmission and reflection data from exactly the same patch of a sample's surface at variable angles of incidence (θ_i) in the range $5° \leq |\theta_i| \leq 85°$ (that is, angles on either side of beam normal noted as +/-). Adding an automated polarizer based on nano-wire grid technology makes it possible to obtain accurate measurements at S, P, or any user-specified polarization angle.

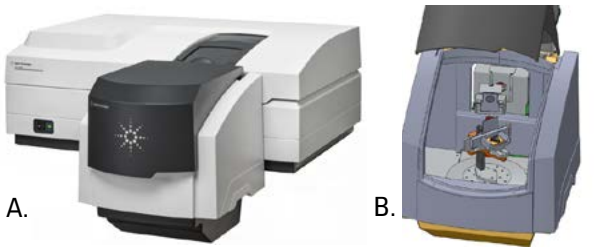

Figure 1. A. Agilent's Cary 7000 UMS. B. The Universal Measurement Accessory, as standard on the Cary 7000 UMS. The UMA is a true multi-modal measurement system capable of absolute reflectance, transmission and scattering analysis.

The centerpiece of the Cary 7000 UMS, the Cary Universal Measurement Accessory (UMA), is available separately to upgrade existing UV-Vis-NIR spectrophotometers from the Cary family, including the 4000, 5000, and 6000i.

Autosampler

The Agilent Solids Autosampler is an independently controlled sample holder especially designed to work with the UMA. The autosampler mounts inside the large UMA sample chamber over the axis of rotation of the sample stage. In this way, the autosampler doesn't limit the basic functions of the UMA. In fact, it enhances the measurement capabilities by adding two degrees of freedom to the sample position. As seen in Figure 2 these additional degrees of freedom are in radial (z) and rotational direction (Φ) about the incident beams axis (I_o). Depending on the type of sample, a variety of sample holders allow mounting of multiple individual samples (up to 32 x 1 inch diameter), or single large diameter samples (up to 200 mm, 8 inch diameter). That makes the Agilent Solid Autosampler the ideal upgrade to the Cary 7000 UMS for the optical characterization of large sets (batches) of optical components or the spatial mapping of larger individual samples down to a practical resolution limit of 2 mm x 2 mm.

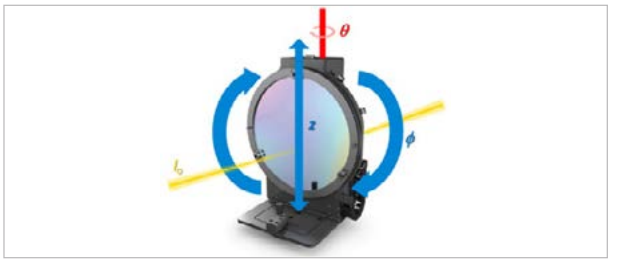

Figure 2. MPS(θ_i,Φ, z) co-ordinate system of the Agilent Solids Autosampler with respect to incident beam *I*o.

Sample holder

The 8-inch round sample holder securely mounts the sample into the autosampler, so the sample holder touches the sample only by a 3.0 mm ring around the edges and three (removable) spring-loaded clamps which minimizes sample contact and upholds the integrity of the sample. This is of great importance for sensitive end products and coated precursors alike.

Figure 3. A 200 mm diameter precut wafer mounted in the 8'' sample holder that attaches into the Solids Autosampler.

Figure 4. Front view of the Cary 7000 UMA sample compartment with the Agilent Solids Autosampler installed and the 200 mm diameter coated wafer mounted into the autosampler.

Experimental Details

Determining the measurement limits

Prior to the actual mapping experiment, we determined the radial limit of measurement optically, recording transmission signals at distances from 90 to 95 mm from the center position at 1 mm increments (Figure 5). A drop in the transmission signal at 95 mm diameter indicates the limit of measurement where the sample holder inner ring starts to obstruct the measurement beam. The maximum measurement point was set to 94 mm radius for all profiles to avoid beam obstruction. The optical interference coating on the wafer doesn't cover the entire substrate but reaches to about 3 mm to the edge of the wafer (Figure 5).

That means we could confidently measure 94% of the total coated wafer surface using the Solids Autosampler.

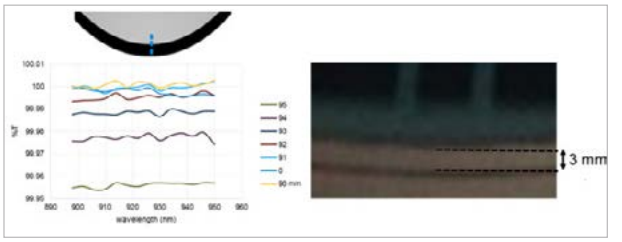

Figure 5. Left: The maximum measurable edge point was confirmed by measuring at 1 mm increments from 90 mm to 95 mm. A signal drop at 95 mm indicates the beam clipping the sample holder edge. Right: The coating reaches 3 mm from the edge of the wafer.

Reflection spectra

Although the Cary 7000 UMS can perform measurements at variable angles of incidence from 5° to 85°, we chose a 7° (near normal). Larger angles will spread the beam patch size on the sample surface, which leads to a reduced spatial resolution during mapping. We set the (adjustable) incident beam cone angles to 3° horizontal and 1° vertical (sample rotation takes place about the vertical axis) and used a 4 nm spectral bandwidth. These parameters lead to a beam patch of approximately 5.0 mm x 1.5 mm (height x width), which is slightly larger than the step size resolution of the autosampler (0.5° steps vertically and rotationally about the beam axis).

Table 1. Agilent Cary 7000 UMS measurement conditions used to acquire the reflection spectrum presented in Figure 4.

Parameter	Value
Angle of incidence	7°
Wavelength range	2500-250 nm
Data interval	UV/Vis 1.0 nm, NIR 4.0 nm
Spectral bandwidth	UV/Vis 4.0 nm, NIR 4.0 nm
Signal averaging time	0.5 sec
Polarization	s-polarization
Incident beam aperture	3° x 1° (vertical x horizontal)
Baseline correction	100% T

Wafer profiling

For the optical characterization of the coating surface, we configured the autosampler to drive the sample according to the mapping profile given in Table 2. The mapping profile consists of 8 chords through the wafer's diameter with an angular resolution of Φ= 22.5°. Each chord represents 27 spatial points spaced 5 mm apart, plus two smaller step intervals toward the edge at 92 mm and 93 mm (Table 2). We set the Cary 7000 UMS to perform short wavelength scans over the analytic wavelength at every measurement point. Once prepared, the Cary 7000 UMS and autosampler worked together—fully automated—to collect the desired data set.

Table 2. Mapping profile and collection conditions applied on the wafer profiling experiment.

Tuning parameter	Value
Angle of incidence	7°
Wavelength range	1065-1063 nm
Data interval	1.0 nm
Spectral bandwidth	4.0 nm
Signal averaging time	1 sec
Detector	silicon photodiode (manually set detector change)
Polarization	s-and p-polarization
Incident beam aperture	3°x1° (vertical x horizontal)
Baseline correction	100% T + 0% T

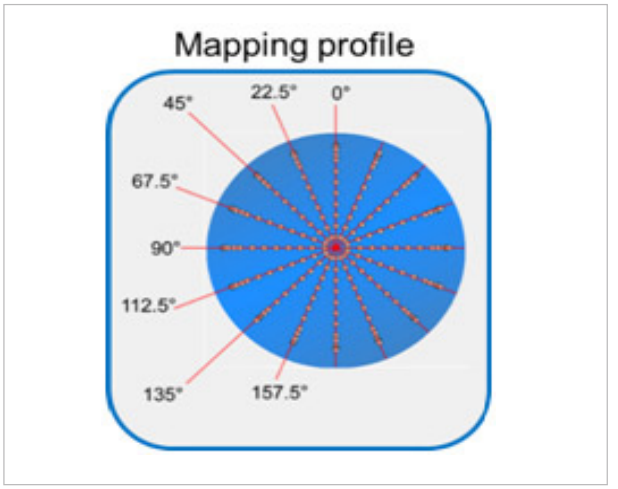

Results and discussion

Figure 6 shows the s-polarized reflectance spectrum from the UV (250 nm) to the NIR (2500 nm) of the coated wafer. We took the spectrum from a spot in the center of the wafer because that is where the quality of the coating can be expected to be best. The spectrum clearly shows the design intent of the optical interference coating with reflection around 1064 nm exceeding 99% over a narrow 950 nm to 1150 nm band pass.

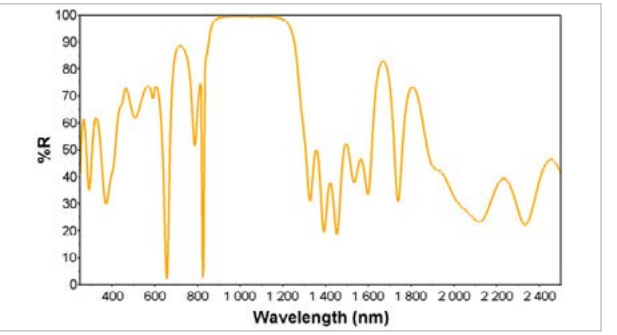

Figure 6. The Rs spectrum of wafer center at 7° angle of incidence

In the mapping experiment, we used the Cary 7000 UMS and the autosampler to collect the reflection characteristics of the wafer at 1064 nm in s- and p-polarization following the mapping pattern given in Table 2. Figure 7 shows the mapping profiles we obtained with the reflection values at 1064 nm plotted against the distance of the measurement point from the center. These profiles reveal a decrease in reflection from the wafer center toward the edge in both s- and p-polarization. The high similarity and consistency between individual profiles indicate a centrosymmetric optical contour of the wafer. Outliners at 80 mm diameter on the 90° chord and at 85 mm on the 67.5° chord both in Rs and Rp could be directly attributed to contamination on the wafer surface by subsequent visual inspection.

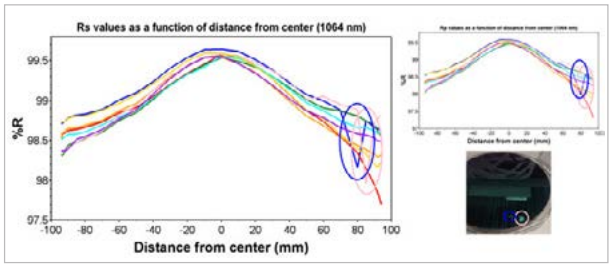

Figure 7. Mapping profiles (%Rs: left and %Rp: right, top) at 1064 nm.

The center position of the wafer was measured repeatedly as part of each chord, and this data was used to estimate reproducibility of the measurement (Figure 8). A reproducibility of <0.1% was achieved over the time course of the mapping experiment (~6.5 h), which is about 10 times better than the %R differences found between points at the center and at the edges (up to 1%). That not only demonstrates the long-time stability of the Cary 7000 UMS but also underlines the significance of the presented profiles.

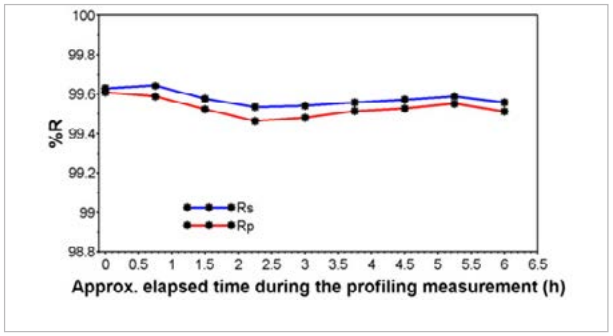

Figure 8. Variability of the system during the time course of the mapping experiment

Conclusions

In this study, we used the Agilent Cary 7000 UMS with Solids Autosampler to successfully analyze the coating uniformity across a 200 mm diameter precut wafer. The system was setup to execute %R measurements centered around 1064 nm in a user-defined pattern across the wafer's surface. The resulting profiles revealed a decrease in coating quality toward the wafer's edges. This knowledge could be used to find and overcome the underlying variability in the coating process.

This mapping analysis could be used for quality control or it could be implemented in development processes to maximize yields and minimize waste and investment. The true-to-life example used for this application note serves to prove the extensive capabilities of the Cary 7000 and Solids Autosampler for automated routine multi-angle spectroscopic characterizations of optical materials, coatings, and components in a wide range of industrial and laboratory applications.

References

1. Burt, T., Haq, F. "High volume optical component testing using Agilent Cary 7000 Universal Measurement Spectrophotometer (UMS) with Solids Autosampler", Application note Agilent Technologies, publication number 5991-4071EN (2014).

2. Burt, T., Haq, F. "Coated wafer mapping using an Agilent Cary 7000 Universal Measurement Spectrophotometer (UMS) with Solids Autosampler", Application note Agilent Technologies, publication number 5991-4072EN (2014).

3. Death, D.L., Francis, R.J., Bricker, C., Burt, T., Colley, C. "The UMA: A new tool for Multi-angle Photometric Spectroscopy", Optical Interference Coatings (OIC) OSA Topical Meeting, Canada (2013).

4. Tikhonravov, A.V., Amotchkina, T.V., Trubetskov, M.K., Francis, R.J., Janicki, V., Sancho-Parramon, J., Zorc, H. and Pervak, V. "Optical characterization and reverse engineering based on multiangle spectroscopy", *Appl. Opt*. 51, 245-254 (2012).

5. Amotchkina, T.V., Trubetskov, M.K., Tikhonravov, A.V., Janicki, V. J., Sancho-Parramon, Razskazovskaya, O. and Pervak, V. "Oscillations in the spectral behavior of total losses (1 – T – R) in the dielectric films", *Opt. Exp.* 20, 16129-16144 (2012).

6. Amotchkina, T.V., Trubetskov, M.K., Tikhonravov, A.V., Schlichting, S., Ehlers, H., Ristau, D., Death, D., Francis, J.J. and Pervak, V. "Quality control of oblique incidence optical coatings based on normal incidence measurement data", *Opt. Exp.* 21, 21508-21522 (2013).

Performance of compact visual displays — measuring angular reflectance of optically active materials using the Agilent Cary 7000 Universal Measurement Spectrophotometer (UMS)

Application note

Materials

Authors

Travis Burt, Huang ChuanXu*, Andy Jiang*

Agilent Technologies
Mulgrave, Victoria, Australia

*Agilent Technologies
Shanghai, China

Introduction

The prevalence of visual displays in everyday use continues to grow as the size, weight and power consumption is reduced and device mobility is subsequently improved. Optical displays, based on light emitting diode (LED) and liquid crystal display (LCD) technology finds broad industrial and domestic use. Examples of devices include mobile telephones, portable computers ranging from hand-held personal digital assistants (PDAs) to laptop computers, portable digital music players, LED/LCD desktop computer monitors, and LED/LCD televisions. In an industry where thickness improvements are measured in tens of microns, LED/LCD packages are becoming thinner as the manufacturers of electronic devices strive for smaller package sizes.

Displays use backlighting to illuminate the full display area and liquid crystals to control the timing and color of the emissions presented to the viewer (Figure 1). The backlighting often takes the form of a solid light guide in the shape of a slab or wedge. The illumination source can be cold cathode fluorescent (CCFL) lighting, more commonly referred to as an LCD TV, or LED based backlighting often referred to as an LED TV. Due to the importance of backlighting on picture quality, the labels overlook the fact that both TV types employ the use of LCD's to control images presented to the viewer.

The solid light guides used in backlighting are often made of an optically transparent polymeric material which is mass produced by, for example, injection molding. The optical and electrical efficiency of solid light guides are enhanced by the use of reflectors. The reflector films are strategically positioned to more efficiently utilize light that would otherwise exit the back surface of the solid light guide or the illuminating source (Figure 1).

Backlight reflectors used in light guides need to have a high reflectivity for efficient transport of light. Reflection values of >98% are typical reflectance targets as multiple (tens of) reflections through the light guide would otherwise quickly extinguish available light if much more than 2% was lost at each reflection event. Multilayer optical coatings are used to generate the high reflectivities of the thin reflector films. The physical properties of the films, which are typically <100 µm thick, can be of a non-metallic multilayer polymeric material which can result in surfaces with optical activity. Optically active materials rotate the polarization state of light on a transmission or reflection event. More common are materials that are optically inactive where polarization interactions introduced by the sample only act to subdue a particular polarization component such as S, or P, not rotate it. While optical activity will typically have no direct consequence in end-use applications inside the display, accurate optical characterization (QA/QC) of the reflector prior to assembly requires careful consideration of these effects to ensure correct %R and %T values are recorded at the detector.

Experimental

Samples

The sample measured was approximately 50 x 50 mm (w x d) and approximately 100 µm thick (Figure 2). The reflective surface was protected by a semi-transparent clear film which could be easily peeled off before measurements were taken. The thickness of the sample and its flexibility was accommodated during mounting

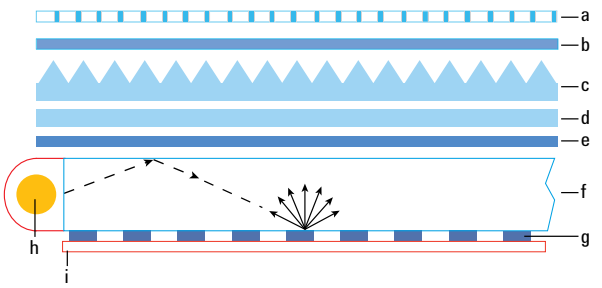

Figure 1. Cross section of products used in LCD construction:

a: LCD

b-d: Varying film types to increase backlighting efficiency

e: Diffuser

f: Light guide

g: Dots for extracting light from the light guide

h: Fluorescent or LED light source

i: Back reflector film (shown in red)

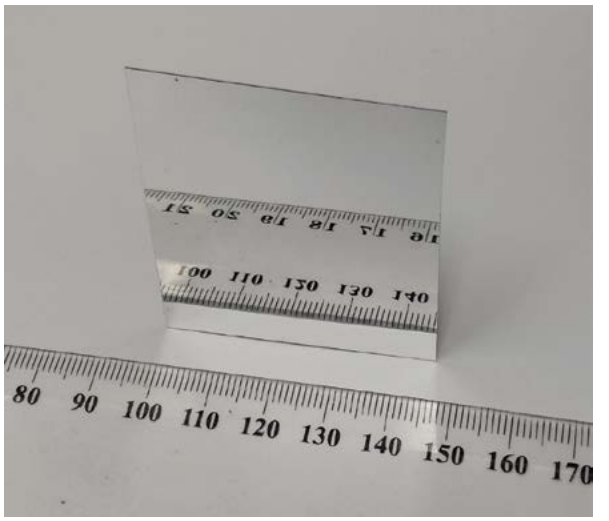

Figure 2. Reflector sample

to ensure that a flat surface was presented to the incoming beam.

Optical activity of the sample was demonstrated before measurement in the Cary 7000 UMS by illuminating the sample with s-polarized visible white light at angle, and viewing the specularly reflected beam from the sample by eye through a second polarizer. Maximum intensity of the reflected beam was observed by rotating the viewing polarizer a few degrees from the S (0 deg) position.

The angular off-set between the incident s-polarized light and the visually detected light confirmed optical activity, or optical rotation of the light. This practical test confirmed that a depolarizer would be required to be inserted before the detector during the spectrophotometric measurements.

Instrumentation

- Agilent Cary 7000 Universal Measurement Spectrophotometer, p/n G6873AA

The Cary 7000 Universal Measurement Spectrophotometer (UMS) is a highly automated UV-Vis-NIR spectrophotometer system. The UMS performs variable angle transmission and absolute reflectance measurements. The linearly polarized beam that is incident on the sample can be used to measure transmission, and by rotating the detector assembly about an axis through the sample and perpendicular to the plane of incidence, in reflection, as indicated in Figure 3.

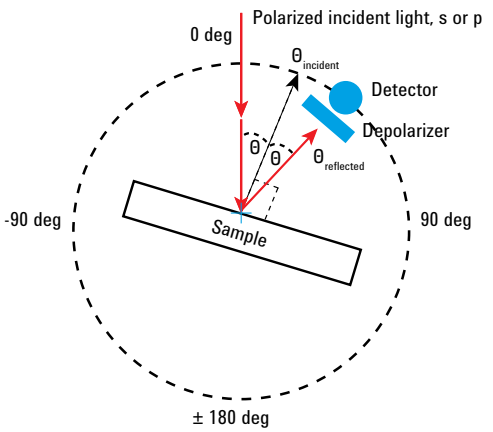

Figure 3. Schematic of the Cary 7000 UMS. Light incident onto the sample can be s, or p polarized. The detector module allows mounting of a depolarizer immediately before the detector. Absolute specular reflection of transmission can be measured

A depolarizer was placed after the sample but before the detector to correct for the optical rotation imposed on the reflected light by the sample. The depolarizer before the detector and the polarizer before the sample were included in the single baseline measurement taken before each sample collect was made. The Cary 7000 UMS only requires a single baseline to be collected for all %R measurements at any angle for a given polarization. This unique feature dramatically improves the speed of analysis and sample throughput possible on this system.

Results and discussion

Reflectance data was collected at four angles of incidence (AOI); 70, 60, 45 and 30 deg over the spectral range 300–1200 nm (Figure 4). The sample demonstrated its design intent by displaying reflectance >98%R over the visible wavelength range (400–800 nm) (Figure 5).

The multi-angle measurements showed consistent performance over a broad angular range in the region of interest (400–800 nm) and angular dependence outside this range (>800 nm). High AOI >60 deg also showed some diminishing of the %R quality in the 600–700 nm and 800–900 nm region. The spectral dependence of the %R profile at these angles demonstrates that some color alterations are to be expected for high angles of incidence.

The importance of depolarizing the light after the sample, but just before the detector, is demonstrated in Figure 6. In this figure, absolute reflectance is measured with and without the use of a depolarizer. Without the use of the depolarizer the optical activity of the sample causes the %R values to artificially exceed 100%. This is compared directly to the result where a depolarizer is used which corrects for the optical rotation of the light and gives the correct values.

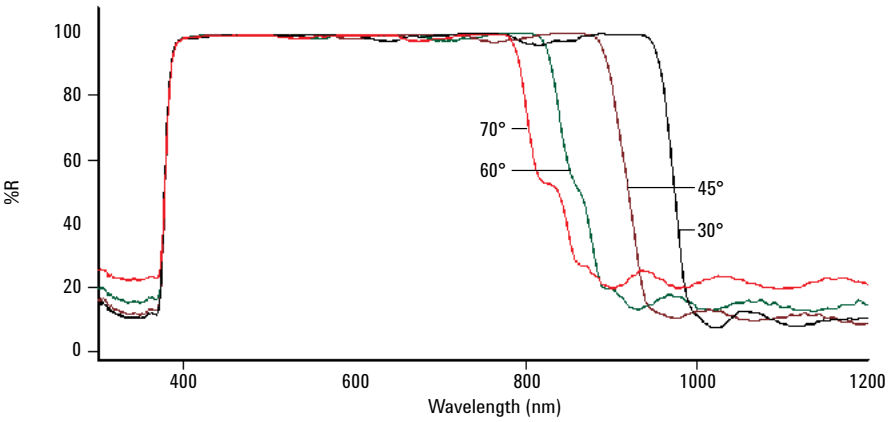

Figure 4: Reflection of backlight material at 70 (red), 60 (green), 45 (brown), 30 (black) degree s-polarized light

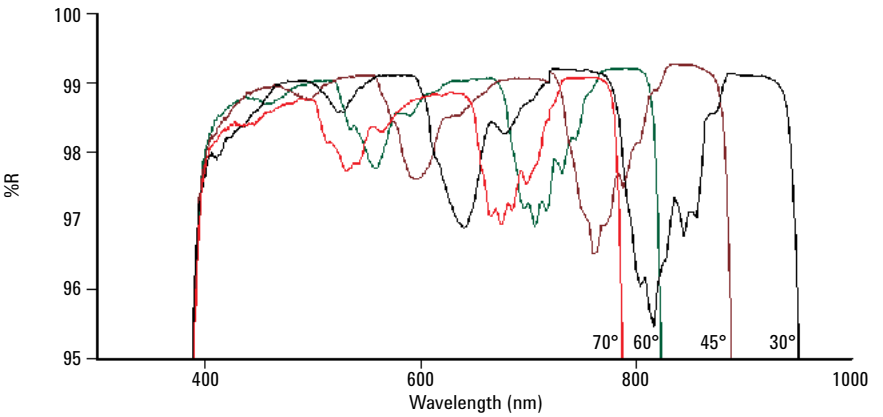

Figure 5: Magnified view of Figure 4 showing reflection of backlight material at 70 (red), 60 (green), 45 (brown), 30 (black) degree s-polarized light

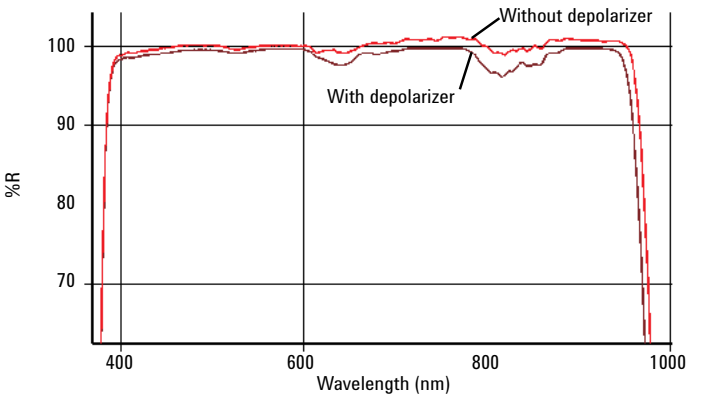

Figure 6: Demonstration of the importance of using a depolarizer after the sample but before the detector. Absolute reflection of backlight material at 30° s-polarized with a depolarizer before the detector (brown) and 30° s-polarized WITHOUT a depolarizer before the detector (red)

Conclusions

The Agilent Cary 7000 UMS was shown to be a valuable tool for measuring the optical properties of next generation materials used in optical displays. The optical rotation imposed by the specialized polymeric coating on the sample was accurately measured by using linearly polarized incident light and depolarizing the reflected light before it was detected and processed.

Optical characterization of thin films using a new Universal Measurement Accessory for the Agilent Cary UV-Vis-NIR spectrophotometers

Application note

Materials

Authors

Robert Francis and Travis Burt

Agilent Technologies
Mulgrave, Victoria, Australia

Introduction

A more detailed account of this work was first published in Applied Optics, 10 January 2012 / Vol. 51, No. 2.

The accurate determination of the optical parameters of thin films and multilayer coatings (using reverse engineering of optical coatings) is paramount to the manufacturing of high quality products. The data provides a feedback to the design/production chain. Reverse-engineering results — where each layer is assessed in turn — can be used to adjust deposition parameters, recalibrate monitoring systems, and improve control of the thicknesses of individual layers.

Typically, optical characterization is based on the analysis of normal- or near-normal-incidence transmittance (T) and/or reflectance (R) data of a thin film sample on a transparent substrate using UV-visible-near-IR (UV-Vis-NIR) or Fourier transform IR (FTIR) spectrophotometry. However, optical characterization based on normal incidence T and R measurements and reliable reverse engineering based on normal-incidence or near normal-incidence T and R measurement data is challenging.

In this application, we demonstrate the applicability of multi-angle spectral photometric data to the optical characterization of single thin films and the reverse engineering of multilayer optical coatings using a Cary 5000 UV-Vis-NIR spectrophotometer equipped with a new Universal Measurement Accessory (UMA). We consider dense thin films and a multilayer produced by magnetron sputtering, as well as electron-beam (e-beam) evaporated thin films, which are typically more difficult to characterize. This data could also be collected on the Agilent Cary 7000 Universal Measurement Spectrophotometer (UMS).

Experimental

Samples

For our study we measured two sets of experimental samples using two different deposition techniques: magnetron sputtering and e-beam evaporation. Details can be found in reference [1].

Instrumentation

- Agilent Cary 5000 UV-Vis-NIR spectrophotometer
- Agilent Universal Measurement Accessory

The UMA is a highly automated variable angle specular reflectance and transmittance system with full software control of the sample, detector and polarizer positions. It provides accurate, rapid and complete optical characterization of samples via transmission (%T) and absolute reflection (%R) measurements at various controllable angles of incident light (0–85 deg %T, 5–85 deg %R). The linearly polarized beam that illuminates the sample can be measured in transmission. It can be measured in absolute reflectance by moving the detector assembly in a plane at a constant radius from the sample. This multiple measurement mode capability of the UMA results in improved productivity and more precise characterization of samples. A schematic of the UMA is presented in Figure 1.

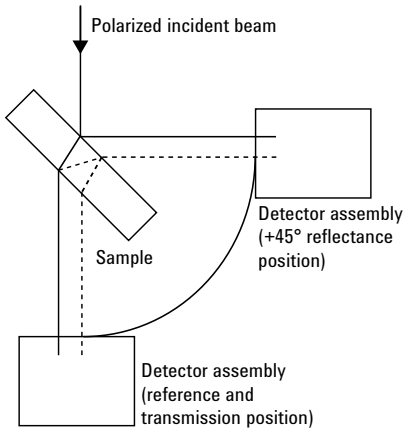

Figure 1. Schematic of the Agilent UMA, an absolute variable angle reflectance and transmission accessory

Results and discussion

Multi-angle spectral photometric measurements were performed for all samples in the spectral range from 300–2500 nm at incidence angles of 7°, 10°, 20°, 30°, and 40° for s- and p-polarized light. In all optical characterization and reverse-engineering procedures throughout this study, we used measurement data taken in the spectral range from 330–1100 nm only. Substrate internal absorption is significant above 1100 nm wavelength, making estimation of accuracy uncertain.

Dense dielectric thin films

The UMA was used to acquire multi-angle spectral photometric data for the optical characterization of Ta_2O_5 and SiO_2 thin films produced by magnetron sputtering. In Table 1, we present numerical results of optical characterization: measured film thicknesses and refractive index values at $\lambda = 600$ nm. There is excellent consistency of the results obtained using T and R data measured at different incidence angles and with different polarization states. For both materials, deviations of thickness and refractive index values (n) from mean values in all columns of Table 1 are lower than 0.1%.

Table 1. Parameters of Ta_2O_5 and SiO_2 films found by using oblique-incidence T and R data acquired using the Agilent UMA

	Ta_2O_5		SiO_2	
Polarization state/angle of incidence	**Physical thickness (nm)**	**n at 600 nm**	**Physical thickness (nm)**	**n at 600 nm**
s, 7°	292.3	2.162	401.4	1.486
s, 10°	292.5	2.160	401.7	1.485
s, 20°	292.4	2.161	401.5	1.484
s, 30°	292.4	2.161	401.9	1.484
s, 40°	292.4	2.161	401.6	1.483
p, 7°	292.7	2.159	401.9	1.484
p, 10°	292.5	2.160	401.4	1.485
p, 20°	292.5	2.160	401.5	1.484
p, 30°	292.5	2.160	401.9	1.486
p, 40°	292.4	2.161	401.7	1.483

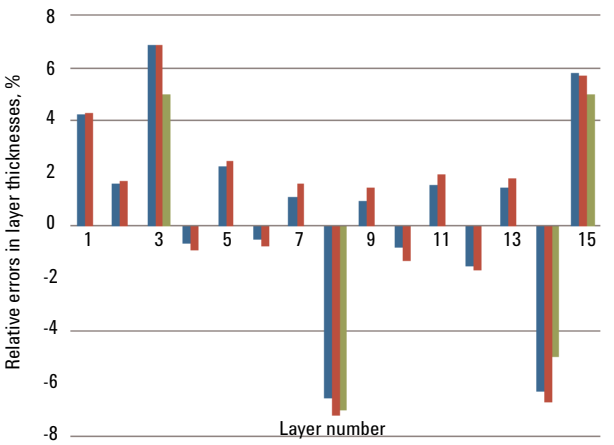

Figure 2. Comparison of errors in layer thicknesses of 15-layer quarter-wave mirror found on the basis of reflectance and transmittance data taken at 7°, 10°, 20°, 30°, and 40°, for the s-polarization case (blue bars) and the p-polarization case (red bars). Green bars show planned errors in the thicknesses of the third, eighth, 14th, and 15th layers.

Reliability of reverse engineering based on multi-angle spectroscopy

To check the reliability of reverse engineering based on multi-angle optical photometric data, we analyzed a specially prepared 15-layer quarter-wave mirror with Ta_2O_5 and SiO_2 as high and low index materials. The mirror was produced by magnetron sputtering by using time monitoring of layer thicknesses. During the deposition of this mirror, intentional errors of +5%, –7%, –5%, and +5% were imposed on the third, eighth, 14th, and 15th mirror layers, respectively. Various combinations of input measurement data was acquired using the UMA and the intentional thickness errors were reliably detected in all cases [1]. A typical example of the consistency of obtained results is presented in Figure 2.

Application of multi-angle spectroscopy to optical characterization of inhomogeneous e-beam evaporated thin films

We also applied multi-angle spectral photometric measurement to the determination of optical parameters of e-beam evaporated HfO_2 and SiO_2 films of various thicknesses. This was achieved by reverse engineering of a specially prepared multilayer mirror. It was found that the optical properties of the e-beam evaporated HfO_2 films are dependent on film thickness. Results of all reverse-engineering attempts were consistent. The offsets of SiO_2 refractive indices determined in the course of reverse engineering were in the range from 1.5% to 1.7% with respect to the nominal refractive index of SiO_2 found from characterization of the single SiO_2 layer. A good agreement in refractive indices of HfO_2 layers was also observed.

The variations of HfO_2 refractive index values, determined from separate oblique incidence T and R measurements, did not exceed 0.5%. It can be seen in Figure 3 that the measured refractive index wavelength dependence of HfO_2 film is in agreement with reference wavelength dependencies from a previous study [2]. This agreement confirms the previous conclusion that the crystalline state of HfO_2 depends on film thickness [3, 4]. As shown in these references, thin films are basically amorphous while thicker films are partially crystalline, and the larger the crystalline fraction, the thicker the film. This can explain the difference in refractive indices of our HfO_2 films that are 197 nm thick in the case of a single layer and approximately 50 nm thick in the case of a multilayer structure.

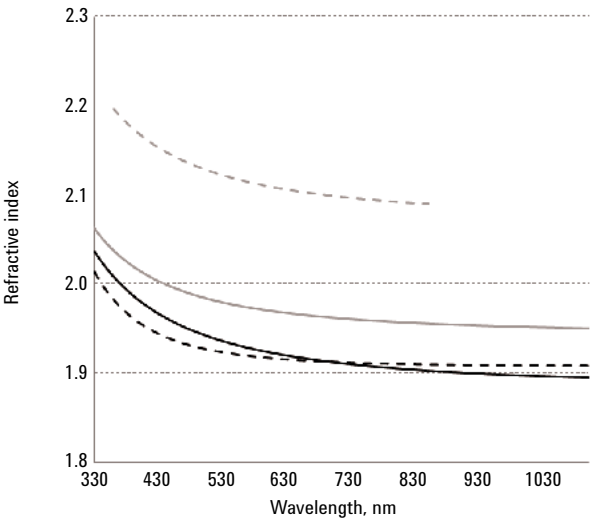

Figure 3. Nominal refractive index wavelength dependence of e-beam evaporated HfO_2 film (solid black curve), and reference refractive index wavelength dependencies of HfO_2 films produced by radio frequency sputtering (gray curve) and ion-beam sputtering (dashed gray curve). The dashed black curve shows the refractive index of thin HfO_2 film found from measurement data related to a 12-layer quarter-wave mirror.

Conclusions

We studied the applicability of multi-angle spectroscopy to the optical characterization of thin films and reverse engineering of multilayer coatings. The UMA, a new advanced spectrophotometric accessory developed by Agilent (and fitted to an Agilent Cary 5000 UV-Vis-NIR spectrophotometer), supplied reflectance and transmittance data for multiple angle and s- and p-polarization states. The accuracy of measurement data was verified and it was confirmed that all measurement data was excellent over a wide spectral range from the UV to the NIR up to the incidence angles of 40°.

Multi-angle spectral photometry provides researchers with more experimental information than conventional spectroscopy. Our study demonstrates that the new UMA spectrophotometer accessory provides experimental information that permits the solving of various optical coating characterization and reverse-engineering problems.

Comparative analysis of various combinations of input multi-angle spectroscopic data provides self-verification of the results obtained. We believe that multi-angle spectral photometry is the perfect tool for the analysis of optical coatings under oblique light incidence or at diverged light illumination.

References

1. A. Tikhonravov, T. Amotchkina, M. Trubetskov, R. Francis, V. Janicki, J. Sancho-Parramon, H. Zorc, and V. Pervak, "Optical characterization and reverse engineering based on multiangle spectroscopy," *Appl. Opt . 51,* 245-254 (2012)

2. A. Tikhonravov, M. Trubetskov, T. Amotchkina, G. DeBell, V. Pervak, A. K. Sytchkova, M. Grilli, and D. Ristau, "Optical parameters of oxide films typically used in optical coating production," *Appl. Opt. 50,* C75–C85 (2011).

3. M. Modreanu, J. Sancho-Parramon, D. O'Connell, J. Justice, O. Durand, and B. Servet, "Solid phase crystallisation of HfO_2 thin films," *Mater. Sci. Eng. B 118,* 127–131 (2005).

4. M. Modreanu, J. Sancho-Parramon, O. Durand, B. Servet, M. Stchakovsky, C. Eypert, C. Naudin, A. Knowles, and F. Bridou, "Investigation of thermal annealing effects on microstructural and optical properties of HfO_2 thin films," *Appl. Surface Sci. 253,* 328–334 (2006).

Investigating the angular dependence of absolute specular reflection using the Agilent Cary 7000 Universal Measurement Spectrophotometer (UMS)

Application note

Materials

Authors

Travis Burt, Chris Colley

Agilent Technologies
Mulgrave, Victoria, Australia

Introduction

When characterizing an optical sample it is common to measure reflection or transmission properties at a single angle of incidence (AOI). However, for a more complete characterization of the sample, it is desirable to measure reflection and/or transmission at multiple AOI's as this can provide a much deeper insight into the sample's optical properties.

This application note illustrates how the Cary 7000 Universal Measurement Spectrophotometer (UMS) can provide rapid and automated absolute specular reflection measurements at multiple AOIs. The value of using 3-dimensional (3-D) plots and 2-dimensional (2-D) contour plots to visualize the data is also demonstrated.

Experimental

Sample
The sample was a large silicon wafer measuring 200 mm in diameter and 0.80 mm thickness. A proprietary optical coating had been applied to the front surface after polishing. A summary of the sample and collect conditions is given in Table 1.

Instrumentation
The data was collected using the Cary 7000 UMS, which is a highly automated variable angle absolute specular reflectance and transmittance system. With the Cary 7000 UMS, operators have independent motorized control over the angle of incidence onto the sample and the position of the detector, which can be freely rotated in an arc around the sample. The independent control of sample rotation and detector position allows for rapid, accurate and unattended measurements.

Traditionally, reflectance and transmittance measurements have been performed using spectrophotometers fitted with different accessory attachments. In practice, this can lead to different areas of the sample being tested due to illumination beam geometry variations between measurement modes (accessories) and movement of the illumination beam over the sample.

Figure 1. Agilent Cary 7000 UMS with a 200 mm diameter silicon wafer sample mounted in the measurement chamber

If the deposition process produces a film with a non-uniform thickness, it is reasonable to expect that reflectance and transmittance measurements would be affected.

With the development of the Agilent Cary 7000 UMS, it is now possible to measure *T* and *R* at the same sample point, without moving the sample, thus overcoming one source of artifacts on the results.

Measurements
Specular reflection measurements were made with AOIs from 6° to 86° in 1° increments. The polarization of the light incident on the sample was controlled with an automated rotatable wire grid polarizer. Reflection with both s- and p-polarization was measured.

The collect conditions were set up using the Cary WinUV software method editor. Only two baselines are required at the start of the full data collection sequence, one for s- and one for p-polarization. These baselines were used for all angles, and the software applied the appropriate baseline to the individual collected spectra. In contrast, other systems require a unique baseline for each polarization at each angle, which dramatically increases the total time of collect. Once the two baselines had been collected, the system was left unattended to collect the entire data set.

As has already been noted, the silicon wafer was particularly large at 200 mm diameter. The Cary 7000 UMS is designed to accommodate samples as large as 275 mm in diameter enabling very high grazing angles of incidence to be measured. With the largest possible samples, angles close to 90° can be measured without the incident light "falling off" the sample.

Table 1. Agilent Cary 7000 UMS collect conditions

Parameter	Value
AOI	6° to 86° in 1.0° intervals
Wavelength range	2500–250 nm
Data interval	UV/Vis 1.0 nm, NIR 4.0 nm
Spectral bandwidth	UV-Vis 4.0 nm, NIR 4.0 nm
Signal averaging time	0.26 sec
Polarization	s and p
Incident beam aperture	3°x 3° (vertical x horizontal)

Results and discussion

Specular reflectance

Figure 2 shows the absolute specular reflection spectra with angles of incidence ranging from 6° to 86° in 1° increments for s-polarized light. A similar plot was generated for p-polarized light as well (not shown in this document).

Analyzing such a large number of spectra can be a significant challenge. Figures 3 and 4 show 2-D contour plots and 3-D plots generated using Scilab software [1], respectively, for the same data set. It can be seen that the reflective properties, in terms of the positions of minima and the associated %R values, are highly dependent on AOI.

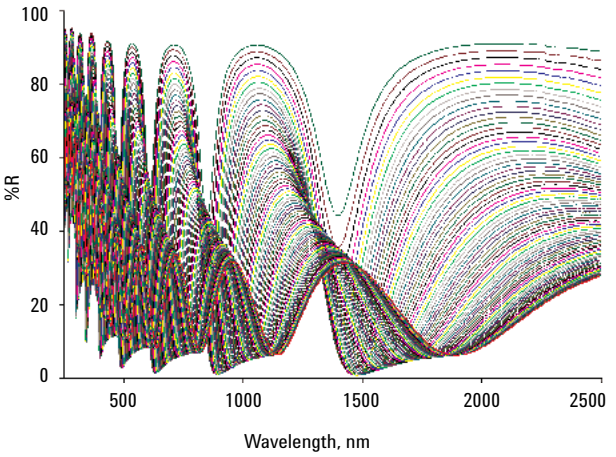

Figure 2. Absolute specular reflectance of s-polarized light from the silicon wafer from 6° AOI to 86° AOI at 1° intervals

For example, in the infrared region, at near normal AOI, there is a broad minimum centered at ca. 1900 nm. At much higher angles of incidence, at ca. 70°, the minimum is centered at approximately 1400 nm. In addition, the minimum is narrower and reaches a %R value that is much closer to zero.

Depending on the intended end use of reflective coatings and the associated performance requirements in terms of AOI, spectral region and %R, these types of observations can be fed back into coating design. Clearly, measuring the coating at one AOI only, as is common, gives no indication of this strong angular dependence.

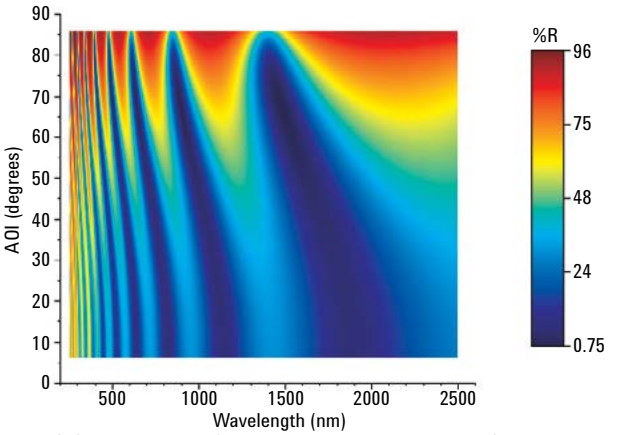

Figure 3. 2-D contour plot of the same data displayed in Figure 2

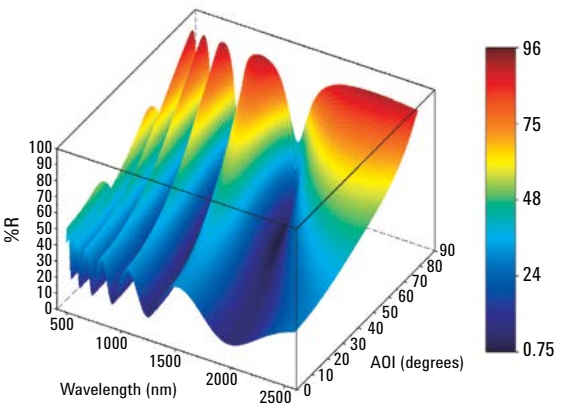

Figure 4. 3-D plot of the same data displayed in Figure 2

Conclusions

It has been demonstrated that the Cary 7000 UMS can be used to automatically collect high quality spectra for a large coated sample at a wide range of AOIs, in both s- and p-polarization. The measurement is made under complete software control and, once the sample is mounted, data collection is entirely unattended. The complete characterization of this sample over a wide wavelength range, AOI and polarization allowed greater insight into the angular dependence of the optical coating.

Furthermore, using 3-D and 2-D contour plots to visualize the large data sets provides a more thorough understanding of the properties of an optical coating. This valuable information can be used to aid coating design and optimization.

References

[1] Scilab is free open source software available at https://www.scilab.org

Quality control of beam splitters and quarter-wave-mirrors using the Agilent Cary 7000 Universal Measurement Spectrophotometer (UMS)

Application note

Materials testing and research

Authors

David Death
Farinaz Haq

Agilent Technologies, Australia

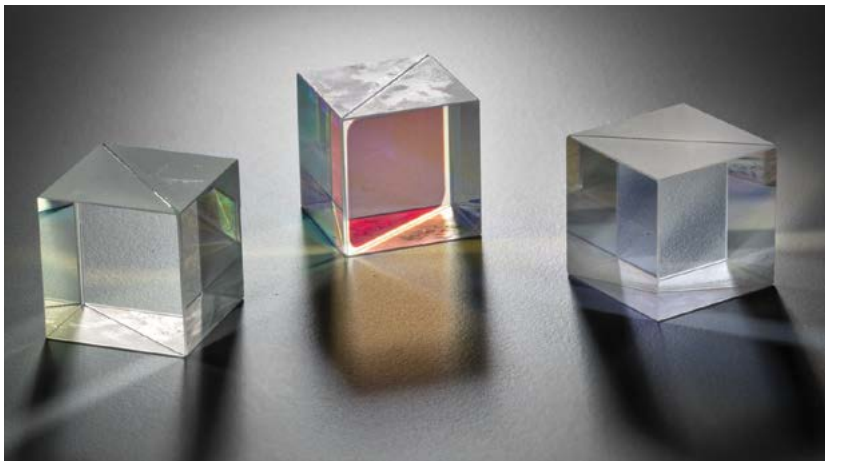

Introduction

Optical coatings and coating technologies have matured over many years in terms of the design, production and characterization processes. Today optical coatings are ubiquitous and can be found in applications from research and space optics to consumer items and industry. The variety of applications include eye wear, architectural and automotive glass, illumination and lighting systems, displays, optical filters, specialty mirrors, fiber optics and communications and medical optics. The performance of optical coatings depends on the specifications of the coating and substrate materials.

The design and manufacture of high quality multilayer optical coatings require accurate measurements of not only the final production component but also the optical constants of the materials in the thin film layers. These measurements enable the detailed design of sometimes very complex multilayer coatings. Measurements made at the end and during production can also be used to reverse engineer optical coatings to provide feedback on the design manufacturing process [1]. A primary aim of reverse engineering is to detect systematic and random errors in individual layer parameters. This helps to improve layer control and optimize the optical coating deposition.

Reliable reverse engineering of an optical coating depends critically on accurate measurements of reflection and transmission. Historically these measurements have been limited to normal incidence transmission (T) and/or near normal incidence reflection (R) data. As may be expected the ambiguity of multilayer reverse engineering grows as the number of coating layers increases. In general it is possible to minimize the ambiguity in reverse engineering by using more measured data. Both T and R measurements made at a range of angles of incidence (AOI) are valuable for the characterization of thin film materials and the reverse engineering of multilayer coatings. Most typical reverse engineering involves the detailed numerical analysis of normal or quasi-normal incidence T and R data related to the coating under study. While this approach is experimentally simple, it can lead to unreliable results due to the limited information available in near normal T and R data sets and the influence of measurement errors within those data sets [1]. In particular, reflection data from broadband reflectors or transmission data from to broadband antireflection (AR) coatings can be considered as examples of such low-information data sets. Historically simple normal incidence T measurements have been available using a wide variety of spectrophotometers and near normal incidence R measurements similarly so by fitting an appropriate reflectance accessory.

This application note demonstrates a new form of multi-angle photometric spectroscopy using a unique automated double beam UV-VIS-NIR multi-angle spectrophotometer, the Cary 7000 Universal Measurement Spectrophotometer (UMS). Example measurements of multilayer coatings used to create a spectral beam splitter and two 43 layer quarter-wave stack mirrors on differing substrates are presented alongside the reverse engineering analysis enabled by the obtained multi-angle spectral photometric data set.

Experimental

Samples

Measurements of three different coatings are summarized from the work of Amotchkina et al. [2]. The first coating, BS-AR-Suprasil, is a specialized beam splitter designed for an oblique AOI of 45°. The 52 layer reflector is deposited on a 1 mm thick Suprasil substrate. The front surface coating specification calls for a spectral transmission profile of greater than 98% T between 935 nm and 945 nm and greater than 98% R between 967nm and 971 nm. Additionally a 10-layer broadband AR coating is deposited on the rear surface. Optical coatings typically consist of alternating layers of varying thickness of high and low refractive index materials. For this first sample the high index material used was Niobium Pentoxide (Nb_2O_5) and the low index

material was Silica (SiO_2) and the coating was deposited using a Leybold Optics GmbH Helios magnetron-sputtering system.

Both the second and third samples are high reflectors constructed of 43 layer quarter-wave stacks with the design wavelength for the reflector at 800 nm. The coatings were deposited on two differing substrate types, 6.35 mm thick fused silica and 1.0 mm thick B260 glass. The sample names were HR800-FusedSilica and HR800-Glass. The high index material used in these coatings was Hafnia (HfO_2) and the low index material used was Silica (SiO_2). The coatings were deposited using e-beam evaporation in a Leybold Optics GmbH SYRUSPro 710 coating machine.

Instrumentation

The reflectance and transmittance of the completed coatings were obtained using the Cary 7000 UMS which is a highly automated variable-angle absolute specular reflectance and transmittance UV-Vis-NIR spectrophotometer. The Cary 7000 UMS provides users with automated independent motorized control over both the sample AOI and the angular positioning of the detector, see Figure 1. This independent control of both sample AOI and detector position allow for rapid, accurate and unattended measurements of optical multilayer coatings.

Reflectance and transmittance measurements have traditionally been performed using different spectrophotometer accessories. This leads to different areas of the sample being measured for reflectance and transmittance. Deposition processes, though well controlled, are not perfect and films are deposited of non-uniform thicknesses. As a result reflectance and transmittance measurements can vary across the surface as the coating thickness changes. With the development of the Cary 7000 UMS, it is now possible to measure R and T from the same point on the sample surface without moving the sample when changing from R to T measurement modes. Additionally the sample can be rotated 180° to permit static transmittance measurements to be performed in the forward or reverse direction. In a similar way the AOI in a reflectance measurement can be varied to either side of the sample normal and the detector can be moved to make R measurements at ±AOI. In either case both R and T can be measured from the same point without removing and replacing the sample in the spectrophotometer or changing to another accessory.

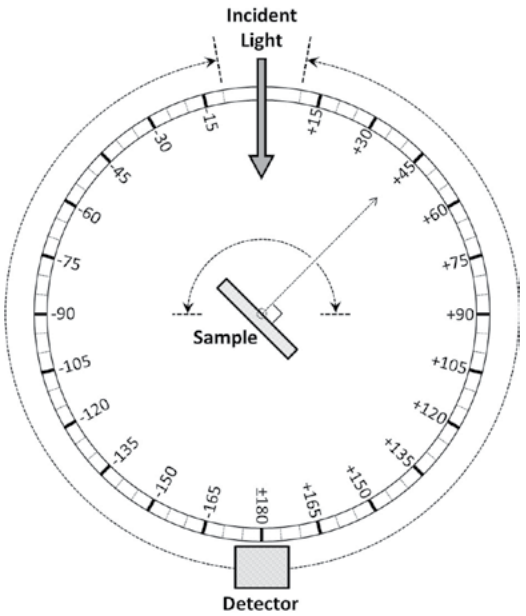

Figure 1. The AOI on the sample and the detector position can be set independently with 0.02° resolution. The AOI on the sample ranges from -85°≤AOI≤85°. The detector can be placed at angles ranging from -10° to 10°. As a result the Cary 7000 is able to determine R over the range 5°≤|AOI|≤85° and T over the range 0°≤|AOI|≤85°.

Results and Discussion

Small variations in the layer thickness as each is deposited and variations in the optical characteristics of the materials used under differing coating conditions result in the overall performance of an optical coating not meeting the original design intent. The design and analysis of optical coatings are accomplished using sophisticated computer software packages which rely on the accurate knowledge of both the physical thickness of each layer and the optical constants of the materials used to build the coating. The three coatings described were designed using OptiLayer, a suite of software consisting of modules for the design of multilayer coatings, prediction of performance, characterization of optical materials and reverse engineering of coatings from measured transmittance and reflectance data.

Some modern coating machines have the facility to monitor the normal incidence transmission of the coating as it is deposited [3-4]. These *in-situ* measurements made at normal incidence are used as a basis for predicting the final design oblique incidence performance of the coating laid down. Detailed analysis of this *in-situ* data using OptiLayer typically shows rough agreement between positioning of the reflectance and transmittance bands with the initial design. However *in-situ* normal incidence measurements are no real substitute for actual oblique angle R and T measurements of the completed coating. In their article Amotchina et al. describe how measurements made using the Cary 7000 UMS allowed them to reverse engineer the deposited coating and hence fine tune the coating process using *in-situ* measurements to more closely match the original design intent of the coating.

In the example of the BSAR-Suprasil beam-splitter the primary uncertainties lie in the thicknesses of the individual layers as the optical properties of the Nb_2O_5 and SiO_2 are quite well understood. In this study, the Cary 7000 UMS was used to measure the sample after coating. The coating specification calls for the beam-splitter to be used at a 45° AOI. Using the Cary 7000 UMS it was possible to measure both R and T at a number of different AOI from the same patch on the surface of the sample. Increasing the number of measurements in the data set (more AOI) served to reduce the level of uncertainty in the results from reverse engineering the coating. Using this data and analysis it was then possible to correlate with *in-situ* measurements and construct an optimization strategy for the deposition. Finally measurements using the Cary 7000 UMS were used to validate the optimization.

Figure 2 compares the predicted and measured spectral transmittance of the optimized BSAR-Suprasil beam-splitter at an AOI of 45° Figure 2(a). The unpolarized transmittance measurements were made using the Cary 7000 UMS. The spectral agreement between the theoretical curve (Optilayer) and the measured data points is exceptionally good. Differences in peak heights are primarily due to the spectral bandwidth used to collect the measured data. Further measurements of the BSAR-Suprasil sample were also made at an AOI of 30° for both S and P incident polarization, this data is shown in Figure 2(b) along with the predicted spectral transmittance. Once again the agreement between measurement and theory is excellent. The close agreement between these measurements made at oblique AOI of 45° and 30° and the model predictions serves to validate the reverse engineering and model refinement used to optimize the coating deposition based on the *in-situ* normal incidence transmittance measurements.

The second and third samples measured were examples of multi-layer quarter wave stack mirrors designed to be oblique incidence high reflectors. Each mirror consisted of 43 quarter wave alternating layers of Hafnia (HfO_2 — high index material) and Silica (SiO_2 — low index material). The difference between the samples being the type and thickness of the substrate used: HR800-FusedSilica — 6.35 mm thick fused silica; HR800-Glass — 1 mm thick B260 glass. In these coatings uncertainty in both the optical properties of the Hafnia and individual layer thickness need to be considered. Once again the mirror is designed for an oblique AOI of 45° with un-polarized incident light.

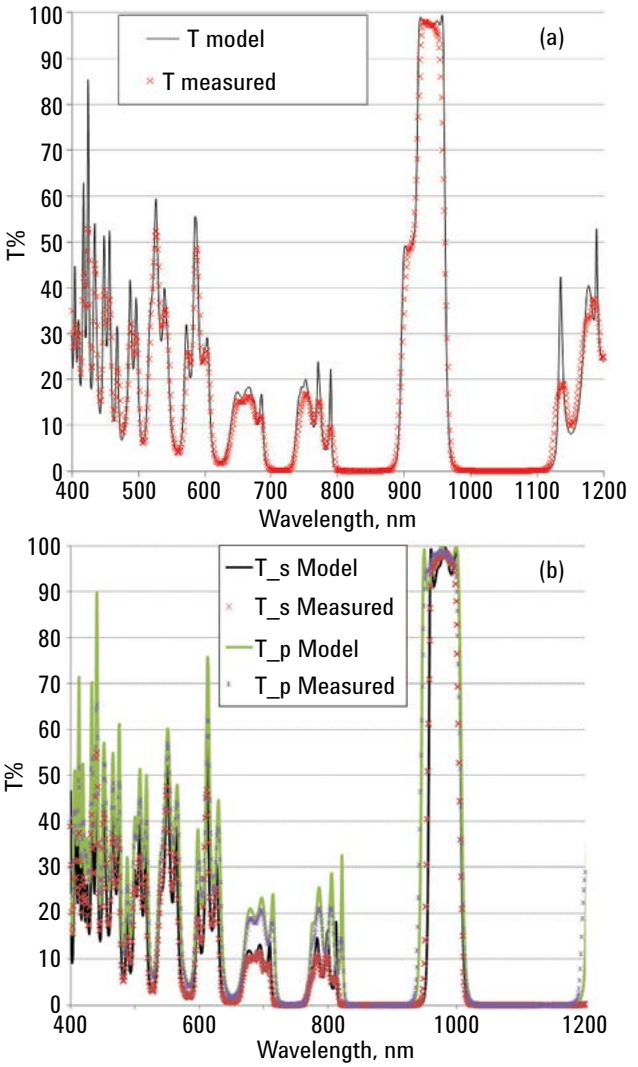

Figure 2. Comparison of oblique incidence experimental transmittance data for the sample BS-AR-Suprasil with model transmittance (a) non-polarized light at 45°, (b) s- and p-polarizations at 30°

As with the first sample, measurements of these samples using the Cary 7000 UMS were used to characterize the final coating performance, optimize the coating strategy and validate the outcomes of the reverse engineering analysis. The strategy developed involved reverse engineering *in-situ* normal incidence measurements during the coating procedure to make adjustments on the fly. As an example of the influence of material and layer thickness variations, Figure 3 compares the desired design specification with the *in-situ* and final transmittance measurement using the Cary 7000 UMS of the un-optimized coating. As can be seen there is significant deviation between the three data sets. The primary difference is observed as a shift of the reflectance band toward shorter wavelength and differences in the width of the reflectance band.

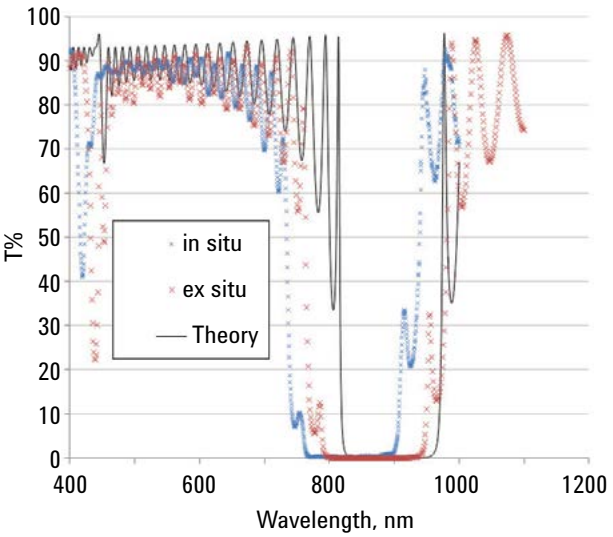

Figure 3. Comparison of *in-situ* normal incidence transmittance data, Cary 7000 UMS (ex-situ) measurements and theoretical transmittance for the HR800-Glass sample

The positioning of the reflectance band towards shorter wavelengths is understood in terms of an underestimation of the individual layer optical thicknesses as they are laid down. This may be associated with either an error in the physical thickness of the deposited layers and/or an uncertainty with respect to the optical properties of the layer materials (refractive index and absorption coefficient). Errors in the geometrical thickness of coating layers can arise from inaccurate calibration of the quartz crystal layer thickness monitors used to control the deposition. Errors in material properties on the other hand arise from incipient variation of the nominal refractive index with deposition temperature. HfO_2 exhibits such a variation of refractive index as a function of deposition temperature and at the relatively low deposition temperature used here (120 °C) there is a degree of uncertainty in its value. Further, the width of the reflection band of a quarter wave mirror stack depends on the ratio of the high and low refractive indices used [5]. On that basis the design specification should result in a width of 126 nm. The normal incidence *in-situ* measurements indicate a width of 133 nm and the Cary 7000 UMS measurements indicates a width approaching 143 nm. Considering that the uncertainties associated with the optical properties and porosity of the silica layers to be small it is apparent that the refractive index of the Hafnia layers is larger than the value assumed in the construction of the coating model. The apparently higher refractive index may be explained by the porous structure of the HfO_2 layers. Under vacuum the porous structure of the HfO_2 layers remains empty and the refractive index is correspondingly low. Exposing the coating to atmospheric air fills the pore structure with water vapor, thereby increasing the refractive index. This process is commonly known as a vacuum shift [6]. These effects can be accounted for reasonably accurately by allowing for random errors in the layer thicknesses and random offsets in the refractive index of the HfO_2 layers [2].

Figure 4 shows the measured transmittance curves for normal and oblique incidence compared with the predicted design curve for the 800 nm high reflectance coating on the 6.35 mm fused silica substrate (HR800-FusedSilica). Once again a wavelength shift is observed, but this time it is toward longer wavelengths. The widths of the high reflectance regions are again also

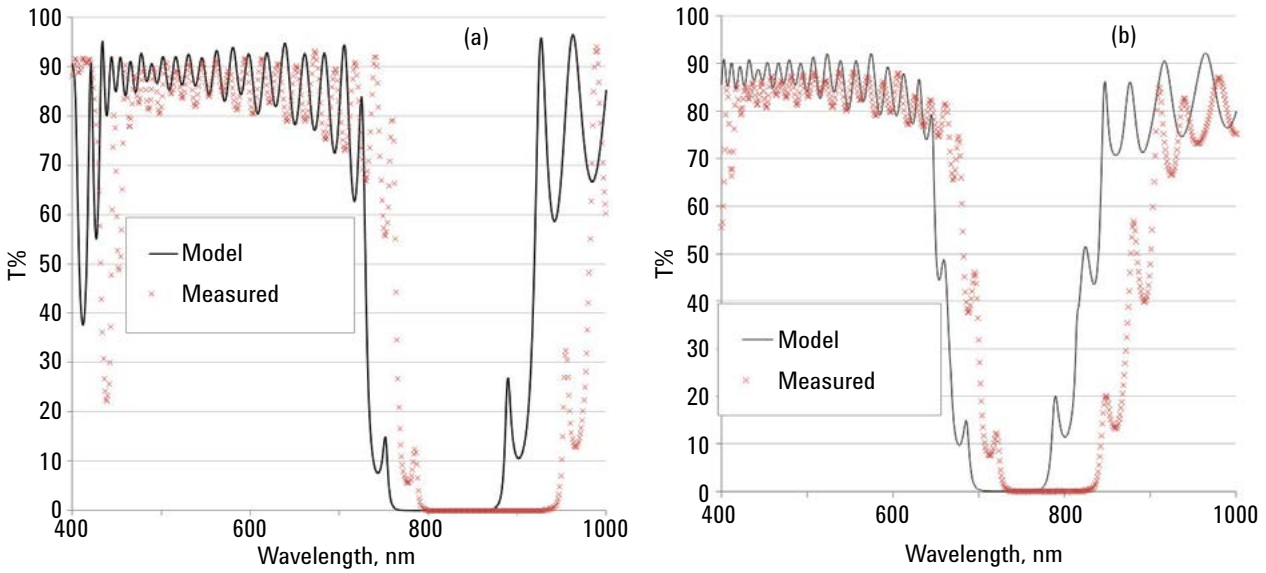

Figure 4. Comparison of normal (a) and AOI = 45° (b) experimental transmittance data related to HR800-FusedSilica sample with model transmittances calculated for intermediate design

different. For this coating the physical layer thicknesses were found to be reasonably accurate. The shift in position of the reflectance band was in this case due to uncertainties in the refractive index values assumed for the HfO_2 layers. The HfO_2 layers are considered to be inhomogeneous due to inter-diffusion of the HfO_2 and SiO_2 coating materials [1]. Random variations in the refractive index of the various HfO_2 layers were thus included in the model and the predicted transmittance recalculated for normal and oblique (45°) incidence and compared with measurements mad on the Cary 7000 UMS.

The final fitting of the normal incidence measurements by model data is shown in Figure 5(a). The model fit to the measurement is reasonable indicating that there is still room to improve the model. The model takes into account all the main features of the deposited coating however it may be further improved by allowing for variations in the degree of material inhomogeneity on a layer by layer basis and the definition of interlayers caused by diffusion of HfO_2 and SiO_2 materials. This level of sophistication cannot be based on the results of one set of transmittance or reflectance measurements at one particular angle of incidence. The Cary 7000 UMS is uniquely placed to provide both R and T data from a given sample at the multiple angles required to provide confidence in modelling these effects.

Figure 5(b) shows the comparison between the coating model and the measured transmittance at 45°. The results demonstrate good agreement between Cary 7000 UMS measurement and the predicted curve. Further the close agreement between measurement and model is confirmed in measurements at all angles made using the Cary 7000 UMS from AOI of 0° to 45° at 5° intervals.

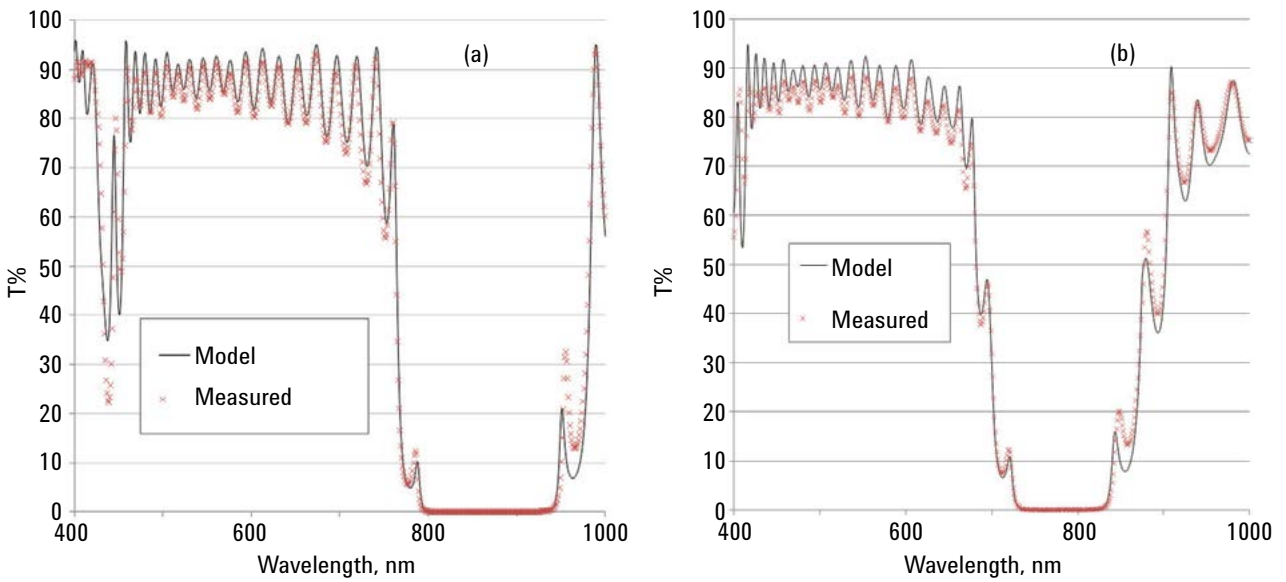

Figure 5. Final fitting of normal (a) and oblique incidence AOI = 45° (b) experimental Transmittance data related to HR800-FusedSilica sample by model transmittances

Figure 6 show the residual difference between the measured and calculated transmittance for both S and P polarization at 800 nm wavelength. As can be seen there is good agreement between the absolute transmittance measured by the Cary 7000 UMS and the value predicted by the model.

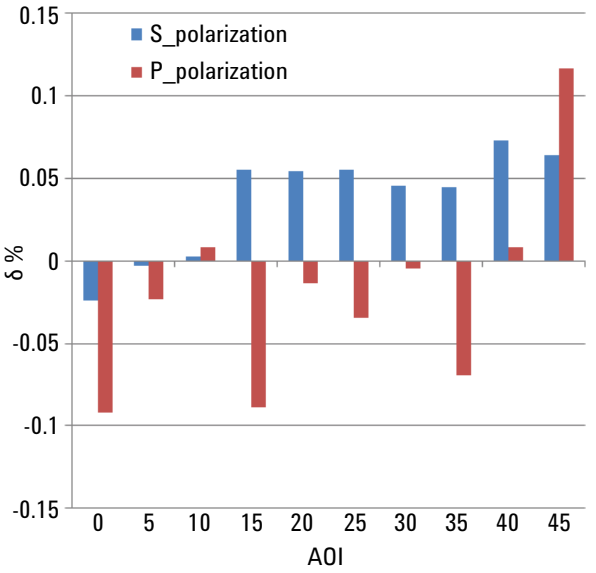

Figure 6. Residual differences between experimental and model transmission measurements data for the HR800-FusedSilica sample at the wavelength of 800 nm versus the AOI

Conclusion

The Cary 7000 UMS has been shown to be a valuable tool for the measurement and characterization of complex multilayer optical coatings. The Cary 7000 UMS provides independent and automated control of sample rotation and detector position giving it the unique ability to measure both reflectance and transmittance at different angles without having to move the sample. The facility of an automated polarizer gives the added benefit of being able to address both S and P polarization measurements, all done with the light incident on exactly the same place on the surface of the sample. The Cary 7000 UMS is an ideal candidate for QA/QC in optical coating environments because of its convenience, ease-of-use and ability to operate and produce accurate data completely unattended.

Amotchkina et al. demonstrate the value that accurate measurements of optical coatings made at a multiplicity of angles has for the accurate characterization, control and optimization of complex optical coatings. Such measurements enable and validate the adoption of intricate optimization strategies in coating deposition, particularly for coatings designed for application at oblique incidence. Such strategies often involve *in-situ* measurements made at normal incidence only followed by reverse engineering of the coating from a limited dataset. The Cary 7000 UMS enables optimization and validation through the provision of accurate measurement across a range of angles.

References

1. A.V. Tikhonravov, T.V. Amotchkina, M.K. Trubetskov, R.J. Francis, V. Janicki, J. Sancho-Parramon, H. Zorc and V. Pervak, "Optical characterisation and reverse engineering based on multiangle spectroscopy," Appl. Opt. 51(2), 245-254 (2012).

2. T.V. Amotchkina, M.K. Trubetskov, A.V. Tikhonravov, S. Schlichting, H. Ehlers, D. Ristau, D. Death, R.J. Francis, and V. Pervak, "Quality control of oblique incidence optical coatings based on normal incidence measurement data," Optics Express, 21,18, 21508–21522 (2013).

3. D. Ristau, H. Ehlers, S. Schlichting, and M. Lappschies, "State of the art in deterministic production of optical thin films," Proc. SPIE 7101, 71010C, 71010C-14 (2008).

4. H.E. Ehlers, S.S. Schlichting, C.S. Schmitz and D.R. Ristau, "Adaptive manufacturing of high-precision optics based on virtual deposition and hybrid process control techniques," Chin. Opt, Lett., 8, 62–66 (2010).

5. S.A. Furman and A.V. Tikhonravov, "Basics of Optics of Multilayer Systems, Editions Frontieres, (1992).

6. O. Stenzel, S. Wilbrandt, S. Yulin, N. Kaiser, M. Held, A. Tunnermann, J. Biskupek, and U. Kaiser, "Plasma ion assisted deposition of hafnium dioxide using argon and xenon as process gases," Opt. Mater. Express, 1(2), 278–292 (2011).

A faster, more accurate way of characterizing cube beamsplitters using the Agilent Cary 7000 Universal Measurement Spectrophotometer (UMS)

Application note

Materials

Authors

Travis Burt, Chris Colley, Hakchu Lee*

Agilent Technologies
Mulgrave, Victoria, Australia

*Agilent Technologies
Santa Clara, California, USA

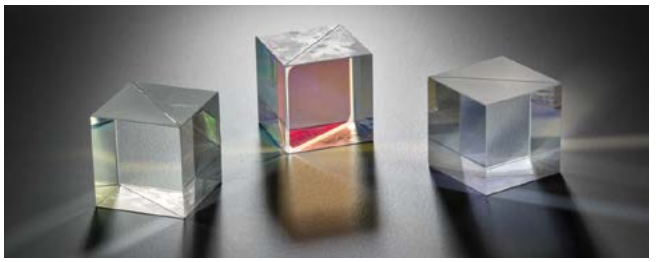

Abstract

Cube beamsplitters (CBS) are critical optical components that have a wide variety of uses in consumer products, high-tech micro positioning equipment, and fiber optic based telecommunication systems. This application note describes *in situ*, automated and unattended, transmission, reflection and absorptance measurements of CBS using an Agilent Cary 7000 Universal Measurement Spectrophotometer (UMS). Spectral information obtained is shown to provide useful insight for optical engineers at the design phase, and provide QA/QC departments better control metrics during final testing; all obtained at highly productive rates amenable to routine volume analysis demands.

Introduction

Typically not much larger than a die (0.5–1", 12.7–25.4 mm), the purpose of a CBS, as the name suggests, is to split a beam of light into two distinct paths — a reflected beam and a transmitted beam (Figure 1).

The separated beam can be used to duplicate images, separate colors or polarization states, or in the case of laser applications, create compact interferometers for nano-positioning systems. In all cases successful CBS design, implementation and quality control rely on detailed spectral knowledge of both the transmitted and reflected beams. Dielectric (optical) coatings deposited on the central hypotenuse, and sometimes also the outside faces, determine the wavelength and polarization characteristics of the CBS. One of the measurement challenges is that the optical behavior of the internal multilayer coating is influenced by its immediate opto-mechanical environment, e.g., the refractive indices of the bonding agent used to combine the two halves. *In situ* measurement of the dielectric coating is imperative as an open air characterization, performed prior to cementing the two prism halves together, renders different results to the completed cube assembly.

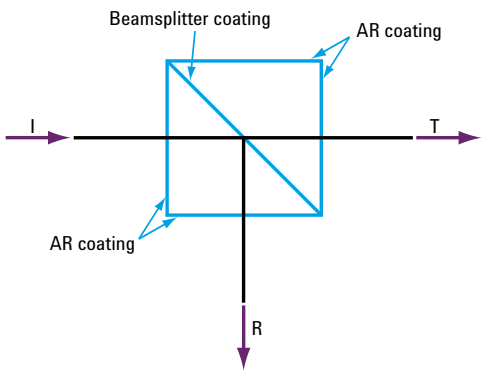

Figure 1. Plan view of a CBS showing reflection (R) and transmission (T) of the incident light (I)

The Cary 7000 UMS permits spectral characterization of the transmitted and reflected beam on the same system without moving the sample, and hence the incident beam. The *in situ* measurement of transmission (T) and reflection (R) from identical locations on the sample permit accurate Absorptance (A = 1–T–R) data to be calculated, providing greater insight into substrate and coating properties.

When analyzing total losses in spectra, researchers have previously reported artifacts which may cause doubt about the quality of the data. Sources of artifact have been reported [1] to include:

- The difference in angles of incidence (AOI) at which T and R are measured
- A slight thickness non-uniformity of the film
- Absorption in a thin film acting in combination with interference effects

In this application note, data collected using the Cary 7000 UMS is presented. Both T and R have been measured without moving the sample and hence, eliminating the source of AOI variations and coating thickness non-uniformities.

Beamsplitter Types

Cube beamsplitters can be broadly categorized according to the optical requirements of their end use. A basic overview will be given here to highlight the optical performance drivers behind each type.

The wavelength range covered can be broadband, covering the entire visible spectrum for example, or narrow band, accommodating a specific laser line, such as from a 632.8 HeNe laser. The wavelength range is controlled by the beamsplitter coating but the substrate material must also transmit the required wavelength range. BK7 glass is a low cost material useful for the visible spectrum but has strong attenuation in the UV and NIR wavelengths. Fused silica has a high cost but lower optical losses and broader wavelength range, making it the preferred choice for high power laser applications.

The bonding method used to join the two halves can be an important consideration in their end use. Optical cement produces a highly stable (mechanical) CBS but this construction is more suited to lower optical power applications. Norland Optical Adhesive 61 ("NOA 61") is an example of an optical cement. It is a clear, colorless, liquid photopolymer that cures when exposed to ultraviolet light. Higher power laser applications, on the other hand, must avoid the use of cement and turn to optical contact methods or refractive index matched oils instead. These have higher power thresholds but must be handled and used appropriately as they are less mechanically stable.

The polarization properties of a CBS are commonly used for laser based interferometry devices. For example, the performance of interferometric nano-positioning systems is partially determined by the requirement for a CBS with a high T_p/T_s ratio and a corresponding high R_s/R_p ratio. The CBS measured in this application note is an example of such a polarizing beamsplitter and behaves as shown schematically in Figure 2.

Experimental

Sample

The CBS was 25 mm cubed with a proprietary beamsplitter and anti-reflection coating made from titanium dioxide and silicon dioxide. The two prisms are bonded with optical adhesive.

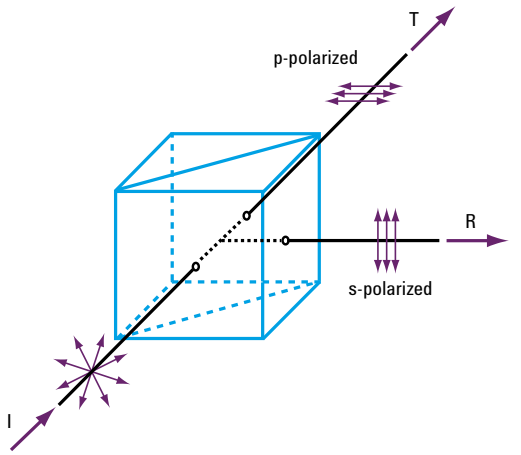

Figure 2. 3-D schematic of the reflection and transmission of light incident on a polarizing CBS

Instrumentation

The data was collected using the Cary 7000 UMS, which is a highly automated variable angle absolute specular reflectance and transmittance system. With the Cary 7000 UMS, operators have independent motorized control over the angle of incidence onto the sample and the position of the detector, which can be freely rotated in an arc around the sample. The independent control of sample rotation and detector position allow for rapid, accurate and unattended measurements of CBS.

Traditionally, reflectance and transmittance measurements have been performed using spectrophotometers fitted with different accessory attachments. In practice, this can lead to different areas of the sample being tested due to illumination beam patch size variations between measurement modes (accessories) and movement of the illumination beam over the sample.

If the deposition process produces a film with a non-uniform thickness, it is reasonable to expect that reflectance and transmittance measurements would be affected.

With the development of the Cary 7000 UMS, it is now possible to measure T and R at the same sample point without moving the sample, overcoming one source of artifacts on the results. In addition, the sample can be automatically rotated 180° to permit static T and R measurements to be performed in the forward or reverse direction. In either case, T and R are measured from the same point without moving the sample.

In this study, the Cary 7000 UMS was used to acquire transmittance data for s-polarized and p-polarized incident light at 0° AOI. Reflectance data was collected at 90° to the incoming beam and transmittance data at 0° (directly) as shown in Figure 3. The sample is mounted such that the center of the cube is at the focal point of the incident beam and on the axis of rotation of both the sample and detector. The cone angle of light incident on the sample was limited by 2° vertical and horizontal apertures.

Spectra were measured over 500–720 nm with a data interval of 1 nm, a spectral bandwidth of 5 nm and a 0.5 sec spectral averaging time.

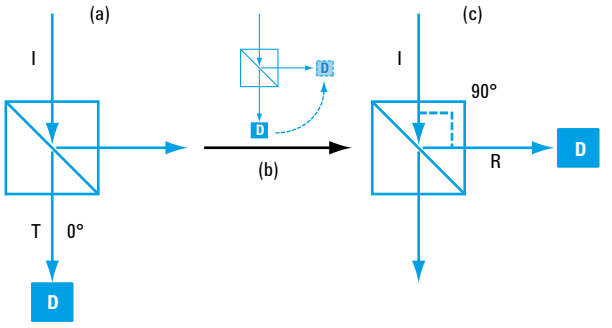

Figure 3. (a) CBS sample and detector (D) orientation for transmission measurement. (b) The detector is rotated around the sample in the plane of incidence so that for reflection measurements (c) the detector is at 90° to the incident beam and sample. NOTE: The sample does not move.

Results and discussion

The CBS is designed for use with a helium neon laser which emits at 632.8 nm. At that wavelength the CBS would ideally transmit 100% p-polarized light and reflect 100% s-polarized light. In reality, the desired transmittance and reflectance of polarized light will not be perfect so it is important to be able to measure the true performance of the CBS.

Figure 4(a) shows s-polarization transmittance and reflectance spectra measured using the Cary 7000 UMS system. By zooming in on each of the spectra around 633 nm (see Figures 4(b) and (c)), the transmission and reflection values at 633 nm can be seen. The transmission of s-polarized light at 633 nm is 0.04 %T which is within the specification for the CBS of <0.2 %T. The p-polarized spectra are shown in Figure 5. The transmission of p-polarized light at 633 nm is 98.19 %T which is within the specification of >98 %T.

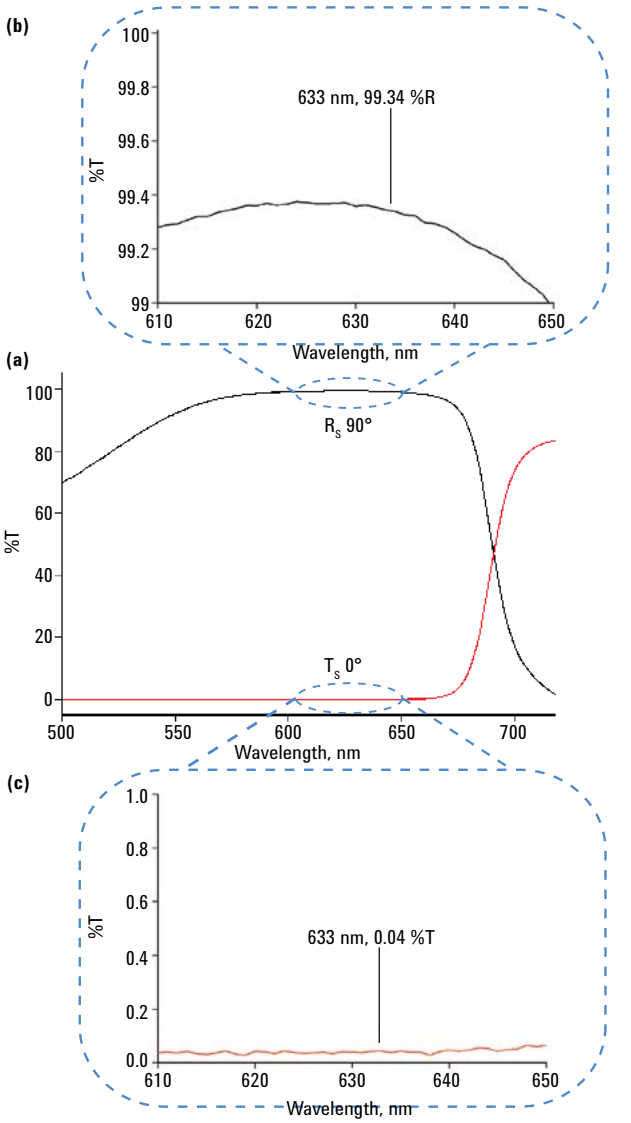

Figure 4. (a) Transmission and reflection spectra for s-polarized light measured on a CBS sample in the Cary 7000 UMS. (b) Reflection spectrum zoomed in around 633 nm. (c) Transmission spectrum zoomed in around 633 nm.

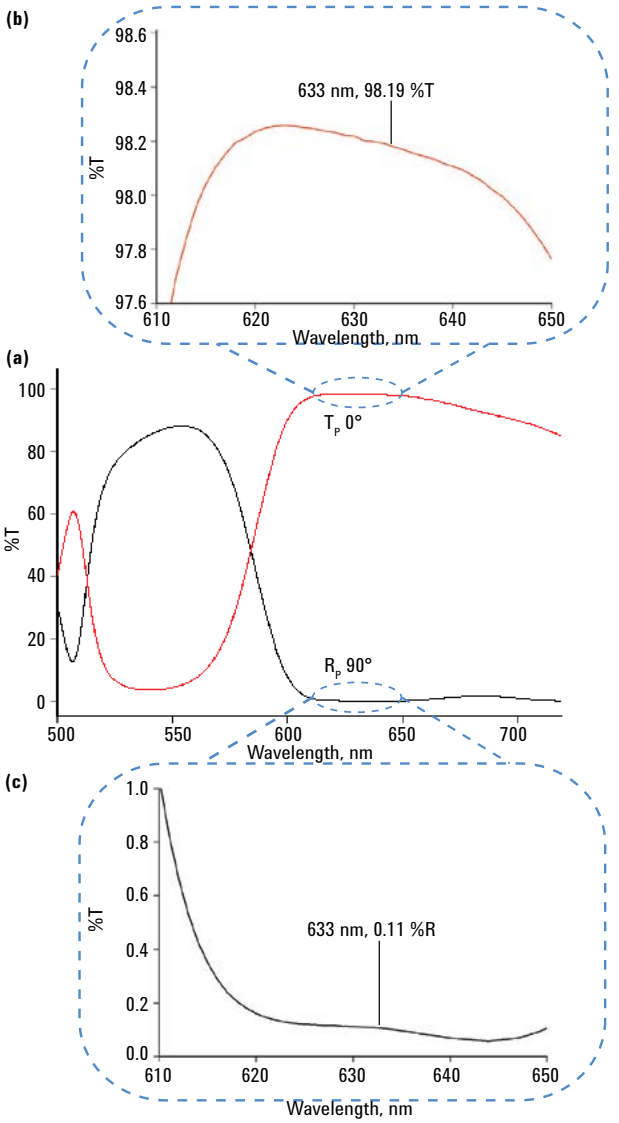

Figure 5. (a) Transmission and reflection spectra for p-polarized light measured on a CBS sample in the Cary 7000 UMS. (b) Transmission spectrum zoomed in around 633 nm. (c) Reflection spectrum zoomed in around 633 nm.

Since we have been able to measure transmission and reflection without moving the sample, we have collected self consistent spectral data which are useful for determining total losses (e,g.. retro-reflection, internal absorption or scattering). Absorptance, A, where A =1-T-R, for s- and p-polarized light are shown in Figure 6 which displays the spectral profile of light associated with these losses.

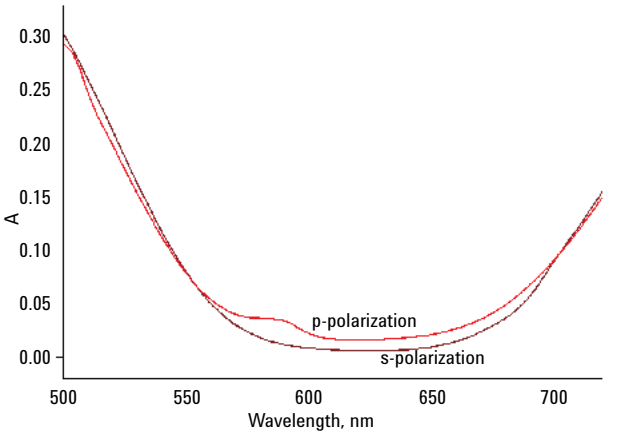

Figure 6. Absorptance spectra for s- and p-polarization

Conclusions

The Cary 7000 UMS has been shown to be a valuable tool for the characterization of cube beamsplitters. The system allows independent and automated control of the sample rotation and the detector position. The unique ability to measure T and R components without having to move the sample, hence, keeping the incident light on the sample unchanged, has also provided detailed spectral information on the absorptance of the beamsplitter.

The Cary 7000 UMS is ideal for QA/QC environments because it offers convenience, ease-of-use and completely unattended data collection.

References

1. "Oscillations in spectral behavior of total losses (1 – R – T) in thin dielectric films", T. V. Amotchkina, M. K. Trubetskov, A. V. Tikhonravov, V Janicki, J. Sancho-Parramon, O. Razskazovskaya, V. Pervak, *Optics Express*, Vol. 20, Issue 14, pp. 16129-16144 (2012).

OTHER COATING TECHNOLOGIES

MOLECULAR SPECTROSCOPY FROM AGILENT

Our molecular spectroscopy instrument range includes:

UV-Vis

From super fast routine instruments through to research-grade, our Cary UV-Vis spectrophotometers are ideal for measuring both liquids and solids.

UV-Vis-NIR

The Cary 7000 UMS is specifically designed for the materials sector – allowing the measurement of virtually any sample; measure absolute reflectance and transmission at any angle and can do it all unattended.

Fluroscence

The Cary Eclipse with xenon flash lamp technology delivers fluorescence sensitivity using fiber optics. A benchtop instrument, ideal for studying coatings, before and after application.

Hand held FTIR

Our 4300 hand held FTIR enables real time measurements to be taken wherever they are needed – regardless of the physical size or location of the object.

Benchtop FTIR

The Cary 630 FTIR provides quantitative and qualitative information for routine analysis of solids, liquids, and gases.

FTIR Imaging and Microscopy

Study the surface of coatings with a Cary 610 or 620 FTIR microscope that provides both microscope images and FTIR analysis of the coating components.

OTHER AGILENT TECHNOLOGIES FOR THE COATINGS INDUSTRY

UV-Vis fiber optic systems

The Cary 60, fitted with the Barrelino Fiber Optic Diffuse Reflectance accessory is ideal for measuring coatings, in-situ.

Applications include: Measuring Diffuse Reflectance

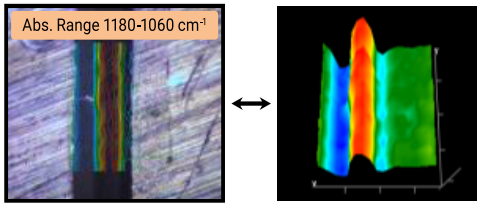

FTIR imaging

Agilent FTIR imaging systems provide the ability to characterize the spatial distribution of components in a coating as well as the ability to identify the specific chemical nature of the coating.

Applications include: Materials characterization using infrared mapping

Chromatography systems

Agilent's GC, GC/MS, HPLC and LC/MS systems are used for a wide range of coating studies – from investigating food packaging coatings to VOC analysis in architectural coatings.

Elemental analysis

Agilent's ICP-OES and ICP-MS systems are used to study metals in solutions, with applications such as investigating the Cr(VI) in corrosion protection coatings.

Agilent vacuum pumps

The Turbo-V 3K-G is more than a pump. It is a dedicated pumping system, designed specifically for thin film deposition equipment. More information

For more information

Learn more:
www.agilent.com/chem/films-coatings

Buy online:
www.agilent.com/chem/store

U.S. and Canada
1-800-227-9770
agilent_inquiries@agilent.com

Europe
info_agilent@agilent.com

Asia Pacific
inquiry_lsca@agilent.com

August 23, 2017
5991-8223EN

Agilent Technologies